

UNIVERSITA' DEGLI STUDI DI PAVIA

FACOLTA' DI INGEGNERIA
DIPARTIMENTO DI INGEGNERIA INDUSTRIALE E DELL'INFORMAZIONE

DOTTORATO DI RICERCA IN BIOINGEGNERIA E BIOINFORMATICA
XXIX CICLO 2013-2014

EVALUATION OF ACUTE ALCOHOL INTOXICATION AS A MODEL OF CEREBELLAR DISEASE

PhD Thesis by
FAUSTO ROMANO

Advisor:
Prof. Stefano Ramat

PhD Program Chair:
Prof. Riccardo Bellazzi



Acknowledgments

I would like to express my truthful gratitude to my advisor Prof. Stefano Ramat for the continuous support of my Ph.D study and related research, for his patience, motivation, and knowledge. His inspiration, insight and feedback have been priceless, allowing me to grow as a research scientist.

I would like to extend my sincere gratefulness to Dr. Giovanni Bertolini for his precious advices, comments and encouragement which incited me to widen my research from various perspectives. Your advice on research as well as on my career have been invaluable.

My sincere thanks also goes to Prof. Dominik Straumann, Dr. Melody Ying-Yu Huang, and Dr. Alexander Tarnutzer, who provided me an opportunity to join their team and access to the laboratory and research facilities in Zurich, and to Marco Penner and Dr. Christopher Bockisch for their technical support. Without their precious support, it would not be possible to conduct this research.

I gratefully acknowledge all Nicoletta, Paolo, Giulia, Fabrizio, Ting Stefan my lab mates for the stimulating discussions, all our work together, and for all the fun we have had in the last years.

Last but not the least, I would like to thank my parents Roberto and Maria Pia for all of the sacrifices that they have made on my behalf, my sister Chiara, my girlfriend Valeria and my friend Emiliano for supporting me in writing, in my life in general, and for spurring me to achieve my goal.

Abstract (Italiano)

La barriera ematoencefalica è un'unità anatomico-funzionale con permeabilità altamente selettiva che separa il sistema circolatorio dal sistema nervoso centrale (SNC). Il cervello è così protetto da potenziali neurotossine, mentre il passaggio delle sostanze nutritive, come acqua, zucchero, vitamine e gas, è permesso attraverso questa barriera. Nonostante ciò, l'etanolo, per le sue proprietà chimico-fisiche, può diffondere attraverso la barriera ematoencefalica ed interagisce direttamente con tutte le strutture del SNC. Tra queste il cervelletto è una delle regioni più sensibili, poiché l'etanolo interagisce direttamente con le sinapsi delle cellule della corteccia cerebellare: le cellule del Purkinje. Tale interazione induce un'alterazione delle frequenze di scarica delle cellule del Purkinje (sia degli *spike* semplici sia di quelli complessi), determinando così il deterioramento delle funzioni cerebellari, come il controllo motorio, l'equilibrio e il controllo dei movimenti degli occhi, determinando così.

Nei pazienti cerebellari le alterazioni delle funzioni del cervelletto sono comparabili, anche se più gravi, a quelle di soggetti in stato da ebbrezza. Sulla base di tali analogie, l'obiettivo del mio lavoro è stato quello di sfruttare la compromissione transitoria del cervelletto prodotta dall'alcol per studiarne le patologie, al fine di ottenere nuove informazioni riguardo il suo ruolo nel controllo motorio.

Per raggiungere questo scopo, l'attività di ricerca descritta in questa tesi si è concentrata sullo studio degli effetti dell'alcol sul controllo dei movimenti oculari, e in particolare sul meccanismo del *gaze holding*, sia nell'uomo che nello zebrafish.

Per *gaze-holding* si intende la capacità di mantenere stabile il nostro sguardo ad una eccentricità desiderata, "vincendo" le forze visco-elastiche di richiamo dei muscoli extra-oculari che tendono a riportare l'occhio in posizione di riposo. Tale capacità permette di mantenere l'immagine della scena visiva stabile sulla retina, evitandone lo slittamento retinico e la conseguente riduzione dell'acuità visiva. Il *gaze-holding* è quindi fondamentale per le attività quotidiane, come la lettura, e viene "implementato" nel nostro SNC attraverso due attori principali: l'integratore neurale e il cervelletto.

L'integratore neurale è una rete nervosa del tronco cerebrale che elabora tutti i movimenti oculari integrando i comandi che codificano la velocità degli occhi e trasformandoli così nei comandi di posizione che verranno trasmessi ai motoneuroni dei muscoli extra-oculari. Tuttavia, tale integratore, che produce la scarica tonica che codifica l'eccentricità cui i muscoli extra-oculari manterranno l'occhio, è imperfetto e la sua uscita

decade rapidamente nel tempo, richiedendo l'azione del cervelletto che ne prolunga la costante di tempo fino a 20s.

I soggetti in stato di ebbrezza e i pazienti in cui la funzionalità cerebellare è alterata presentano un segno clinico tipico, detto "gaze-evoked nystagmus" (GEN), cioè un'anormale deriva centripeta dell'occhio alternata da saccadi centrifughe che riportano lo sguardo nella posizione eccentrica.

Nonostante il GEN sia stato ampiamente studiato in pazienti cerebellari, in letteratura non sono presenti analisi dettagliate dell'influenza dell'alcol sul meccanismo di *gaze-holding*.

Di conseguenza, il primo obiettivo della mia ricerca è stato quello di studiare il *gaze-holding* in due gruppi di soggetti prima e 30 minuti dopo l'assunzione di una quantità di alcol stimata per raggiungere un contenuto alcolico nel sangue (BAC), rispettivamente di 0,06% e 0,10%.

Per la prima volta, le alterazioni del *gaze-holding* legate alla concentrazione di alcol nel sangue sono state dunque quantificate analizzando la velocità di deriva dell'occhio in funzione dell'eccentricità dello sguardo, considerando un intervallo di angoli ampio e continuo ($\pm 40^\circ$). Inoltre, per valutare le prestazioni del *gaze-holding*, è stato impiegato un nuovo approccio che ha permesso di sintetizzare la relazione tra velocità di deriva e posizione dell'occhio tramite una funzione tangente. Sfruttando questo modello è stato possibile descrivere le anomalie indotte dall'alcol nel *gaze-holding* e, in seguito, compararle con quelle riportate nei pazienti cerebellari acquisiti in uno studio precedente realizzato presso lo stesso laboratorio a Zurigo.

I risultati hanno dimostrato che l'alcol causa un aumento della velocità di deriva degli occhi rispetto alla condizione di controllo per tutte le eccentricità dello sguardo. In particolare l'incremento della velocità di deriva, detto effetto di scala, è risultato correlato alla concentrazione di alcol nel sangue, così che i risultati sperimentali ottenuti possono essere ben interpolati considerando un fattore moltiplicativo pari a 2 nei soggetti con 0.06% BAC e uno fattore pari a 3 in quelli con 0.10%.

Un sottogruppo di soggetti con 0.10% di BAC ha mostrato un effetto secondario indotto dall'alcol. Tale effetto aggiungendosi "all'effetto di scala", ha causato un incremento non-lineare della velocità di deriva per angoli molto eccentrici.

Considerato che simili trasformazioni lineari e non-lineari sono state riscontrate anche in pazienti affetti da degenerazioni cerebellari, i nostri risultati suggeriscono che il GEN indotto dall'alcol può essere considerato come un buon modello del GEN nei pazienti cerebellari.

La seconda parte della mia ricerca ha cercato di comprendere quanto i risultati ottenuti nell'uomo sotto l'effetto dell'alcol potessero essere generalizzati, verificando se lo zebrafish potesse rappresentare un organismo modello per le malattie cerebellari. Per perseguire questo obiettivo abbiamo sfruttato sia i vantaggi legati all'utilizzo di un organismo vertebrato come modello, sia le analogie tra gli effetti indotti dall'alcol e quelli causati dalle patologie cerebellari sul sistema oculomotorio.

Il SNC dello zebrafish, come quello di altri vertebrati, presenta infatti strutture neurali comparabili a quelle umane, come il cervelletto, la corteccia visiva e il tronco encefalico.

Nonostante lo Zebrafish sia un organismo non foveato, presenta una rete neurale situata nel romboencefalo, struttura analoga al tronco encefalico nell'uomo, che svolge un'attività d'integrazione matematica dei segnali di velocità degli occhi e viene generalmente considerata analoga a quella del VPNI nell'uomo. Tuttavia, il coinvolgimento del cervelletto nel *gaze-holding* non è stato invece esplicitamente testato nei pesci.

Proprio per tale motivo il mio studio sullo zebrafish ha avuto come oggetto due temi principali: la quantificazione degli effetti dell'etanolo sul sistema oculomotorio e l'identificazione del ruolo del cervelletto nel *gaze-holding* del pesce.

La ricerca sullo zebrafish è stata quindi effettuata analizzando i movimenti oculari spontanei in due stadi dello sviluppo del pesce, quello larvale e quello di giovane adulto, evitando così errori nella valutazione degli effetti dell'alcol dovuti ad un eventuale sviluppo parziale del SNC nella larva.

L'effetto dell'alcol sul *gaze-holding* è stato valutato stimando la costante di tempo dell'integratore. Inoltre, per verificare altri effetti dell'alcol sul controllo cerebellare dei movimenti oculari, sono state valutate le alterazioni del sistema saccadico mediante l'analisi della *main sequence*.

Lo studio sulle larve non ha rivelato alcun effetto macroscopico sul suo sistema oculomotore, ma solo un effetto non omogeneo e variabile da esemplare ad esemplare.

Nei giovani adulti, invece, l'esposizione all'etanolo ha indotto delle anomalie sia nel *gaze-holding* sia nel sistema saccadico.

In particolare, per quanto riguarda il meccanismo del *gaze-holding*, l'alcol sembra indurre un'alterazione non-lineare della velocità di deriva in funzione dell'angolo di eccentricità, senza modificare la costante di tempo dell'integratore neurale. Nel sistema saccadico, invece, è stata osservata una riduzione della velocità di picco e dell'ampiezza delle saccadi legata alla concentrazione dell'etanolo.

Nonostante l'esposizione all'etanolo produca delle anomalie nel sistema saccadico dello zebrafish che sono parzialmente paragonabili a quelle riscontrate nell'uomo in stato di ebbrezza, le diverse alterazioni nel meccanismo di *gaze-holding* suggeriscono un limitato coinvolgimento del cervelletto nel controllo oculomotorio dello zebrafish. Queste limitazioni mostrano quindi che lo zebrafish potrebbe non essere un adeguato organismo modello per le malattie cerebellari, anche se ampiamente utilizzato nella ricerca oftalmica.

La tesi qui presentata ripercorre tutta la mia attività di ricerca, partendo con una dissertazione sulle conoscenze di base necessarie al mio studio, per finire con la descrizione dettagliata dei risultati ottenuti sull'uomo e sullo zebrafish.

- Nel capitolo 1, sono state introdotte le caratteristiche principali del controllo oculomotorio, trattando con particolare attenzione quelle riguardanti il meccanismo del *gaze-holding*. Si prosegue

con la descrizione dell'anatomia e della fisiologia del “*plant*” oculomotorio, ricapitolando i modelli matematici più comunemente usati. In seguito vengono presentate le strutture neurali coinvolte nel *gaze-holding*: il cervelletto e l'integratore neurale del tronco encefalico. Il capitolo si conclude presentando i vantaggi dell'utilizzo di organismi modello nel campo della ricerca dei movimenti oculari, mostrando le analogie tra le strutture neurali presenti nell'uomo e nello zebrafish coinvolte nel controllo dei movimenti oculari.

- La prima parte del secondo capitolo tratta del ruolo critico del cervelletto nei movimenti oculari umani e descrive le anomalie oculomotorie causate da patologie cerebellari. Nella seconda parte viene illustrata l'azione neurotossica dell'alcol, spiegando il suo meccanismo di azione dal livello molecolare fino a quello cerebellare. Inoltre, sono presentate le alterazioni oculomotorie indotte dall'alcol, concludendo con una breve digressione sui danni cerebellari indotti dal consumo cronico di alcol.
- Nel capitolo 3, verrà presentata la ricerca da me svolta sugli effetti, nell'uomo, dell'intossicazione acuta da alcol sul *gaze-holding*. Tutte le fasi della procedura di analisi sono approfonditamente descritte, spiegando l'utilità dell'analisi del PV-plot per valutare le prestazioni del *gaze-holding*. In conclusione sono presentati i risultati ottenuti, confrontando l'instabilità oculomotoria indotta dall'alcol con quella dovuta a patologie cerebellari.
- Nel capitolo 4 è stata affrontata l'utilizzo dello zebrafish come organismo modello delle patologie cerebellari. Il capitolo descrive l'effetto dell'alcol sul *gaze-holding* e sul sistema saccadico nello zebrafish. Inoltre, tutte le procedure sperimentali e le metodologie di analisi adottate sono approfonditamente spiegate, mostrando i vantaggi e gli svantaggi dell'utilizzo dello zebrafish come organismo modello. Per concludere sono presentati i risultati ottenuti nelle larve e nello zebrafish, analizzando le analogie e le diversità tra l'effetto dell'alcol sul sistema oculomotorio dell'uomo e dello zebrafish.

Abstract (English)

Blood-brain barrier is a highly selective permeability barrier that separates the circulating blood from the central nervous system (CNS). All nutrients such as water, sugar, vitamins and gases are allowed to pass through, while the brain is protected from potential neurotoxins. Despite that, ethanol can diffuse through such barrier for its chemical and physical properties and it interacts with all structures of the CNS. Among them, the cerebellum is one of the most sensitive brain region, since ethanol directly interacts with the functioning of synapses in the cerebellar cortex, i.e. Purkinje cells. Such interaction alters the Purkinje cells discharge rate (both simple and complex spikes) and produces a deterioration of cerebellar functions, such as motor control, balance and eye movement control.

Cerebellar patients manifest deficits of cerebellar functions comparable, although stronger, to those experienced by alcohol-intoxicated subjects. Based on such similarities, my work aimed at model cerebellar diseases and get new insights on cerebellar role in motor control exploiting the transient impairment caused by alcohol.

To achieve this goal, the research activity described in this thesis has concerned the study of the alcohol-induced effect on the control of eye movements in humans and zebrafish, focusing on the gaze-holding mechanism.

Gaze-holding is defined as the ability to hold our gaze stable at a desired eccentricity, overcoming the visco-elastic forces of the orbital tissues and extraocular muscles that tend to rapidly pull eyes back towards the resting position.

Such ability allows keeping the image stable on the retina, avoiding retinal slip and the related reduction in visual acuity. The gaze-holding mechanism is therefore fundamental for everyday activities, such as reading, and is “implemented” in our CNS by means of two actors: the neural integrator and the cerebellum.

The neural integrator is a brainstem neural network that processes all eye movements commands converting them from encoding eye-velocity to encoding eye-position, suited for driving ocular motor neurons. However, such integrator, responsible for producing the tonic firing that will keep the eye in its eccentric position, is imperfect, i.e. leaky, so that its output decays over time, requiring a cerebellar involvement, which improves and enhances neural integration to a time constant around 20s.

Both cerebellar patients and alcohol-intoxicated subjects manifest a typical clinical ocular motor sign called gaze-evoked nystagmus (GEN): an

abnormal centripetal eye drift with centrifugal correcting saccades while at eccentric gaze.

Despite GEN has been extensively investigated in cerebellar patients, a detailed analysis of the influence of alcohol on gaze-dependent eye drift is still missing.

Thus, as a first aim of my research, we examined gaze-holding in two groups of healthy human subjects recorded before and 30 minutes after intake of the estimated alcohol amount needed to reach a blood alcohol content (BAC) of 0.06% and 0.10%, respectively.

For the first time, changes in gaze-holding were quantified by analyzing eye drift velocity as a continuous function of gaze position over a large range ($\pm 40^\circ$) of horizontal gaze angles. A novel approach was used to assess the gaze-holding performance, summarizing the eye eccentricity-drift velocity relationship by means of a tangent model with 2-parameters. Such model allowed to describe the alcohol-induced abnormalities in gaze-holding mechanism and to compare them with those reported in cerebellar patients, which were previously recorded in the same laboratory in Zurich.

The results presented here showed that alcohol intoxication caused a linear increase of drift velocity for all gaze eccentricities. Specifically, compared to the baseline, the drift velocity increased by a factor 2 at 0.06% BAC and by a factor 3 at 0.10% BAC.

A secondary effect, instead, was found in a subgroup of subjects tested at 0.10% BAC, which showed an additional nonlinear increase of drift velocity at large gaze angles.

Considering that similar linear and nonlinear transformations were described in patients affected by cerebellar degenerations, our results suggest that alcohol-induced GEN could provide a model of GEN in cerebellar pathology.

The second part of my research aimed at understanding whether the results found in alcohol intoxicated human subjects, could be generalized to zebrafish, which has been frequently considered as potential candidate for modeling cerebellar diseases in the scientific literature. To pursue such aim, we exploited the advantages of using a simpler vertebrate as a model organism and the analogies between alcohol-induced and cerebellar-induced ocular motor abnormalities.

The zebrafish CNS presents, such as other vertebrates, neural structures that are comparable to the human CNS. Specifically, the cerebellum, the visual cortex and the brainstem are preserved in zebrafish, although its visual system presents relevant structural differences with respect to the human, such as the lateral eyes and the lack of a fovea.

Such analogies are not only anatomical, so that the neural integrator in the fish has extensively been used to investigate how the human brainstem performs such integration.

Despite the zebrafish cerebellum shares relevant functions with the human one, the involvement of the cerebellum in the gaze-holding mechanism of fish has not been explicitly tested yet.

Thus, my study was designed to face two purposes: quantifying ethanol effects on the zebrafish ocular motor system, and elucidating the role of the cerebellum on the gaze-holding mechanism.

The research on zebrafish was carried out analyzing the spontaneous eye movements at two developmental stages, i.e. larval and juvenile, hoping to overcome any potential partial development of the gaze-holding structures in the larvae.

The alcohol-induced effect on gaze-holding was assessed by estimating the integrator time constant and PV-plot analysis. Additionally, the other alcohol effects on cerebellar control of eye movements were evaluated based on assessing the potential alteration of the saccadic system by means of the main sequence analysis.

The study on larvae did not reveal any macroscopic effect on their ocular motor system, showing only a nonhomogeneous effect of ethanol on their eye movements.

In juvenile zebrafish, instead, ethanol-dependent abnormalities were induced both in gaze-holding and in the saccadic system. In the former system, a nonlinear transformation of the position-drift velocity relationship was observed, although any reduction in the time constant of the neural integrator was not statistically significant. In the latter, instead, only a reduction of saccade peak velocity and amplitude was found.

Despite the observed saccadic abnormalities are partially comparable to those documented in intoxicated humans, the dissimilar alteration found in gaze-holding system after alcohol exposure suggests that cerebellar involvement in eye movement control may be limited in zebrafish. Such limitation pointed out that zebrafish may not be a suitable model organism for cerebellar diseases, although it is widely used in ophthalmic research.

The thesis presented here summarizes all my research activity, beginning from an introduction on the basic knowledge needed for carrying out the study I performed, to a detailed description of our results in humans and zebrafish.

- Chapter 1 details the main features of ocular motor control which are introduced focusing on the gaze-holding mechanism. Beginning from the anatomy and physiology of the ocular motor plant, a review about the most commonly mathematical models used to describe the plant is presented. The focus is then moved on the neural structures involved in the gaze-holding task: the cerebellum and the velocity-to-position neural integrator. Eventually, the advantages of using model organisms in eye movement research are still discussed, showing the analogies between humans and zebrafish neural structures involved in ocular motor control.
- The first part of chapter 2 presents the critical role of the cerebellum in human eye movement control and describes the eye movement abnormalities induced by cerebellar diseases. In the second, the neurotoxicity of alcohol is presented, showing its action mechanism from the cellular level to the cerebellar one.

Additionally, the alcohol-induced abnormalities in the ocular motor system are discussed, and a short digression on cerebellar damages induced by chronic alcohol consumption is presented.

- Chapter 3 presents my research on gaze instability induced by alcohol intoxication in humans. All steps involved in the analysis approach implemented in this study are described in depth, showing how to evaluate the performance of gaze-holding by means of PV-plot analysis. Eventually, our findings are presented comparing alcohol-induced gaze instability with the cerebellar-induced one.
- In the last chapter we dealt with the concerns regarding whether zebrafish can be used as model organism for human cerebellar diseases or not. Specifically, chapter 4 describes the effect of alcohol on gaze-holding and on the saccadic systems in zebrafish. All experimental procedures and methodologies are explained in depth, showing all the advantages and disadvantages of using zebrafish as model organism. Eventually, our findings on larvae and juvenile zebrafish are discussed, showing the possible analogies and dissimilarities between the alcohol-induced effect on the human and the zebrafish ocular motor systems.

Contents

Abstract (Italiano)	I
Abstract (English)	V
List of abbreviations	XI
Chapter 1: Ocular motor control	1
1.1. <i>Why study eye movements?</i>	2
1.2. <i>The ocular motor plant</i>	4
1.2.1. Anatomy and physiology.....	4
1.2.2. Ocular motor plant: 3D proprieties and kinematics.....	6
1.2.3. Ocular motor plant model.....	8
1.3. <i>Gaze-holding mechanism</i>	10
1.3.1. Coding of ocular motor signals in the final common path.....	11
1.3.2. Quantitative aspects of neural integration	13
1.3.3. Pulse-Slide-Step: a nonlinear approach	15
1.3.4. Neural Substrates for gaze-holding	16
1.4. <i>Abnormalities of Neural Integrator: Gaze Evoked Nystagmus</i>	20
1.5. <i>Eye movements in Zebrafish</i>	22
1.5.1. Zebrafish as a model organism.....	22
1.5.2. Neural architecture analogies with humans	25
Chapter 2: Disorder of cerebellar ocular motor control	27
2.1. <i>A survey of cerebellar disorders implication on eye movements control</i>	27
2.1.1. Ocular motor deficits of flocculus and paraflocculus lesions.....	29
2.1.2. Ocular motor deficits of nodule and uvula lesions	29
2.1.3. Ocular motor deficits of dorsal vermis and fastigial nuclei	30
2.2. <i>Effect of alcohol intoxication on cerebellar functions</i>	31
2.2.1. Molecular and cellular action of acute ethanol intoxication	31
2.2.2. Effect of acute alcohol intoxication on vestibular and ocular motor systems.....	33
2.2.3. Alcohol-related damages of Cerebellum: chronic intoxication	35
Chapter 3: Alcohol-induced Gaze-evoked Nystagmus	39
3.1. <i>Background</i>	39
3.2. <i>Materials and methods</i>	40
3.2.1. Subjects.....	40
3.2.2. Experimental settings.....	41
3.2.3. Experimental procedure	41
3.2.4. Data-preprocessing	42
3.2.5. Data grouping	43
3.2.6. Data analysis	45
3.2.1. Gaze-holding dataset comparison	47

3.2.2. Statistical analysis.....	48
3.3. <i>Results</i>	49
3.3.1. Gaze-holding baseline comparisons.....	49
3.3.1. BAC 0.06%: Alcohol effects on gaze-holding	51
3.3.2. BAC 0.06%: Differential analysis two eyes.....	52
3.3.3. BAC 0.06%: Differential analysis for temporal and nasal hemifield...55	
3.3.4. BAC 0.10%: Overall effect of acute intoxication on gaze-holding.....56	
3.3.5. BAC 0.10%: Pure scaling vs Shaping and scaling effect.	57
3.3.6. Evaluation of model parameters.....	61
3.4. <i>Discussion: Alcohol-induced GEN a model of cerebellar GEN</i>	62
Chapter 4: How can Zebrafish contribute to the understanding of ocular motor disorders?	67
4.1. <i>Background</i>	67
4.2. <i>Materials and methods</i>	69
4.2.1. Maintenance and breeding of Zebrafish	69
4.2.2. Experimental setup	69
4.2.3. Experimental procedure	70
4.2.4. Eye movements extraction.....	71
4.2.5. Data post-processing	72
4.2.6. Data analysis	73
4.2.7. Statistical analysis.....	75
4.3. <i>Results</i>	75
4.3.1. Ethanol effect on larvae	75
4.3.2. Ethanol effect on Juvenile zebrafish	80
4.4. <i>Discussion: human vs zebrafish, analogies and differences in ethanol intoxication</i>	86
Conclusions	91
References	93

List of abbreviations

AA	After Alcohol
AE	After Ethanol
BA	Before Alcohol
BAC	Blood Alcohol Content
BBB	Blood-Brain Barrier
BE	Before Ethanol
CN	Cranial Nerve
CNS	Central Nervous System
dpf	days post-fertilization
EPN	End-point Nystagmus
GEN	Gaze-evoked Nystagmus
GPP	Granule cell Parallel fiber-Purkinje cell
LE	Left eye
MAD	Median Absolute Deviation
MGG	Mossy fiber-Granule cell-Golgi cell
MLBN	Medium-Lead Burst Cells
MVN	Medial Vestibular Nucleus
NH	Nasal Hemifield
NPH	Nucleus Prepositus Hypoglossi
OKR	Optokinetic Reflex
PMT	Paramedian Tract

PPRF	Paramedian Pontine Reticular Formation
PS	Pure Scaling
RE	Right eye
RN	Rebound Nystagmus
SS	Scaling and Shaping
TH	Temporal Hemifield
VOR	Vestibulo-ocular Reflex
VPNI	Velocity to Position Neural Integrator
VSM	Velocity Storage Mechanism

Chapter 1

Ocular motor control

After the earth formation, sunlight has played a fundamental role in the evolution of living organisms [1]. From rudimentary eye formed only by photosensitive cells, up to complex human eye, almost all organisms exploited light energy converting it into electro-chemical impulses in neurons, to take evolutionary advantages and benefits.

Due to evolutionary pressure derived by visually guided behavior, up to 96% of animal species possess a complex optical system, and mollusks, chordates and arthropods shared eyes with image-resolving ability [2], [3]. Thus, since millions of years ago, vision became the primary source of information for the vertebrates, to perceive and locate themselves in the surrounding environment, allowing them to navigate and interact with the world.

As solid ground of reliable visual information, a proper functioning of ocular motor system is needed to focus the image of the object-of-interest (i.e., the visual target) on the retina. The complexity of such task is even greater for foveate animals such as human beings, since only 1% of the retinal area (i.e., fovea) is responsible for sharp vision (limited to two degrees of the visual field [4]), the image of interest has to be centered in the foveal region of retina.

The steadiness of gaze is therefore one of the fundamental aims of the ocular motor system, as motion of the scene on the retina (so-called retinal slip) is a serious threat of vertebrates' vision capability. Hence, several neural structures were developed in the vertebrates' central nervous system (CNS) and were surprisingly preserved during biological evolution, such as the circuitry of basal ganglia (from cyclostomes to humans) or motor centers located into the brainstem [5].

Despite keeping in focus the object-of-interest on our retina might appear as one of the easiest tasks for the brain, maintaining fixation is in fact a complex task, especially when either the target or our head or both of them are moving. The ocular motor control system, indeed, ensures proper

gaze behavior in a semi-automatic way exploiting several functional classes of eye movements (Table 1-1) regardless of adopted solution.

Due to the high level of complexity of such mechanisms, beginning with a digression on the important of research in eyes movements, this chapter will introduce the reader to the “world of ocular motor control”, with a special focus on the neural structures involved in the gaze-holding task. Besides, it will be introducing the amazing analogies between humans and zebrafish, a teleost fish commonly used as a model organism, which uses human-like neural strategies for eye movements control despite the lack of a fovea. Most literature information was taken from [6], [7].

Table 1-1: Functional classes of human eye movements (adapted from [7])

Class of Eye Movements		Main Function
	Vestibular	Holds images of the visual field steady on the retina during brief head rotations or linear translation
Gaze holding	Visual Fixation	Holds the image of a stationary object on the fovea minimizing ocular drifts
	Optokinetic	Holds images of the visual field steady on the retina during sustained head rotation or linear translation
	Smooth Pursuit	Holds the image of a small moving target on the fovea; or holds the image of a small near target on the retina during linear self-motion; with optokinetic responses, aids gaze stabilization during sustained head rotation
Gaze shifting	Nystagmus quick phase	Reset the eyes during prolonged rotation and direct gaze towards the oncoming visual scene
	Saccades	Bring images of objects-of-interest focus on the fovea
	Vergence	Moves the eyes in opposite directions so that images of a single object are placed or held simultaneously on the fovea of each eye

1.1. Why study eye movements?

Regarding all scientific production over the past 150 years, the research in field of eye movements has never stopped. More than 80.000 articles have been published from 1874 to 2015 [8], and about 10% of them concern ocular motor control.

The remarkable findings in the field of eye movements are helping basic science and clinicians, from otolaryngologists to neurologists passing through neurobiologists, psychologists and neuroscientists, to solve one demanding question: how does the brain work?

But how can basic eye movements contribute to unravel the complex neural networks of the brain?

To answer this question, it is important to keep in mind that vision is the key sense of almost all vertebrates, and a right response to external stimuli is essential to survive. From this point of view, it is not surprising that the development of a reliable ocular motor control system has guaranteed a better chance of survival, by allowing clear vision.

Thus, after millions of years of vertebrates evolution, a stereotypical relationship between stimuli and reflexive eye movements, such as vestibulo-ocular reflex (VOR) [9]–[11] or optokinetic reflex (OKR) [12]–[14], was developed. Even voluntary eye movements (such as saccades and smooth pursuit in foveate animals) are automatic in many circumstances, and normally have stereotypical trajectories and relationships between velocity and amplitude [15]–[19].

Exploiting the stereotyped features of eye movements, researchers have investigated the structures of the human CNS involved in ocular motor control, such as the medulla, pons, midbrain, cerebellum, and prefrontal, parietal posterior and visual cortex [20]–[23], and the physiology of the extraocular muscles, ocular motor neurons, afferent visual pathways, inner ear and retina.

Abnormalities of eye movements are, indeed, often detectable when any of these areas are damaged or influenced by drugs. Thus, relationships between specific pattern of eye movements and the pathophysiology or the anatomical localization of lesions have allowed to shed light on brain function, such as in [24], where *Robison and Fuchs* investigated the role of the frontal eye fields in the control of saccadic eye movements using electrical stimulations.

Moreover, the neural structure of CNS shared by vertebrates has been giving the opportunity to use several model organisms for a better understanding of the human brain. For instance, studies on mammals [11]–[13], [16], [20], [24]–[26], such as cats and rhesus monkeys, provided new insights how the cerebellum is involved in adaptive control of gain in VOR [25] or to maintain a steady eye position (i.e., gaze-holding) [26], while “simpler” vertebrates, such as gold fish or zebrafish, allowed to study extensively ontogeny of optokinetic and vestibulo-ocular behaviors [27]–[30] or the mechanism of congenital nystagmus [31], [32].

However, a question may arise: why should eye movements be easier than other movements? Today we already know that not only eye movements have highly stereotyped features, but also other simple motor tasks follow similar principles, such as goal-directed arm movements [33]. Despite that, several findings would not be possible without using eye movements. First, eye movements are inherently simpler than limb or whole body movements. The movements of each eye are limited to rotations of the eye bulbs around three axes, produced by means of three pairs of muscles. Second, the relatively simple relationship between the discharge of ocular motor neurons and the obtained bulb rotations is fully characterize [6], [34]–[37]. Third, eye movements are easy to measure and

they can be conveniently represented through mathematical models which can be easily simulated.

A good knowledge of the motor physiology of eye is therefore essential for research in the ocular motor system. In the following paragraph, the models proposed in literatures for describing eye movement dynamics are extensively discussed.

1.2. The ocular motor plant

1.2.1. Anatomy and physiology

The ocular motor plant, which consists of the eyeball, its suspensory tissues, and motor units (i.e., six extraocular muscles, and the synapses from the motor neurons innervating them), is one of the best understood muscular plants in motor physiology. This is mostly due to the fact that no external disturbances normally perturb the relationship between motor neuron firing rate and eye position [34].

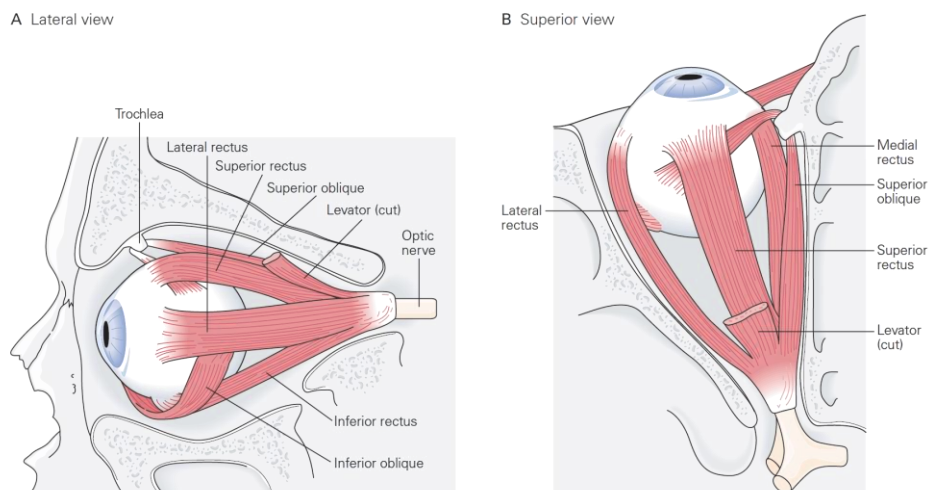


Figure 1.1: The origins and insertions of the extraocular muscles in human eye. A. Lateral view of the left eye. Each rectus muscle inserts in front of the equator of the globe so that contraction rotates the eye toward the muscle. Conversely, the oblique muscles insert behind the equator and contraction rotates the eye away from the insertion, producing an ocular torsion. The superior oblique muscle is the only extraocular muscle that passes through a bony pulley, the trochlea, before it inserts on the globe. The *levator palpebrae superioris*, also known as superior levator muscle, elevates and retracts the superior eyelid. **B.** Superior view of the left eye. The superior rectus passes over the superior oblique and inserts in front of it on the globe. The four recti muscles share a common origin in the apex of the orbit, called annulus of Zinn (Taken from [6]).

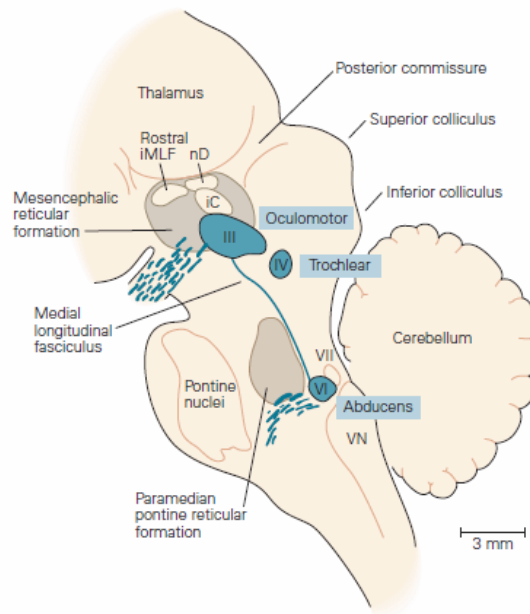


Figure 1.2: The oculomotor nuclei in the brainstem. Parasagittal section of a rhesus monkey thalamus, pons, midbrain, and cerebellum. The nuclei or bodies of oculomotor neurons (blue areas) lie in the brainstem. The oculomotor nerve (CN III) arises from the anterior part of mesencephalon (midbrain) at the level of the mesencephalic reticular formation. The trochlear nucleus (nerve IV) is slightly caudal and lies in the lower midbrain at the level of the inferior colliculus, and gets its name from the trochlea, the bony pulley through which the superior oblique muscle travels. The abducens nucleus (nerve VI) is located below the fourth ventricle in the caudal portion of the pons, at the level of the paramedian pontine reticular formation, adjacent to the fasciculus of the facial nerve (VII) (iC, interstitial nucleus of Cajal; iMLF, interstitial nucleus of the medial longitudinal fasciculus; nD, nucleus of Darkshevich; VN, vestibular nuclei.) (Taken from [6]).

As a first approximation, the eyeball can be considered as a sphere, constrained by the orbital wall and passive orbital tissues. Due to such constraints, the eye movements are limited to rotations, while the translations are negligible.

The six extraocular muscles (shown in Figure 1.1) are organized in three pairs of agonist-antagonist muscles, and allow any rotation in three-dimensional space. Specifically, each muscle pair rotates the eye around one principal axis (horizontal, vertical or torsional) defining its plane of action. The two pairs of rectus muscles, the later-medial and superior-inferior, control eye motion in the horizontal and vertical planes respectively. Contraction of one later recuts causes an abduction movement (i.e. the eye moves temporally), while contraction of medial recuts pulls the eye toward the nose, causing an adduction movement. The movements in vertical plane of elevation and depression are primarily obtained by

contraction of superior and inferior recti, respectively. Conversely to the recti muscles, the oblique muscles are inserted behind the equator of the eye globe, and contraction of superior and inferior oblique muscles is primarily responsible for in-torsion and ex-torsion of the eye (i.e. clockwise and counterclockwise torsion of the eye). A secondary action of superior/inferior muscles is related to torsional movements, likewise the oblique muscles contribute to elevation/depression of the eye. The relative contribution in vertical and torsional rotations produced by such muscles depends on eye position.

Like skeletal muscles, two fundamental laws govern the behavior of extraocular muscles. First according to the Henneman's size principle, the motor units are recruited in fixed order, small and red muscle fibers first and large and white later [38]. Second, as visible in the anatomical arrangement of extraocular muscles (Figure 1.1), Sherrington's law of reciprocal innervation rules excitation-inhibition of agonist-antagonist muscles pairs [39].

The six extraocular muscles are innervated by three groups of motor neurons, whose cells bodies are located in the brainstem, clustered in the nuclei of three cranial nerves (CN) (Figure 1.2): the III CN, the ocular motor nerve; the IV CN, the trochlear nerve; and the VI CN, the abducens nerve. The lateral rectus is innervated by the abducens nerve, while the superior oblique muscle is innervated by the trochlear nerve (cranial nerve IV). Conversely, the ocular motor nerve has four subdivisions, and supplies for all the other extraocular muscles, the medial, the inferior and superior recti and the inferior oblique. Despite that, the abducens nuclei also contain internuclear neurons that excite medial rectus motor neurons.

Eventually, the ocular motor nerve supplies also the levator muscle of the upper eyelid, which has also a sympathetic innervation. Due to such strict relationship between extraocular muscles and cranial nerves, characteristic abnormalities in eye movements are used as clinical signs to detect specific lesions of CN.

1.2.2. Ocular motor plant: 3D proprieties and kinematics

As summarized above, the anatomical structure of the ocular motor plant allows 3D rotations. Consequently, in theory, it allows an infinite number of eye positions for each desired gaze direction, each one with a different amount of torsion.

In reality, though, this is not the case and the solution to such uncertainty is provided by Listing's Law: a kinematic principle that governs 3D eye movements, explaining how, for any gaze direction, the eye always assumes the same unique orientation in 3D when the head is stationary. Specifically, Listing's law states that all achieved eye orientations can be reached by starting from one specific "primary" reference orientation and then rotating about an axis that lies within the Listing's plane. For instance,

such plane is orthogonal to the visual axis when the eye is in ocular primary position, and the the allowed ocular positions as defined by Listing's rules are shown in Figure 1.3.

Listing's law can be expressed using different coordinates' systems such as Helmholtz coordinates. In Helmholtz's system, an eye position is divided into a series of three sub-rotations. Expressed mathematically in Helmholtz coordinates, Listing's law states:

$$T = -HV/2 \quad (1.1)$$

where T, H and V represent torsional, horizontal and vertical angles in radians, and with positive angles defined from the subject's point of view as clockwise, rightward and upward, respectively. As clearly expressed in Eq.(1.1), Listing's law quantitatively specifies the degree of ocular torsion for any given horizontal and vertical eye position. Thus, torsions that do not follow such relationship are not assumed by eye, violating Listing's law such as the eye position drawn in dashed lines in Figure 1.3.

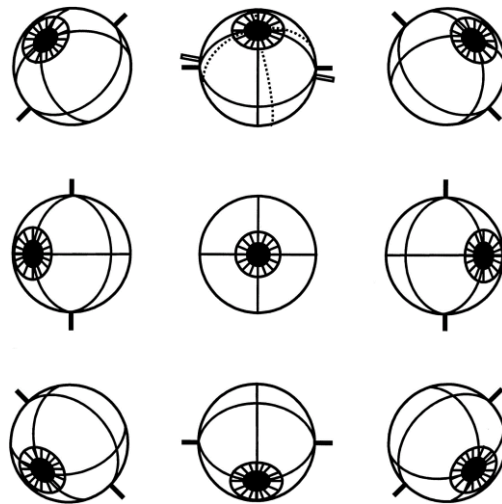


Figure 1.3: Ocular positions as defined by Listing's rules. The nine orientations drawn in solid lines are in accordance with Listing's law, because all achieved eye orientations are achieved rotating from the primary position (center) around axes lying in Listing's plane (the plane of the paper). The position drawn in dashed lines at top center does not fit Listing's law, because the rotation to this position from the primary position occurs around an axis that is tilted out of primary position. (Taken from [40]).

Almost all classes of eye movements shown in Table 1-1 obey Listing's law. Specifically, when the eye is in its primary position, all saccadic and smooth pursuit eye movements are executed with rotation axes lying in Listing's plane (i.e., horizontal/vertical plane). Such relationship is not preserved when the eye starts its rotation from a non-primary position (e.g. an eccentric angle), since Listing's half-angle rule specifies that the angular

velocity axis (i.e. rotation axis) lies in a new plane, the velocity plane, which deviates towards the initial direction of gaze by half its eccentricity angle.

During VOR and OKR, however, Listing's law is not respected. On the other hand, a similar rule, called “quarter angle rule” (the rotation axes have to rotate of a quarter of the angle of the eye), was introduced to describe the behavior of the VOR.

Several hypotheses were proposed to explain why CNS controls the eye movements in order to follow the Listing's law. Helmholtz and Hering proposed separately two theories [41], [42], but both of them are essentially based on optimization of the visual processing related to image flow across the retina, simplifying the neural processing of visual information. Other authors [42], [43] suggested that Listing's rule was a CNS strategy to optimize motor control, improving motor efficiency by minimizing the rotational eccentricity of the eye. Thus, such optimization allows to reduce elastic recoiling forces minimizing the work load on the eye muscles to maintain the eye eccentrically.

1.2.3. Ocular motor plant model

Due to the high degree of complexity of ocular plant kinematics and 3D proprieties, several models have been proposed for describing the ocular motor plant.

Commonly, eye plant behavior is described in terms of elastic and viscous properties of extraocular muscles, simplifying each muscle pair as a single element which has the ability of pushing and pulling the eye. Such single element models have been extensively used, providing a precise description of plant behavior for most classes of eye movements (see Table 1-1).

As first introduced by Robinson's model [34], the input to the plant is the instantaneous motoneurons' discharge rate in terms of number of spikes per seconds $R(t)$, while the instantaneous eye position in the orbit $E(t)$ (or gaze eccentricity) is the output of the system. Such relationship is formally expressed by:

$$R(t) = k_{plant} \cdot (E(t) - E_{null}) + r_{plant} \cdot \frac{dE(t)}{dt} \quad (1.2)$$

where k_{plant} represents the elastic coefficient of the ocular motor plant, E_{null} is the *null* position, r_{plant} is the viscous coefficient of the plant.

The two terms comprised in Eq.(1.2) describe two physiological features of the ocular motor plant.

The former member describes the motoneurons discharge rate $R(t)$ during the fixation, related to eye eccentricity $E(t)$. The discharge rate, indeed, must remain constant during eccentric fixation, in order to maintain the muscle contraction force needed to counterbalance the elastic force, i.e. $k_{plant} \cdot (E(t) - E_{null})$, that would pull the eye back to its primary position.

According to such model, the relationship between the different eye positions and the corresponding discharge rate can be linearly approximated. Thus, the discharge rate has to increase if the eye moves farther from the null position (called the on direction) or to decrease if it moves toward it. The motor neurons cease firing, instead, when the fixation point corresponds to the “null” position of eye E_{null} (also called moto neurons threshold).

The second term, $r_{plant} \cdot dE(t)/dt$, describes the dynamic proprieties of ocular motor plant. Discharge rate, indeed, is also related to eye velocity, since it is necessary to overcome viscous drag imposed by orbital supporting tissues opposing motion (i.e. instantaneous changes in eye eccentricity). Thus, the higher the desired eye velocity $dE(t)/dt$ the higher the moto neurons firing rate $R(t)$.

Eventually, it is worth taking note that this first order model proposed by Robinson does not take into account the inertia of eyeball, as it is negligible as suggested in [44].

Despite that, experimental observation of discharge patterns of ocular motor neurons [34], [35], confirmed that such first-order differential equation is compatible with a first order system with a single visco-elastic term. The patterns of moto neuron discharges, the so-called “pulse and step” (as detailed in the following paragraph), is described by means of two actions. A tonic innervation is needed to keep the gaze stable and overcome the centripetal elastic forces of the plant (“step”), and a phasic innervation is needed to overcome the viscous drag, and consists of a burst in activity of neurons (“pulse”).

Recordings of firing rate over a large population of motoneurons allow to estimate the parameters of Eq.(1.2), i.e. $k_{plant} = 4 \text{ nspike}/^\circ$, $E_{null} = 25^\circ$, and $r_{plant} = 0.95 \text{ nspike}\cdot\text{sec}/^\circ$, resulting in the following relationship between $R(t)$ and $E(t)$:

$$R(t) = 4 \cdot (E(t) - 25) + 0.95 \cdot dE(t)/dt \quad (1.3)$$

The first-order approximation of the transfer function of the ocular motor plant in Eq. (1.2), using the Laplace transform notation, is therefore as follows:

$$\frac{E(s)}{dR(s)} = \frac{1/k_{plant}}{(sT_e + 1)} \quad (1.4)$$

where $T_e = r_{plant}/k_{plant}$ is the time constant of the plant with a typical value of about 240 msec.

Despite the model shown in Eq.(1.2) describes appropriately almost all eye movements, Robinson suggested that a second order model could take into account the presence of two elastic elements and two viscous terms in plant, as at least a pair of muscles are responsible for each rotation [45].

Several models [45]–[47] were later proposed as a better approximation of ocular motor plant dynamics. In [47], *Keller et al.* introduced a third term in Eq.(1.2), considering the dependency between motoneurons firing rate and eye acceleration, as follows:

$$R(t) = k_{plant} \cdot (E(t) - E_{null}) + r_{plant} \cdot \frac{dE(t)}{dt} + m \cdot \frac{d^2E(t)}{dt^2} \quad (1.5)$$

Considering also a delay τ equal to about 8ms, the Laplace transform of the ocular plant model proposed in Eq.(1.5) becomes:

$$\frac{E(s)}{dR(s)} = \frac{(1/k_{plant}) \cdot e^{-s\tau}}{(sT_{e1} + 1) \cdot (sT_{e2} + 1)} \quad (1.6)$$

where $T_{e1} = 0.18s$ and $T_{e2} = 0.016s$ represent the two time constants of the plant due to the presence of two elastic and viscous coefficients[45].

However, since the third term of Eq.(1.5) affects model behavior only for high accelerations (above $1000^\circ/s$), Eq.(1.2) can be considered a good approximation for almost all purposes. Despite that, several studies suggest that a fourth-order model is the most accurate to represent the behavior of the ocular motor plant [44], [45], [48].

1.3. Gaze-holding mechanism

To clearly see a stationary object, our CNS controls visual fixation in order to hold its image stable on the fovea. Gaze stability is therefore a fundamental function to allow a clear vision. However, such functionality is not only related to visual fixation, as it is possible to sustain gaze eccentrically even in the dark without visual stimuli [49], [50].

As already mentioned in the anatomical description of the ocular motor plant, the elastic recoiling forces of the orbital tissues and extraocular muscles tend to rapidly pull eyes back towards the resting position. Thus, to counteract these forces, and hold the eyes steady in an eccentric position in the orbit, the ocular motor neurons must maintain a sustained rate of discharge inducing a tonic contraction of the extraocular muscles.

Such physiological function is called “Gaze-holding”, and is strictly related to a network of neurons located in the brainstem, called Velocity-Position Neural Integrator (VPNI)[20], [51], [52], that integrates velocity signals into position commands. All neural commands generating eye movements are processed by such VPNI network. The signal processing performed by this network is equivalent to the mathematical integration of the incoming velocity command. Although the VPNI plays a fundamental role in gaze-holding mechanism, its integration is not perfect, and a second “actor”, the cerebellum, compensates for its non-ideal behavior [22], [53]–[56].

1.3.1. Coding of ocular motor signals in the final common path

Understanding how brainstem neurons encode eye movement signals is the first step toward understanding the neural basis for the gaze-holding mechanism.

To move the eye quickly to a new position in the orbit and keep it there, the motor signal must include information about the velocity and position of the eye, to overcome respectively a velocity-dependent viscous force that opposes rapid movement, and an elastic one, which tends to restore the eye to the central position in the orbit.

Such information is conveyed and coded in the discharge frequency of extraocular motoneurons [6], [35], generating a motor command called “pulse and step”. Specifically, the pulse component of motor signal is generated by the firing rate of motoneurons which rises rapidly producing saccade, while a tonic innervation of muscles (i.e. steady action of neurons which fire at a constant frequency) produced the step component.

The pulse and step are generated by different brainstem structures, clustered in three groups of neurons (as shown in block diagram in Figure 1.4A)[6], [7]. The pulse of a saccadic command is generated by a class of neurons called burst cells which fire only during the saccade (Figure 1.4B). The step of innervation is instead “computed” by means of a neural network, the VPNI, producing a tonic discharge directly derived from the pulse innervation (Figure 1.4B). The appropriate step is, indeed, obtained by mathematical integration of the pulse as first suggested by Robinson[57].

Since burst neurons are inherently unstable a further population of neurons, the pause or omnipause cells, is needed to prevent undesired saccades by constantly inhibiting burst cells. Indeed, omnipause neurons fire continuously before and after a saccade, while they pause firing during a saccade in any direction.

The anatomical localization of every cluster of neurons is related to its functionality. Focusing only on horizontal eye movement, the neural circuit needed for a movement in the left hemifield is shown in Figure 1.4C.

The pulse needed for a horizontal saccade is generated by a family of burst neurons laying in the paramedian pontine reticular formation (PPRF), the medium-lead burst cells (MLBN) that project to ipsilateral abducens nuclei and, through an interneuron, to contralateral ocular motor nuclei (red cells in Figure 1.4C), allowing precise coordination of conjugated eye movements.

Two more types of burst neurons are located in the pons: the long-lead and the inhibitory burst cells. The former receive excitatory input from higher centers, projecting directly on medium lead cells. The latter are excited by the activity of MLBN and act as inhibitory cells, suppressing the activity of contralateral abducens neurons and contralateral excitatory burst neurons.

The integration of the pulse is performed by tonic cells (violet cells in Figure 1.4C) in the medial vestibular nucleus and in the nucleus prepositus

hypoglossi (NPH) that are linked through commissural connections (see the Section 1.3.4, for a detailed description). The neural integration is improved by interconnection with the flocculus in the cerebellum as explained below.

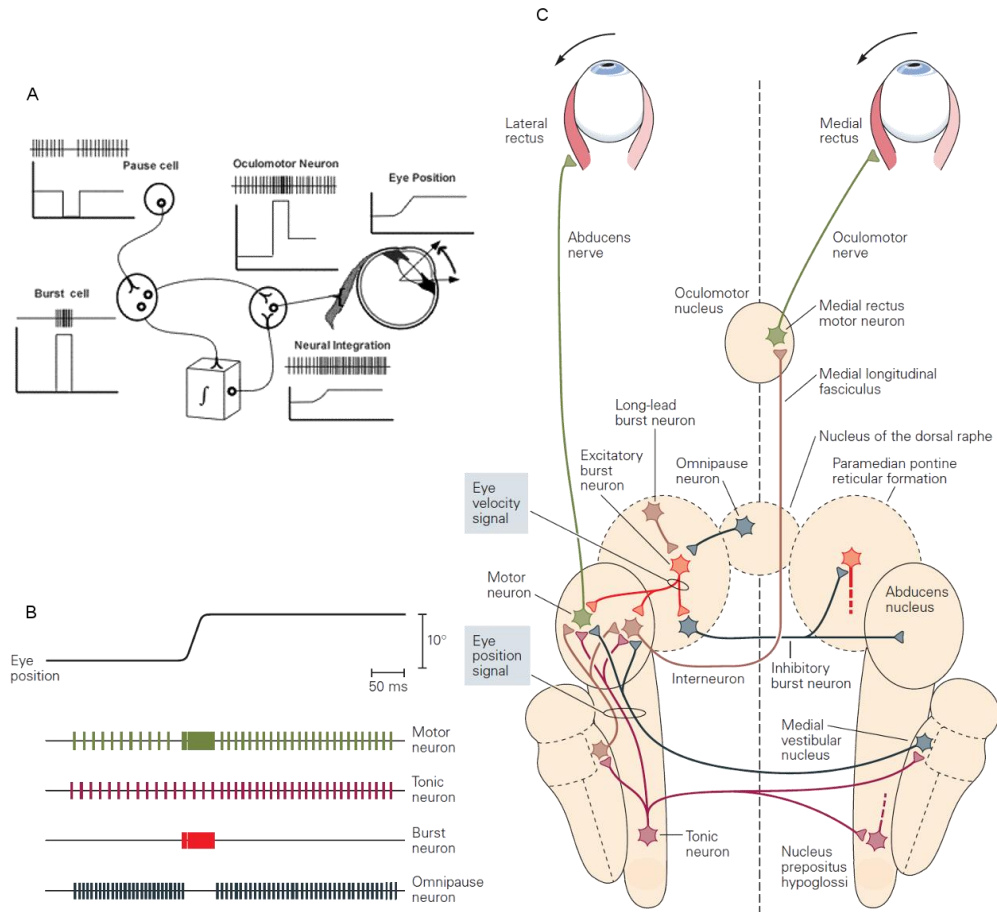


Figure 1.4: Pulse-step motor command generated in brainstem structures. **A.** The pulse of the motor command is generated by burst cells that project to ocular motor neurons, causing a phasic contraction of the extraocular muscles. This same pulse signal is sent to neural integrator cells, which generate a step of innervation causing a tonic contraction of the extraocular muscles. **B.** Different patterns of firing rate code the different information conveyed by specific family of neurons. The motor neuron provides both position and velocity signals. The excitatory burst neuron signals code the eye velocity, firing only during the saccade. In the neural integrator, the tonic neuron signals convey only eye position information integrating eye velocity. The omnipause neuron discharges, instead, avoid unwanted saccades inhibiting the burst neurons and stop firing only during saccades. **C.** The motor circuit for horizontal eye movements (Modified from [6], [58]).

Eventually, the omnipause cells are located in the pons, and project to contralateral pontine and mesencephalic burst neurons inhibiting their activity (GABA-ergic inhibition).

As a final remark, it is worth noting that the ocular motoneurons (with the extraocular muscles) represent a final common pathway for all eye movements. The combined position-velocity motor commands, indeed, are coded in the motoneurons firing rate irrespective of which ocular motor subsystems generate it (e.g. the vestibular, vergence, optokinetic smooth pursuit or saccadic systems).

1.3.2. Quantitative aspects of neural integration

Despite the eyeball position depends on firing rate of motoneurons (see Eq.(1.2)), the motor commands are assembled using several sensory or premotor inputs which encode velocity signals. Single-unit recordings of vestibular afferents and secondary vestibular neurons have shown that their the firing rate encodes and head velocity [59], while Purkinje cells of the flocculus encode the gaze velocity [60].

Such issue is solved by the VPNI that performs a mathematical integration of velocity input for all conjugate eye movements [7], supplying the position information for the common pathway.

As extensively explained in Section 1.3.1, the VPNI generates the step of innervation allowing to keep the eye at any desired eccentricity (Figure 1.5A). However, the neural integrator is not perfect, and since the firing rate of such network declines with time, the eye position decays with a time course that approximates a negative exponential [20] (Figure 1.5B). The VPNI is therefore called “leaky integrator”, that is an integrator that gradually leaks a small amount of input over time.

Mathematically speaking, such behavior is described through a first-order differential equation as follows:

$$dE/dt = -E(t)/\tau_c \quad (1.7)$$

where τ_c is the rate of leak, or the time constant of VPNI (in healthy human subjects typically between 20 and 70 seconds [7]).

The quantitative evaluation of the VPNI time constant is a measure of the behavior of its integration ability. As shown by Eq.(1.7) when the value of $\tau_c \rightarrow +\infty$ the neural network behaves as a perfect integrator, while the shorter is the time constant, the faster the eye position signal decays.

To estimate the time constant of the VPNI, several methods have been proposed in the literature [7], [50]. Among them, a useful approach is to plot the eye drift velocity versus the eye eccentricity, drawing the so-called PV-plot and fitting the PV relationship with nonlinear function (such as a tangent function as proposed in [50]). Alternatively, when only a few data are available, the fit of exponential decay on eye position data versus time or the initial slope method (Figure 1.5C) are possible solutions. The first two methods, the PV-plot and the exponential fit, have been used in this research to estimate the time constant in humans and zebrafish. Both

approaches are fully explained in the Method Sections of the last two chapters.

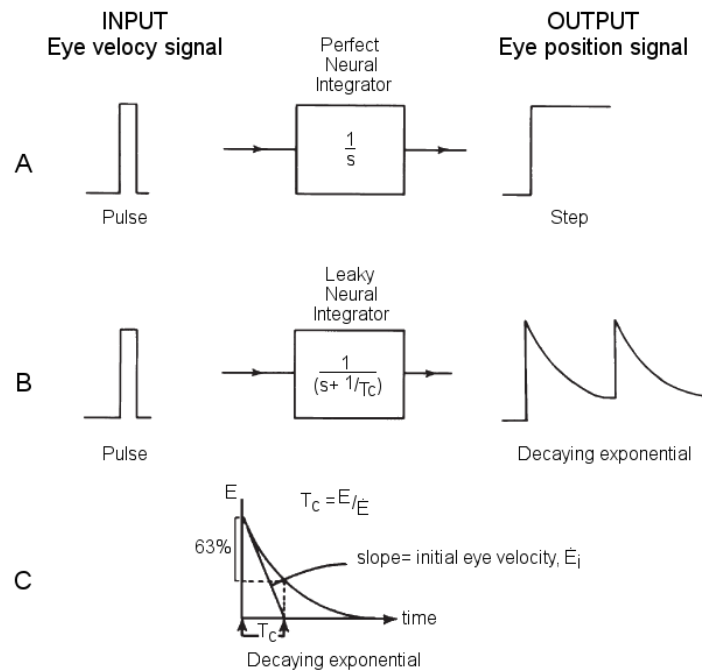


Figure 1.5: Quantitative aspects of neural integration. **A.** Impulsive response of a perfect neural integrator. The eye velocity input, a pulse, is perfectly integrated by the network, obtaining a step as output. Therefore, the eye is held stable in the new position for an infinite time. **B.** Impulsive response of leaky neural integrator. The leak of the system is described by the time constant T_c . Since the integration is not perfect the eye position decays toward the null position, until a corrective saccade brings the eye back. **C.** The time constant of exponential decay represents the time at which the value of response has decreased by 63.2% (i.e. the new eye position). The time constant can be approximated using the initial slope method, as the ratio of the eye displacement (from the null position) to the slope of straight line fitting the initial portion of exponential decay (Modified from [7]).

Experimental observation on cerebellar patients [22], [53], [55] and model organisms [26], [61] suggested that the integration of the described brainstem VPNI does not provide a sufficient stability of gaze, hypothesizing a boosting action of the cerebellum through a feedback circuit. In [22], *Zee et al.* proposed a simplified model supported by clinical observation, where the VPNI time constant is prolonged by the positive feedback loop of the cerebellum when the cerebellum gain K is appropriate (for further details see Section 1.3.4.2 and Figure 1.6).

Despite the cerebellum provides an excellent improvement of VPNI time constant (from 1-2 to 20-40 seconds)[22], [62], [63], in absence of adequate visual stimuli, when the visually mediated mechanism (e.g. visual

fixation, or smooth pursuit) are “switched off”, even healthy subjects show a centripetal drift from eccentric gaze positions [7].

Additionally, when the eye is displaced more than 20° , the centrifugal drift velocity increases nonlinearly with gaze eccentricity [50]. Consequently, a physiological centrifugal nystagmus (End-point nystagmus, EPN) may be observed to compensate high drift velocities at extreme gaze angles, with fast phases bringing the eyes back in the desired position [64]–[68].

The rate of centripetal drift could be also influenced by several factors which impair or alter the process of neural integration [53], [68]–[72]. The mental perception or sensory context of the subject, as well as its state of alertness or physical status (e.g. sleep deprivation, fatigue and loss of concentration) may decrease the VPNI time constant. A similar or enhanced effect is induced by drugs, chemical substances (e.g. alcohol) or pathological conditions affecting the cerebellar function (see Section 1.4 and Chapter 2).

1.3.3. Pulse-Slide-Step: a nonlinear approach

The actual dynamic mechanism of ocular plant is nonlinear and such nonlinearity is neglected in the first order model shown in Eq.(1.2). Such nonlinearity is due to the fibromuscular pulleys and functional compartmentalization of rectus muscles which are fundamental to simplify the planning of eye movement by the brainstem [73]. Robinson’s fourth-order model [45] helps us representing the nonlinear behavior of ocular motor plant, and it is described in Laplace notation as follows:

$$\frac{E(s)}{dR(s)} = \frac{sT_z + 1}{T_{e1}T_{e2}s^2 + (T_{e1} + T_{e2})s + 1} \quad (1.8)$$

where T_{e1} , T_{e2} represent the time constant of the ocular plant of the two elastic and viscous elements as shown in Eq.(1.6), while $T_z = 92\text{ms}$ is the time constant of the zero, needed to model the post-saccadic drift.

Nevertheless, the pulse-step model used to explain the encoding of motor signal, does not take into account other nonlinearities enhanced during the saccades or in far eccentric gaze angles (due to the nonlinear features of VPNI, such as the drift velocity-position relationship). The pulse-step model, indeed, well describes the steady-state properties of ocular motor behavior but not the dynamic ones in high frequency domain. As hypothesized by *Optican et al.* [48], the motor program may be generated by three components, called “pulse-slide-step”, which are likely derived from the velocity command along the final oculomotor pathway, in order to take all linear and non-linear factors of the ocular motor plant into account.

The overall transfer function (the ratio of the output to the input, i.e. the velocity command and the discharge rate of motor neurons, respectively) of

the “pulse-slide-step” network is defined in the Laplace notation as follows:

$$\frac{dR(s)}{V(s)} = A + \frac{B}{s} + \frac{C}{T_s s + 1} = \frac{BT_s s^2 + (AT_s + B + C)s + A}{s(sT_s + 1)} \quad (1.9)$$

where the three terms represent the pulse, step, and slide components of motor control signal with their DC gains (i.e. A, B and C, respectively).

The overall transfer function of the final common path is therefore obtained multiplying Eq.(1.8) and Eq. (1.9). If the parameters of the neural network in Eq.(1.8) are correctly tuned, the dynamics of the ocular motor plant can be almost completely compensated by the brainstem network. Specifically, the slide has to match the zero time constant of the plant (i.e. $T_s = T_z$), while the pulse, step, and slide gains must be $A=1$, $B= T_{e1}T_{e2}/T_s$ and $C = T_{e1} + T_s - T_{e1}T_{e2}/T_s$.

Optican et al. also provided an experimental proof of the existence of the slide component of innervation [48]. They proved that the data recorded when adaptive mechanisms are at stake was explainable only by using the pulse-slide-step model, and the parameters of Eq.(1.9) can be tuned by modifying the visual condition (e.g. drifting the visual scene). Their finding implies when pulse-slide-step components match the ocular motor plant dynamics, the eye is perfectly stable after a saccade, conversely, a post-saccadic drift appears when parameters are mistuned.

As a final remark, the step component could be also modeled using the leaky integrator (shown in Figure 1.5B), describing the longer time constant of VPNI (20-40 seconds considering the reinforcement of cerebellum).

1.3.4. Neural Substrates for gaze-holding

As pointed out in previous section, the gaze-holding mechanism relies on two components, the VPNI, a distributed neural network in the brainstem, and the flocculus, an anatomo-functional structure of the cerebellum.

The VPNI and the cerebellum perform the neural integration for all eye movements providing a reliable motor command to allow the gaze stability.

The integration of horizontal and vertical conjugate eye movements is performed by different groups of neurons in the brainstem. Specifically, the nucleus prepositus hypoglossi (NPH) and the medial vestibular nucleus (MVN) are involved in integration of horizontal eye movements, whereas the interstitial nucleus of Cajal in vertical ones.

Conversely, the cerebellum contributes in neural integration irrespective of movement direction, as the flocculus forms several connections with the neurons of the paramedian tract (PMT) in brainstem.

1.3.4.1. The brainstem contribution to horizontal eye movements

The NPH and MVN are located in the caudal pons and specifically in the medulla oblongata, performing the neural integration of horizontal conjugate eye movements [6], [7], [74]. As mentioned in Section 1.3.1, to accomplish such task, the parocellular portion of MVN and the NPH neurons encode a combination of position-velocity signals, similarly to the extraocular motoneurons. The caudal portion of NPH located in paramedian tract (PMT) projects to the contralateral NPH and the flocculus, allowing synchronized, conjugate eye movements [74], and linking the cerebellum in the neural integration [52], [56].

As shown in Figure 1.4C, both NPH and MVN receive velocity signals from excitatory burst neurons and from the other structures (e.g. vestibular nuclei) involved in velocity encoding of motor signal for motoneurons [7], [74].

Several mechanisms likely contribute to the VPNI integration, from the intrinsic property of neuron membrane, to the positive feedback between the cerebellar circuit and cerebellar cortex [20], [22], [52], [75]. Among them, *Miri et al.* suggested that NPH comprises a local network with temporal-spatial proprieties which integrates velocity signals. In such network, the neurons encode gradually signals related to eye position, to those related to eye velocity creating a rostral-caudal gradient (i.e. from rostral to caudal portion of NPH) [76].

Useful information about the MVN and NPH contribution to the neural integration has been provided by pharmacology studies or chemical lesions, inactivating or inhibiting selected neural components or portions [7].

Notable example is unilateral injection of an excitotoxin in MVN-NPH region [20], that produce an acute, partial failure of both ipsilateral and contralateral gaze-holding, and a shift of the null or neutral point (the eye position where eye velocity is zero) towards the side of the lesion. In the same study [20], *Canon and Robison'* further confirmed that the MVN-NPH region integrates every conjugate horizontal eye movement, as vestibular, optokinetic and smooth pursuit were also affected by excitotoxin injection.

1.3.4.2. The contribution of cerebellum

The vestibulo-cerebellum (or archicerebellum) is the oldest part in evolutionary terms of the cerebellum, and plays a pivotal role in control of eye movements, balance and motor learning [6]. As extensively described in the next Chapter, the vestibulo-cerebellum comprises two main anatomic-functional substructures, the tonsil (i.e., flocculus and paraflocculus) and the caudal portion of cerebellar vermis (i.e. nodulus and uvula).

Experimental evidences [26], [61], [77] and clinical cases of cerebellar patients [22], [53], [55], [62] suggest that the cerebellum improves the performance of the brainstem inherently leaky neural integrator.

Specifically, the flocculus and paraflocculus are involved in such process, as their lesion makes the neural integrator deficient [77], [78]. The onset of post-saccadic drift is a characteristic abnormality in eye movements that follow flocculus-paraflocculus lesion, due to pulse-step mismatch (i.e. the step is relative smaller than pulse) [56]. Moreover, an increased gaze instability and the onset gaze-evoked nystagmus (GEN, see Section 1.4) are related to damages in such cerebellar areas, arising from a decrease of the time constant of the neural integrator (from 20-40 to 1.5 seconds)[7].

Cerebellar integration is achieved through the Purkinje cells within the flocculus and paraflocculus. Purkinje cells encode signals related to the position of the eye in the orbit during fixation, to eye movements during smooth pursuit or vestibular responses, and also to gaze velocity (i.e. the velocity of eye in space)[56], [60], [79]. Such neurons are linked reciprocally with cells in the PMT and NPH-MVN regions which in turn encode combined position-velocity signals [52], [74], [79], creating an anatomical pathway between the cerebellum and brainstem. Furthermore, new insights of reciprocal innervation of Purkinje cells suggest that neural integration may be also realized directly onto the cerebellar cortex [7].

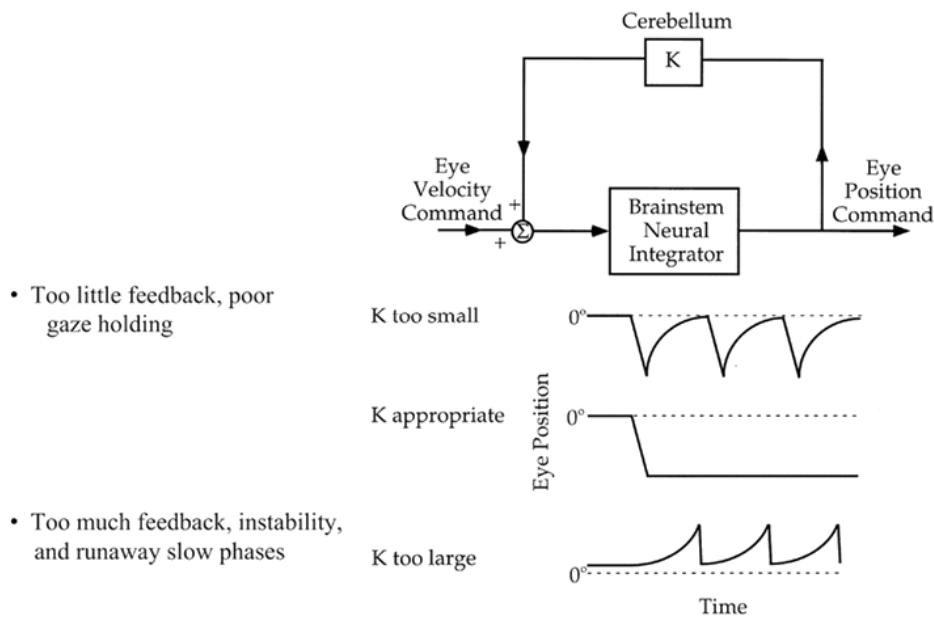


Figure 1.6: Model for cerebellar effect on neural integrator function. A positive feedback loop improves the time constant of an inherently leaky brainstem neural integrator. The effect of positive loop varies with the value of K. Only if the feedback is adequate, a perfect steady tonic eye position command is sent to motoneurons. Conversely, gaze-holding mechanism is impaired or gaze is unstable if feedback action is deficient or excessive (Taken from [56]).

Zee et al. proposed a simplified but useful model to describe the cerebellar-brainstem pathway [22]. Such model summarizes cerebellar function in a positive feedback loop, where neural integration could be performed through neurons which excite themselves perseverating their own activity. This idea is based on the reciprocal connection between the brainstem and cerebellum, ideally creating a feedback loop.

Thus, the short time constant of brainstem VPNI (1-2 seconds) [22], [62], [63] is prolonged by the action of the cerebellum, represented by the feedback factor K (or gain, Figure 1.6). Different behaviors of the gaze-holding mechanism can be modeled by tuning the feedback factor: 1) When K is appropriate, the cerebellum integration is nearly perfect, and gaze is held stably on the new planned position. 2) If the K increases, the neural reinforcement is too strong and the integrator becomes unstable, as commonly happens in positive feedback process. Such instability causes an exponential increase of eye velocity, producing a centrifugal drift. 3) If the K falls, the neural reinforcement is not enough to preserve the neurons' firing rate, and the integrator becomes leaky. The eyes drift back to the neutral position, as the innervation level of motoneurons does not overcome the elastic recovery force of muscles.

Despite such model does not take into account the information encoded by the neurons in the cerebellar-brainstem circuits, it well describes the physiological and pathological conditions of the gaze-holding mechanism. Specifically, the two waveforms of the model shown in Figure 1.6 (when K is too small or large) match the ones observed in the eye movements of cerebellar patients.

The horizontal downbeat or upbeat nystagmus are two examples of centrifugal nystagmus, which are observed in patients with combined floccular-parafloccular lesions, tumor, multiple sclerosis or Wernicke's encephalopathy [7], [80], [81]. The horizontal GEN, instead, is a centripetal nystagmus commonly observed in degenerative cerebellar ataxia [53], or after alcohol intoxication [71].

The proposed model simplifies the actual behavior of the cerebellum-brainstem circuit, but some properties cannot be explained through a positive feedback loop only. For instance, the acquired pendular nystagmus (Figure 1.7A.c) is caused by an instable integration of eye moments due to multiple sclerosis [82]. The description of this phenomenon is not provided by the model in Figure 1.6. Moreover, the key role of the cerebellum in adaptive and learning processes is neglected. The neural integrator, indeed, can be tuned by new visual-vestibular demands inducing changes in gaze stability [83]–[85].

Some observations can be moved also to the structure of the model. When a process is modeled using a positive feedback loop, in control theory, the system tends to be unstable and barely controllable. However, the gaze-holding is a quite stable mechanism, and a robust neural integration is provided even after cerebellar lesions [7]. Thus, several models have been proposed to explain how an anatomically distributed neural network performs neural integration in a neurobiological fashion [86]–[89].

1.4. Abnormalities of neural integrator: Gaze Evoked Nystagmus

As previously noted, all neural commands generating eye movements are processed by a brainstem neural network producing adequate sustained positional signals. Several diseases affecting the brainstem or cerebellum cause ocular motor disturbances related to gaze stability, and are often accompanied with symptoms of blurred vision, double vision, tendency to fall, or gait disturbances [90].

Even healthy subjects do not have a “perfect” neural integrator [20]. Despite the cerebellum sufficiently compensates for inherently poor action of VPNI [26], a physiological centripetal eye drift is manifest in darkness (i.e. decay of tonic neurons’ firing rate) [50]. Furthermore, some normal subjects show a physiological gaze-evoked nystagmus, also known as end-point nystagmus (EPN), in darkness. Despite that, experimental observations have shown that some healthy subjects exhibit deficient gaze-holding (i.e. slight eye drift) even while fixating a visual target [66], [67].

Commonly, the EPN and in wider terms gaze-holding deficit occur when the gaze is brought in far lateral or up eccentric angles (e.g. $>30^\circ$). Despite that, the occurrence of EPN is quite variable and some healthy subjects showing no EPN, regardless of eccentricity, have been reported [64], [66], [67] while others presented with nystagmus already at small gaze eccentricities [50], [64], [68]. These contrasting findings have been explained by the influence of the physical status of the subjects [69], [71], [91].

However, the existence of EPN suggests that the performance of gaze-holding system degrades at larger eccentricities. As confirmed in [50], the relationship between gaze eccentricities and drift velocity remains linear only in small range of gaze ($\pm 15^\circ$), while increased drift velocity, and in turn the EPN, could be observed in more eccentric angles, suggesting that the VPNI-cerebellum networks may be optimized only for the most common range of gaze angles used in everyday life. Such optimization may be due to the motor-strategies implemented by the brain when an object of interest is placed in far eccentric angles in a head reference system ($>20^\circ$). In these cases, combinations of head and eye movements may be preferred over only saccadic ones to maintain the eyes at less eccentric angles.

The pathological form of gaze-evoked nystagmus, or just only GEN, is caused by a broad range of neural disorders or pharmacological reasons [7]. The EPN and GEN share the same characteristic waveform of eye movements: a centripetal drift (slow-phase) followed by corrective quick phase (Figure 1.7A). The slow-phase drift may be exponential or linear (Figure 1.7A.a, b), as it is related to nonlinear features of the neural integrator [50], [53]. Close to the null position of the eye (the central position of gaze), eye drift is more linear due to constant eye drift velocity, while the eye position decays exponentially for more eccentric angles [50].

Despite such analogies, several clinical features of EPN allow to distinguish it from its pathological form. Typically, the EPN is poorly sustained (less than 20 seconds) and its amplitude and frequency are lower than the GEN ones [92]. Moreover, eye drift velocity in GEN is higher than in EPN and the angle of insurgence of nystagmus is significantly decreased [50], [53]. Asymmetric nystagmus is often observed in pathological conditions, conversely to EPN.

A sustained form of nystagmus, called “fatigue nystagmus” [64], [66], may also appear in healthy subjects, but it is easily discernible from the pathological GEN, as it is caused by a prolonged (60-120 seconds) fixation in extreme eccentric angles.

On lateral gaze in healthy subjects, the nystagmus is primarily horizontal, and vertical component is absent or very rare, while strong downbeat component is a common sign of dysfunction in central connections [7].

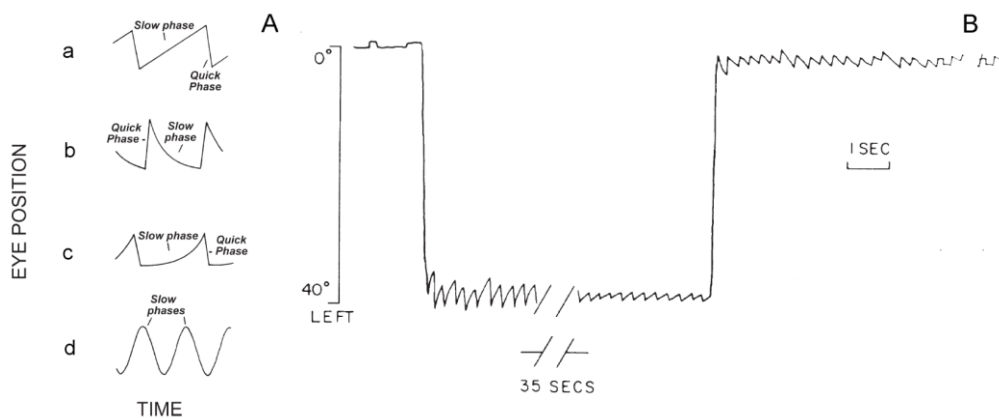


Figure 1.7: Waveforms of nystagmus. **A.** Four common slow-phase waveforms related to different neural abnormalities. **a.** Constant velocity of drift, causing a linear decay. Such nystagmus is commonly observed in peripheral or central vestibular diseases. **b.** Centripetal nystagmus toward the null position of the eye, showing a negative exponential time course. Typical waveform of gaze-evoked nystagmus, is related to impaired neural integrator. **c.** Centrifugal nystagmus away from the null position of the eye, showing a positive exponential time course (i.e. increasing velocity). This nystagmus is usually caused by an unstable neural integrator. **d.** Pendular nystagmus, which may be congenital or acquired. **B.** Nystagmus caused by familiar cerebellar degeneration. On far left, the patients showed a strong gaze-evoked nystagmus. The drift velocity declined, and after 35 seconds the nystagmus amplitude is clearly reduced. Such process may be induced by adaptive mechanism to reduce excessive eye drift. When the eyes returned to the central position, the patient showed a reversed nystagmus (i.e. toward the previous direction) called rebound nystagmus. (Modified from [7], [93]).

In general, GEN is easily identified by means of clinical inspection, accompanied with other ocular motor abnormalities (e.g. smooth pursuit and VOR [92], [94]). GEN is indeed caused by neural disorders and/or

lesion of brainstem-cerebellar networks, which are involved in control of other functions (e.g. motor control, short memory, ocular motor control and motor learning) [7].

Specifically, regarding the pathogenies, GEN is mainly caused by cerebellar disorders that involve the vestibulo-cerebellum structures, and especially when midline/paramedian vermal and caudal structures are affected [55], GEN is elicited, irrespective of directions.

Omnidirectional GEN is also shown in patients affected by neurodegenerative disease, as well as side effects of benzodiazepines or alcohol [7], [92]. Moreover, different patterns of GEN were observed in patients with neurodegenerative cerebellar disease, possibly related to their age at disease onset [53].

Pure horizontal or vertical GEN can instead indicate lesions in the area of the brainstem involved respectively for horizontal (NPH and VN) or vertical (interstitial nucleus of Cajal) gaze-holding function [90], [92]. Eventually, GEN is also a common clinical sign shown in patients with hereditary cerebellar ataxias [95].

Rebound nystagmus (RN) is another feature related to GEN shown in patients with cerebellar syndromes (Figure 1.7B)[96], although, in weaker form, it has been sometimes found in healthy subjects [67], [97]. The RN is likely induced by brainstem or cerebellar mechanisms to correct centripetal drift of GEN. RN manifests when redirecting fixation to gaze straight ahead after sustained eccentric gaze and it is caused by a transient ocular drift in the direction of the preceding gaze eccentricity [7], [13] (Figure 1.7B).

Its existence is hypothesized to be due to a mechanism which reduces the excessive drift velocity during a sustained fixation at the cost of modifying the relationship between ocular drift velocity and gaze direction at all angles. In patients with cerebellar disease, these adaptive mechanisms may become overactive, leading to a residual drift upon returning to gaze straight ahead, which is strong enough to cause rebound nystagmus [98], [99]. *Zee et al.* suggested that RN could be caused by the optokinetic system [93] while trying to explain why RN could be also elicited in some healthy subjects. Despite that, up to now, RN was never extensively studied and the few reported findings are contradictory.

1.5. Eye movements in Zebrafish

1.5.1. Zebrafish as a model organism

Several model organisms have been extensively used for the study of biology and neurophysiology. Since there is a surprising degree of evolutionary conservation of basic cellular processes among all organisms, both invertebrates and vertebrates have contributed to our understanding of human physiology. Despite the use of invertebrates as model organisms

(such as *C. elegans* or *Drosophila melanogaster*) is growing, vertebrate organisms share striking similarities with humans at many levels spanning from genomic homology to anatomy and physiology, that invertebrates cannot supply.

However, ethical questions are limiting the use of primates in medical research, thus, *Danio rerio*, better known as Zebrafish, is becoming a common and useful scientific model organism mainly used for studying development processes, gene functions, neurophysiology of shared neural structures and behaviors in vertebrates [100].

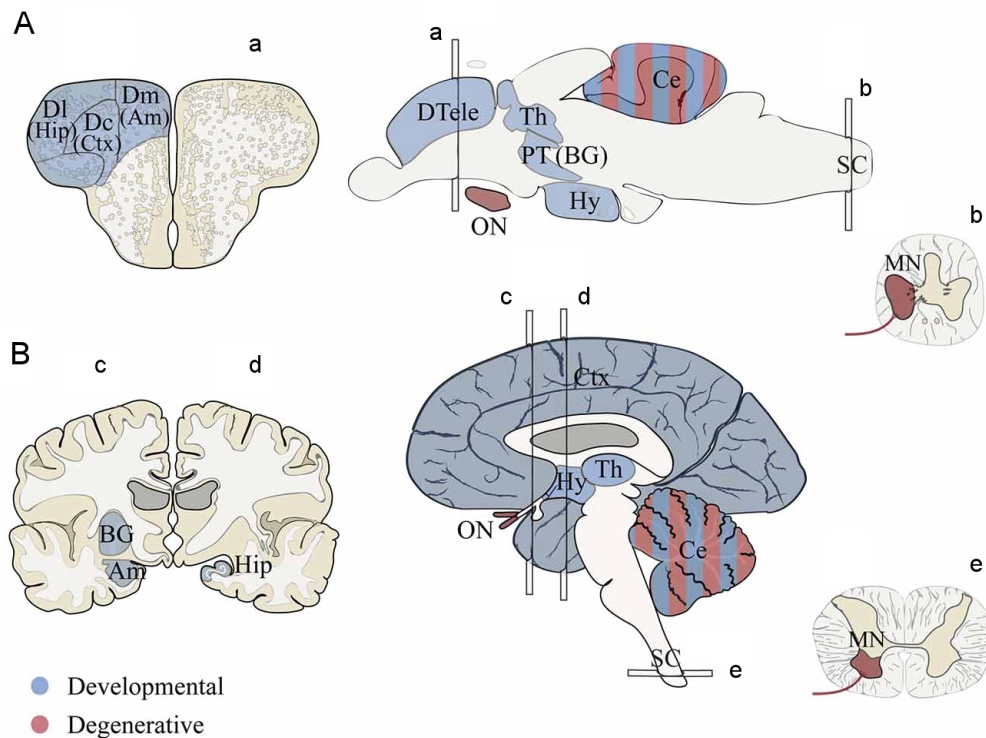


Figure 1.8: Structural homologies between zebrafish and human brain.

A. Adult zebrafish brain and sections for telencephalon, brain (a) and spinal cord (b). **B.** Adult human brain and sections for telencephalon (anterior forebrain, showing basal ganglia, hippocampus and amygdala), brain (c, d) and spinal cord (e). Regions in blue and red represent homologous structures between human and zebrafish associated with developmental disorders and axon degenerative diseases, respectively. The former includes cortical and subcortical regions in vertebrate animals which may be involved in cognition and emotional behavior. The latter, instead, includes portions of the motor circuit and optic nerve. (Am, amygdala; BG, basal ganglia; Ce, cerebellum; Ctx, cortex; Dc, dorsal central pallium; Dl, dorsal lateral pallium; Dm, dorsal medial pallium; DTele, dorsal telencephalon; Hip, hippocampus; Hy, hypothalamus; MN, motor neuron; PT, posterior tuberculum; Th, thalamus; ON, optic nerve) (Modified from [101]).

Zebrafish is a freshwater fish from South and East Asia and, since it belongs to vertebrate subphylum, it shares a common progenitor with human beings. Zebrafish genome has been fully sequenced, and a strict relationship has been found between its genome and the human one. Specifically, about 70% of human protein-coding genes is related to genes in zebrafish and 84% of the genes involved in human disease could be identified in this model organism [102]. Thus, exploiting such analogies, zebrafish has been extensively used to shed light on cancer growth [103], such as melanoma, kidney cancer, liver tumors, malignant peripheral nerve sheath tumors, and the development process of muscles and organs (e.g. eyes) [100], [104].

The reason for zebrafish popularity is not only due to genic affinity, but also to its breeding and maintaining process that are easier, cheaper and faster than with others vertebrates.

A pair of adult zebrafish specimen is indeed capable of producing up to 4200 fertilized eggs per week, and only a small space is required to maintain a large number of zebrafish [100]. Moreover, fertilized eggs almost immediately become transparent, thus during all the stages of zebrafish development, a visual inspection of morphogenetic movements or organogenesis is possible just by using a microscope [100], [105].

Developmental time of zebrafish is one of the shortest among vertebrates. After 24 hours post fertilization (hpf) almost all principal organs are formed, concurrently embryos show spontaneous muscle contractions driven by nervous system activity [106]. Once the zebrafish larvae hatch (48-72 hpf), they immediately exhibit robust swimming [107].

From 5 days post-fertilization (dpf), instead, larvae start to hunt and capture live preys [108]. Since hunting behavior appears to be primarily guided by vision, the visual system develops precociously and the retina becomes mature enough to support visually mediated responses already after 68 hpf [109]. The optokinetic response (OKR), a visual reflexive response, is completely developed after 73dpf, and 24 hours later (4 dpf) the OKR gain is comparable to adult performance [110]. Besides visually guided responses, the vestibulo-ocular reflex develops after 81 hpf despite VOR gain is not still measurable in larvae. Even spontaneous saccades have comparable velocity to those in adult fish just after 96 hpf [110], [111].

Due to analogies between VOR and OKR in humans, zebrafish is indeed useful in ophthalmological research already at the larval stage [30], despite significant differences in eye anatomy such as lateral eyes and lack of fovea. Several human ocular diseases have been modeled in zebrafish mutant strain, such as cataract, glaucoma, diabetes retinopathy and age-related macular degeneration [112], [113]. Moreover, abnormal ocular motor behavior in zebrafish mutants allows to shed light on neuroanatomical pathology providing new insights on ocular motor diseases in humans. The zebrafish mutant *belladonna* is a relevant example of congenital nystagmus and infantile nystagmus model [31], [114]–[116]. *Belladonna* homozygous mutants were indeed found to display a reversed

OKR of misrouting effect at the optic chiasm (i.e. alteration of the optic nerve projection to the optic tectum). Such abnormalities and the wide range of spontaneous eye oscillation patterns match the diagnostic waveforms of infantile nystagmus syndrome, helping researchers to identify the underlying mechanism of such a rare ocular motor pathology.

1.5.2. Neural architecture analogies with humans

In the CNS, the anatomical regions of forebrain, midbrain, hindbrain and spinal cord are generally conserved in vertebrates [100]. As visible in Figure 1.8, several neural structures of the human brain are preserved in zebrafish [101]. Such similarities are not only anatomical. Several neurophysiological observations revealed a comparable regional connectivity of several sub-structures (such as cerebellum, optic tectum and medulla oblongata), implying a strict relationship between zebrafish and human neural functionality [117], [118].

As previously mentioned, due to the thorough understanding of the final motor pathways and behavior, eye movements provide an excellent model system for studying the neural structures involved in motor control, such as cerebellum. Thus, exploiting the neural analogies between zebrafish and human beings, such model organism is extensively used to investigate how neural networks work, and how complex functionalities are implemented in the brain [119].

The success of zebrafish in ocular motor research is mainly due to the amazing analogies of its neural structures with human ones, which are principally involved in eye movements control [100].

Specifically, in zebrafish CNS a primitive form of mammals' visual cortex is located in midbrain: the optic tectum. In simpler vertebrates such as fish, birds and reptiles, the optic tectum acts indeed as a visual cortex, and consequently it executes the first processing of visual information receiving direct projections from retinal cells [120]. Analogies with humans are not limited to optic tectum, but also in neural connectivity of such structure. Direct and indirect projections between the zebrafish optic tectum, mesencephalon and rhombencephalon, form a neural circuitry comparable to the human visuo-cerebellar circuit [101].

Even a structure similar to the human brainstem is present in the zebrafish CNS. Like for other vertebrate organisms, zebrafish CN nuclei (such as IV CN abducens nerve which is involved in horizontal eye movements) and the primary motor and sensory centers are indeed located into the zebrafish rhombencephalon or hindbrain [100].

Physio-anatomical similarities are found between teleost and human cerebellum, as the local circuit of cerebellum formed by granule cells parallel fibers and Purkinje cells is preserved [121]. Moreover, even functional homology of the zebrafish cerebellum during visual-motor

behaviors has been confirmed in behavioral studies using calcium imaging or loose patch recordings from cerebellar Purkinje neurons [101], [122]

The neural structures involved in gaze stability in humans are preserved in zebrafish. A neural integration is indeed needed for every kind of eye movement (see Section 1.3.2). The location and neural components of the integrator were firstly identified in mammals (cats and monkeys) [20], [26], [52] and subsequently in goldfish and zebrafish [119], [123], [124].

Despite several hypotheses and models have been proposed [86]–[88], [125], single-unit recordings on mammals cannot allow to accurately identify the circuit connectivity and cell physiology. Only recent studies on fish have helped us understanding how the brain actually implements mathematical integration [119].

New insight on neural integration was proposed in [126], where the authors used in vivo intracellular recordings from the ocular motor neural integrator in fish. Specifically, *Aksay et al.* suggested that at least part of neural integration is due to synaptic feedback among neurons of brainstem, while other studies revealed a functional relationship between bilateral integrator circuits in medulla [75], [127].

Calcium imaging in zebrafish, instead, allowed to improve our knowledge about the circuit architecture for neural integration [76]. *Miri et al.* suggested that neurons in brainstem encode signals related both to eye position and eye velocity, showing a strict relationship between temporal response of individual neurons and their spatial location.

Chapter 2

Disorder of cerebellar ocular motor control

The cerebellum is located caudally to occipital and temporal lobes within the cranial fossa, and is connected to the dorsal region of the brainstem. Anatomically, the cerebellum is formed of three lobes (Figure 2.1): the anterior and posterior lobes, which together form the body of the cerebellum, and the smaller flocculonodular lobe. A different subdivision is commonly used to identify the three functional areas of cerebellum: the vestibulocerebellum, spinocerebellum, and cerebrocerebellum. Each cerebellar area has a distinctive role in different functions concerning motor control and learning, cognitive function, coordination, posture and equilibrium. The vestibulocerebellum and vermis are the main neural structure involved in eye movements control, and their action is a prerequisite for optimal ocular motor performance.

This chapter will be focused on cerebellar control of eye movements. Specifically, a review about clinical and experimental findings concerning cerebellar disorders will be introduced. The knowledge about abnormalities of eye movements caused by cerebellar disorders has indeed been extensively used to investigate cerebellar functionality.

After that, the focus will be moved to the effect of alcohol on the cerebellum. Starting with a biochemical survey on ethanol interaction with cerebellum cells, the cerebellar effects induced by acute and chronic intoxication will be described.

2.1. A survey of cerebellar disorders implication on eye movements control

Following the classification proposed in [7], [56], cerebellar syndromes are classified in three principal categories which are related to the

anatomical localization of cerebellar lesion causing specific ocular motor abnormalities. In simplified terms, it is possible to classify the effects of cerebellar syndromes as follows: flocculus and paraflocculus syndromes, that provoke alterations in dynamic vestibular responses, sustained pursuit and gaze-holding; nodule and ventral uvula damages, that cause abnormality in sustained vestibular responses; and syndromes of dorsal ocular motor vermis and fastigial ocular motor region, concerning abnormalities on saccades and pursuit initiation.

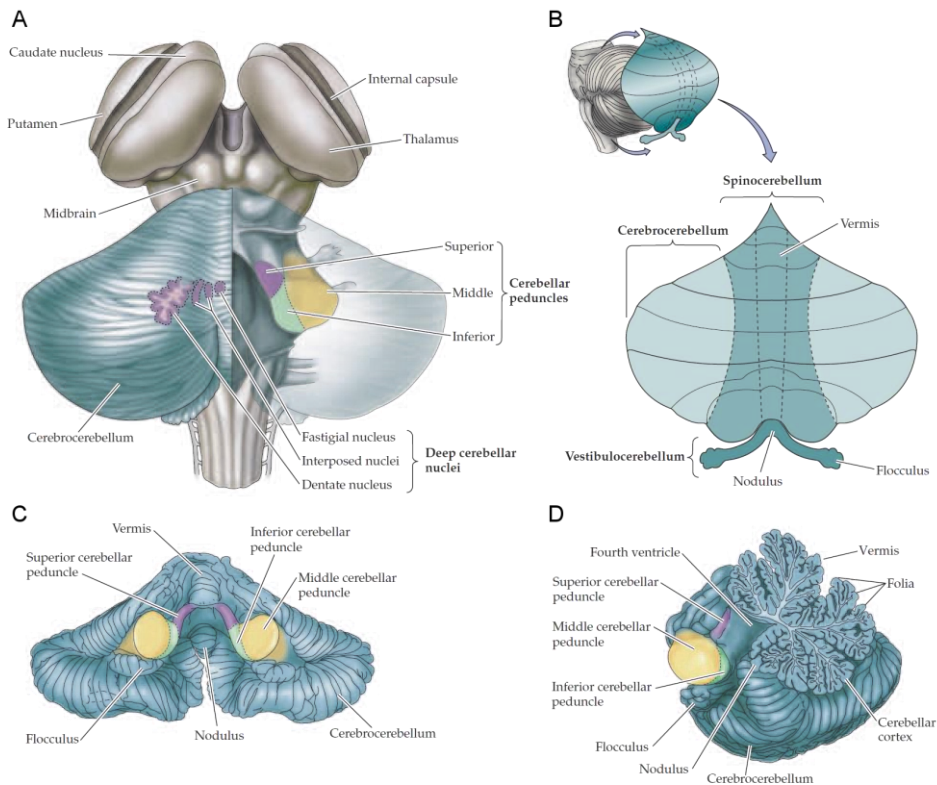


Figure 2.1: Organization and subdivision of the cerebellum. **A.** Dorsal view and anatomical localization of cerebellum. **B.** Unfolded view of cerebellum. Cerebellum is divisible in three functional areas involved in controlling different movements. The vestibulocerebellum is the phylogenetically oldest region of the cerebellum, first appearing in fish. It receives and projects to the brainstem, and controls eye movements and balance. The spinocerebellum receives somatosensory and proprioceptive inputs from the spinal cord and is involved in coordination of voluntary movements. It also comprises the vermis, which governs posture and locomotion and participates in eye movements control. The cerebocerebellum mainly involves connections with the cerebral cortex and participates most extensively in planning and executing voluntary movements. **C.** Cerebellar peduncles on the anterior aspect of the inferior surface. **D.** Paramedian sagittal section through the left cerebellar hemisphere showing the cerebellar cortex (Adapted from [128]).

2.1.1. Ocular motor deficits of flocculus and paraflocculus lesions

Flocculus and paraflocculus ocular motor regions are localized in vestibulocerebellum (Figure 2.1), and their neurons form reciprocal connections with NPH and MVN in the brainstem, coding a combination of eye position and velocity [6].

As extensively described in Chapter 1, the flocculus and paraflocculus are directly involved in neural integration [77], [78]. GEN, RN and downbeat nystagmus are indeed some of the most evident clinical signs of damages in such areas, as a result of deficient neural integration (see Paragraph 1.3.4.2 for further information about deficient neural integration and Section 1.4 for a detailed description of GEN, RN) [22], [92].

Onset of post-saccadic drift is another clinical sign due to flocculus-paraflocculus lesion. Such abnormality is caused by a mismatch of pulse-step component of motor signal as the amplitude of tonic component (i.e. the step) is abnormal [56]. In physiological condition, instead, eye abruptly stops after a saccadic movement, consequently post-saccadic drift is not easily identifiable.

Ocular abnormalities concern also smooth pursuit impairment, during head fixed tracking of a moving target [78]. Despite wide damages of the flocculus and paraflocculus cause a decrease in gain of pursuit during sustained tracking, pursuit function recovers significantly [56]. Such recovery ability is likely due to redundancy of the cerebellum, as both dorsal and caudal areas of the vermis are also involved in smooth pursuit [129], [130].

Clinical observations of unilateral cerebellar infarcts located in flocculus or tonsil (i.e. paraflocculus) showed, respectively, abnormality in head impulse response (VOR suppression deficit) and ipsilateral deficit of the smooth pursuit and gaze-holding system [131], [132]. Such observations suggest that the flocculus is more involved in vestibular processing, while tonsil control concerns more smooth pursuit and gaze-holding function.

2.1.2. Ocular motor deficits of nodule and uvula lesions

The cerebellar vermis is divided by short and deep fissures forming nine lobules. Among them, the nodule and uvula are localized in the inferior part of the vermis (Figure 2.1) [133].

Like the flocculus and paraflocculus, even the nodule and ventral uvula are involved in neural integration, yet their function is completely different from the floccular one [7]. Specifically, the nodule and uvula play a pivotal role in visual-vestibular integration implementing a central process called “velocity storage mechanism” (VSM) [134]–[136].

Thus, damages in such areas lead to the alteration of VSM provoking abnormality in VOR and OKR, such as increased duration of vestibular

responses, inability to habituate the time constant of nystagmus on repeated stimuli and impairment of the normal ability to suppress post rotatory-nystagmus or optokinetic after-nystagmus [135]. Moreover, experimental observations during “cross-coupling” stimulation showed that altered VSM caused erroneous orientation of the eye velocity component of the angular VOR to the gravito-inertial acceleration [134].

Nodule and uvula lesions also elicit downbeat and horizontal nystagmus [56], [137]. Despite flocculus and paraflocculus syndromes share such clinical signs, nodule and uvula lesions have distinctive features. Specifically, downbeat nystagmus can be suppressed with visual fixation and its amplitude is irrespective of gaze position [56], while horizontal nystagmus seems to be characterized by increasing slow-phase velocity and direction changes [137].

2.1.3. Ocular motor deficits of dorsal vermis and fastigial nuclei

The deep cerebellar nuclei are masses of grey matter embedded in cerebellar white matter. The fastigial nucleus is one of such nuclei located nearest to the midline at the anterior end of the superior vermis (Figure 2.1) [133]. Some aspects of the smooth pursuit and saccadic systems are directly controlled by the V, VI and VII lobes of the vermis (i.e. the dorsal region of vermis) and by the fastigial nuclei.

Clinical observation of patients with cerebellar infarction suggests that dorsal vermis contributes in saccades generation [138]. Saccadic dysmetria is indeed a typical sign of dorsal lesion [139]. Specifically, localized lesion of the dorsal vermis alone causes hypometric saccades only, while wide damage involving fastigial nuclei provokes hypermetric saccades [140]. Changes in velocity, acceleration, direction and accuracy of saccades are also other features that may be identified in patients with cerebellar damages to the dorsal vermis [56].

Conversely to flocculus and paraflocculus lesions that affect sustained pursuit, both dorsal vermis and fastigial nuclei damages affect the “open-loop” portion of pursuit [141] (i.e. initialization part of pursuit with highest retinal slip). Specifically, alteration of eye acceleration occurs in the first 100ms of tracking after changes in target velocity.

Dorsal vermis activity is fundamental in saccadic and pursuit adaptation, as confirmed by its temporary inactivation with GABA agonist and antagonist injection or its permanent ablation [139], [141]–[143]. Inactivation of fastigial nuclei, instead, does not affect adaptation and alters the reliability of adapted premotor commands for saccades, suggesting that adaptation takes place mainly in the dorsal ocular motor vermis [144].

2.2. Effect of alcohol intoxication on cerebellar functions

Nowadays, ethanol is commonly consumed during leisure activities. However, its effect is comparable to any psychotropic drug, as it affects the central nervous system. Despite ethanol has a diffuse action on CNS, cerebellar function seems to be strongly impaired by alcohol intoxication. Thus, both acute and chronic intoxication induce a wide range of clinical signs concerning ocular motor abnormalities and impaired motor control.

Following a bottom-up approach, this section will clarify the ethanol mechanism of action from cellular to cerebellar level, focusing on alcohol-induced ocular motor abnormalities. Moreover, cerebellar damages induced by chronic alcohol consumption will be introduced in the last paragraph.

2.2.1. Molecular and cellular action of acute ethanol intoxication

The blood–brain barrier (BBB) is a highly selective permeability barrier that separates the circulating blood from the CNS. All nutrients such as water, sugar, vitamins and gases are allowed to pass through, while the brain is protected from potential neurotoxins. The BBB is indeed impermeable to more than 98% of large and small molecules of neurotherapeutic drugs [145].

However, almost all psychoactive drugs, using a simple diffusion mechanism, pass the BBB and reach brain neurons exploiting their lipid-solubility [146]. Among psychoactive molecules, ethanol, nicotine and caffeine are very lipid-soluble, thus are completely extracted from the blood during a single passage. Moreover, the rapid effect of ethanol on CNS is also due to its water solubility that allows it to enter the blood stream readily.

Once ethanol passed through the BBB, multiple and complex biochemical effects are induced on the CNS (Figure 2.2). Specifically, as summarized in [147], two main pharmacological effects are induced by ethanol: non-selective effects on membrane organization, membrane-bound enzymes functionality, enzymes and proteins involved in signal transduction, and gene expression; selective and direct interactions with the protein amino-acidic structures involved in neurotransmission (such as inhibitory receptor of the GABA and glycine), or associated with the gating mechanism of neurotransmitter-coupled ion channels.

Overall, ethanol interferes directly with neurotransmission and brain metabolism, altering the firing activity of neurons and in turn the specific encoded physiological functions. In CNS, several neurotransmitter systems are affected, including: the glutamatergic pathways, the gamma-aminobutyric acid GABAergic pathways, the serotonergic and noradrenergic systems [147].

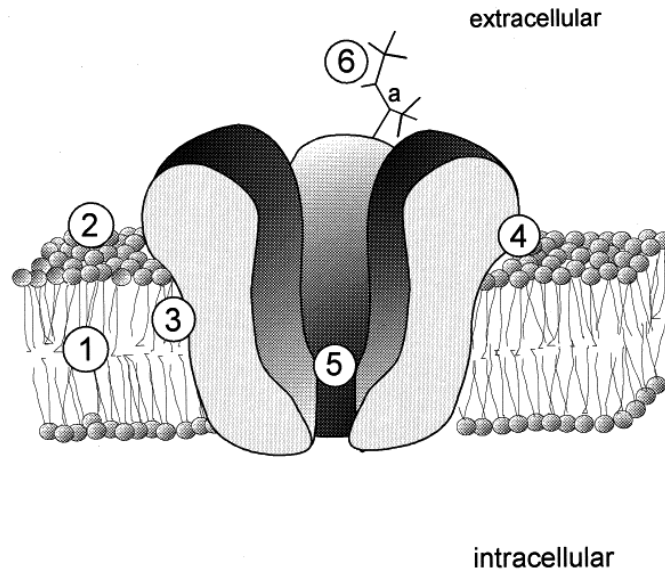


Figure 2.2: Some sites of cellular interaction of ethanol. High concentration of ethanol (>100mM) may produce non-selective effects such as perturbation of membrane architecture by altering the order of the membrane core (1) or the phospholipid structure (3). However, major non-selective interactions of ethanol are the hydrogen bonds formed with the polar head groups of phospholipids (2). Specific, direct interaction of ethanol with the protein amino-acidic structures causes major effects. These structures can be close to the water–lipid interface (4), such as for the GABA_A and glycine receptor, or can be associated with the gating mechanism of the channel (5). Moreover, ethanol can bind allosteric sites in the extracellular amino-acidic domain (a) occupying the recognition site of endogenous ligand (6) (Taken from [147]).

Despite the ethanol action seems to affect the entire CNS, the cerebellar cortex is one of the most sensitive brain regions as its function is tightly controlled by GABAergic inhibitory inputs [148].

GABA receptors are indeed one of targets of ethanol, and consequently GABA_A receptor-dependent neurotransmission is altered impairing cerebellar functions [149].

Purkinje cells are directly involved in such process being a class of GABAergic neurons that provide powerful inhibitory input to control deep cerebellar nuclei. Thus, ethanol depresses Purkinje neuron firing enhancing GABA-induced inhibition of Purkinje cells. Such effect was confirmed by in-vitro and in-vivo electrophysiological recordings showing that ethanol exposure may alter the firing pattern of Purkinje cells [150]–[154]. Despite findings on cycling and spontaneous activity are contrasting, it is generally accepted that the alcohol effect on GABAergic neurotransmission significantly limits the inflow of information into Purkinje cells [149].

Purkinje cells are not the only cerebellar cells involved by ethanol-induced increases in GABA release, as granule cells and molecular layer interneurons (basket and stellate cells) are affected too [155]. Specifically,

GABA release is increased at two synaptic levels: between molecular layer interneurons and Purkinje cells synapses, and reciprocal synapses of molecular layer interneurons. In granule cells instead, ethanol increases tonic and spontaneous inhibitory postsynaptic current affecting both extra-synaptic and synaptic GABA_A receptors.

The ethanol effects on Purkinje cells are not limited to GABA receptors, but even the excitatory glutamatergic inputs of climbing fibers are involved [156]. *Carta et al.* suggested that ethanol inhibits climbing fiber long-term depression, an important form of synaptic plasticity. Such findings provide new insights on how ethanol affects motor activity, as climbing fibers activation of Purkinje cells plays a central role in motor adaptation and learning.

Eventually, recent studies shed light in ethanol-induced cerebellar ataxia, that may be led by ethanol interactions with mossy fiber-granule cell-Golgi cell (MGG) and granule cell parallel fiber-Purkinje cell (GPP) synaptic sites [155]. *Dar et al.* suggested that two ethanol-induced concurrent molecular events cause cerebellar dysfunction, decreasing excitatory output of deep cerebellar nuclei, and cerebellar ataxia [157]. The first event is due to neural nitric oxide synthase inhibition at the MGG synaptic site. Such event causes an abnormal Golgi cell activation, which provokes granule cell deafferentation. The second event is related to adenosine uptake inhibition occurring at the GPP synaptic site. The adenosine accumulation decreases glutamate release and induces strong activation of Purkinje cells.

Overall, the alcohol-induced cerebellar dysfunction is mainly provoked by an alteration of the mechanism of actions of both Purkinje and granulate cells. Moreover, the increased amount of alcohol is associated with increasing severity of the related impairment. Such evidence suggests that Purkinje and granulate cell impairment is alcohol related.

2.2.2. Effect of acute alcohol intoxication on vestibular and ocular motor systems

The effect of alcohol on the CNS is not limited to cognitive or behavioral impairments, and a wide range of motor deficits is related to the level of acute intoxication. Barany reported vertigo, alteration of nystagmic responses and subjective reactions following alcohol ingestion [158] already in 1911. Since then, decades of research have shown multiple and widespread alcohol effects on CNS functions [159]–[161] and human sensory systems [162]–[164].

Cerebellum is directly involved in motor control and its molecular and cellular features make such neural region a sensitive and favorite target for alcohol [148]. Consequently, gait ataxia, impaired motor coordination and balance, are clear signs of acute alcohol intoxication due to deficient function of cerebellum [165]. Besides that, an intact cerebellar functionality is a prerequisite for correct control of eye movements, thus

alcohol intoxication results in less well-known vestibular and ocular motor abnormalities [166], [167].

Clear evidences of alcohol alteration of vestibular responses were documented already over 40 years ago, although mainly described as a dumping effect of alcohol on slow phase velocity of vestibular nystagmus during whole-body acceleration and caloric stimulations [168]–[171]. Afterwards, several studies on vestibular reflexive responses [172]–[175], such as VOR and ocular counter-roll reflex (OCR), revealed alterations of detection and processing of sensory information by alcohol consumption. Such alterations have been further confirmed by clinical tests performed after alcohol consumption, where a reduction in VOR gain, visual acuity and amplitude of ocular vestibular myogenic reflex were observed (respectively in vHIT, DVA and oVEMPs test)[173], [176]. Taken together all these evidences suggest an inhibitory effect of alcohol on reflexive responses to vestibular stimuli, suggesting that alcohol alters functionality of both nervous and sensory systems (i.e. cerebellar and semicircular channels).

Acute alcohol intoxication is also known to cause dysfunctions in other ocular motor systems [166], [167], which induce alterations of visual inputs. Specifically, high doses of alcohol lead to an increase of saccade onset (i.e. increasing reaction time) and decrease velocities of saccades, as well as to a decrease of the gain of smooth pursuit, which becomes increasingly saccadic, inducing greater retinal slip and blurred vision [166], [167], [177]–[179]. Moreover, the gain and slow phase velocity of optokinetic nystagmus is decreased by alcohol, thus the ability to stabilize vision when exposed to a full field visual motion is impaired [169], [177]. Similarly, the ability to suppress the VOR during head motion is diminished, leading to an enhanced nystagmus while fixating a head-fixed target, conversely to the reduction of nystagmus reported during stimulation in full darkness [170], [178], [180].

Even impaired gaze stability and GEN are distinctive features induced by alcohol intoxication [71], [181]–[183]. Although a persistent nystagmus can occasionally appear in healthy subjects at small gaze angles independent of alcohol consumption (see Section 1.4), acute intoxication with levels of blood alcohol content (BAC) above 0.1% lead to a significant increase of the incidence of nystagmus and a significant decrease of the gaze eccentricity at which nystagmus appears [183]. Moreover, despite some controversies [69]–[71], [91], [184], performances of gaze-holding and smooth pursuit systems (Horizontal gaze nystagmus sobriety test) are tested for assessing the “Driving while intoxicated” condition in the United States [185].

Besides ocular motor abnormalities, acute alcohol may alter the visual-vestibular perceptual responses. Anecdotally, the disturbance induced by feeling of drunkenness is commonly renowned to be related to misperception of self-motion. Such belief has been experimentally confirmed by [186]–[188], where alcohol has been shown to be a contributing factor to the development of spatial disorientation, reducing

ability to detect angular motion. Moreover, the self-motion perception after angular velocity step seems to be weakened by ethanol [170], while vection perception (i.e. illusory self-motion) induced by optic flow is enhanced [189].

Despite alcohol effect concerns cerebellar-cortical pathway involved in visuo-vestibular perception, such alterations may be similar to those reported in cerebellar patients, where a consistent alteration of reflexive and perceptual responses have been observed [190], suggesting a cerebellar deficit.

2.2.3. Alcohol-related damages of Cerebellum: chronic intoxication

Despite neurotransmission and neural functionality are already affected by acute alcohol ingestion, chronic abuse provokes worsening of damages inducing neurodegeneration. Specifically, chronic intoxication impairs the function and morphology of most, if not all, brain structures (such as frontal, pontine, thalamic, and cerebellar brain sites) [147].

As mentioned, the cerebellum is directly affected by the neurotoxic effect of alcohol, and approximately in 40% of cases its degeneration occurs after 10 or more years of heavy drinking [191].

Chronic abuse of alcohol induces two main effects on cerebellar structures, a cell death and tissue shrinkage which represent respectively the permanent loss of function and recovery of cerebellum [147], [192], [193]. Specifically, postmortem neuropathology studies reveal several cerebellar abnormalities comprising: widening fissures and sulci in the cerebellar lobes, loss of cells in all layers of the cerebellar cortex, and alteration of the cerebellar pathways functionality (such as the deep cerebellar and the inferior olive) [194]. The volume of cerebellar white and gray matter is also reduced in alcoholics [195] and loss of vermal white matter is reported with ataxia [196].

Experimental observation in alcoholic patients with SPEC tomography confirmed that cerebellar neurons containing GABA_A and benzodiazepine receptors in the anterior superior cerebellar vermis are severely damaged [192]. Furthermore, *Gilmar et al.* showed a glucose hypo-metabolism in such areas, suggesting that the decreased cellular and synaptic activity may be due to alcohol-induced neural loss [197].

Direct ethanol-neuronal interaction is not the only cause of cerebellar degeneration, in fact even side-effects of nutritional deficiencies and hepatic dysfunctions contribute indirectly to cerebellar degenerative process [192], [198], [199]. The compromised liver capacity indeed does not allow to detoxify ethanol and thereby protects the brain from the toxic effects of ethanol and acetaldehyde [191]. In addition, chronic liver injury leads to production of toxic metabolic, and inflammatory mediators provoking diffuse damages of CNS.

Thiamine (B1 vitamin) deficit is a common alcohol-related malnutrition, and seems to be a key factor of neuronal injury [198]. Specifically, chronic alcohol abuse induces a thiamine deficiency by decreasing absorption of thiamine from the gastrointestinal tract [199]. A direct consequence is Wernicke’s encephalopathy, which causes intracellular edema with swelling of oligodendrocytes, myelin sheaths and neuronal dendrites [192]. Although such damages concern the whole CNS, the cerebellum seems to be selectively vulnerable and sensitive to thiamine deficiency [199]. Thus, typical cerebellar degeneration of chronic alcohol abuse (such as reduction in Purkinje cell density and molecular layer atrophy) is exacerbated by Wernicke’s encephalopathy [191], [198]. In addition, the untreated form of Wernicke’s encephalopathy, the Wernicke-Korsakoff syndrome, provokes cerebellar ataxia with worsening of volume deficits in gray matter of cerebellar cortex and white matter in anterior superior vermis [200].

Table 2-1: Neurological features in alcoholic patients (adapted from [192])

Cerebellar signs	Gaze-evoked nystagmus	Ataxic gait
	Ocular dysmetria	Slurred speech
	3 Hz postural leg tremor	Hypotonia
	Kinetic tremor	Titubation
Wernicke’s encephalopathy	Mental confusion	
	Ophthalmoparesia	
	Ataxic gait	
Alcohol withdrawal syndrome	Hallucinations	
	Agitation	
	Autonomic overactivity	
Wernicke-Korsakoff Syndrome	Psychosis	
	Dementia	
	Cerebellar ataxia	
Other signs	Cerebellar atrophy	
	Amyotrophy	
	Decreased tendon reflexes	
	Extensor plantar reflexes	

As a consequence of alcohol-induced pathological changes in the cerebellum, alcoholics develop several deficits related to ocular motor and motor control, motor learning and coordination (Table 2-1). The alcohol-induced damage of cerebellar structures involved in eye movements control provokes ocular motor abnormalities similar to those of cerebellar syndromes (see Section 2.1). For instance, alcohol-induced damages of structures at the base of cerebellum (e.g. flocculus) affect smooth pursuit, gaze-holding and saccadic systems inducing increasing retinal slip [71], [92]. Consequently, the apparent displacement of a visually perceived object leads to visual illusions, postural instability, and visual misperception altering eye-hand or eye-foot coordination [193].

Degeneration in the anterior portion of the cerebellar cortex in patients with chronic alcohol abuse affects movement in the lower limbs, which are

represented in the anterior spinocerebellum [6]. The consequences include a wide and staggering gait, with impairment of arm or hand movements. Moreover, chronic alcohol abuse can cause heterogeneous degeneration of the anterior cerebellum while leaving other cerebellar regions intact [128]. In such cases, patients show only few of the typical alcoholics signs (e.g. strong walking impairment but weak worsening of arm movements or speech), likewise cerebellar patients with localized damages.

Chapter 3

Alcohol-induced Gaze-evoked Nystagmus

3.1. Background

All neural commands generating eye movements are processed by a brainstem neural network [51], [52] the velocity-to-position neural integrator, converting eye-velocity into position commands for ocular motoneurons. As mentioned, the VPNI alone does not provide an appropriate level of tonic innervation to hold gaze in an eccentric position, as the integrator is inherently leaky [26], [201]. Thus, in healthy individuals, the cerebellum compensates the VPNI leakiness [22], [54], [55], preventing the eyes to be rapidly pulled back towards the resting position by the elastic forces of the extraocular muscles [20].

Despite cerebellar control, physiological horizontal centripetal eye-drift that increases with gaze eccentricity occurs in darkness [50].

Cerebellar diseases may cause an increased centripetal drift velocity, which, in turn, elicits centrifugal saccades that aim to keep the eyes at their eccentric position. This sequence of centripetal slow phases and centrifugal quick phases, so called gaze-evoked nystagmus (GEN), appears especially when midline/paramedian vermal and caudal structures are affected [7], [55].

The end-point nystagmus (EPN), is physiological centrifugal nystagmus which may also appear in healthy subjects at extreme gaze eccentricities [64]–[67].

Deficient cerebellar control of the VPNI leads to prominent centripetal eye-drift already at small gaze-angles [53], resulting in blurred vision and oscillopsia [7]. Previously, we described different patterns of eye-drift in patients with neurodegenerative cerebellar disease of various origins and unknown neuropathological differences, possibly related to the age at

disease-onset [53]. With cerebellar ataxia being a rare disease (estimated prevalence=0.2‰ [202]), data from patients are indeed limited.

Impaired gaze stability has also been demonstrated in healthy individuals under the influence of alcohol [71], [182], [203]. Acute alcohol intoxication (BAC>1‰) significantly increases the incidence of EPN [183] and decreases the gaze eccentricity causing nystagmus [181], [182], [185]. Additionally, chronic ethanol consumption alters the function and morphology of several brain structures involved in eye movement control [147], [204], [205], and is one of the most common causes of progressive cerebellar degeneration in adults [206].

We hypothesized that a transient cerebellar inhibition by defined amounts of alcohol may provide a model to study gaze-holding deficits in cerebellar disease. A description of changes in gaze-evoked drift associated with alcohol-intake, however, is missing. Previous studies focused on the occurrence of nystagmus, without reporting the amount of eye-drift [68]–[70], [91], [181], [183], [185]. Thus, measuring eye-drift velocity induced by consumption of two controlled amount of alcohol (0.06% and 0.1%), we aimed to: 1) identify the alterations of the normal gaze-holding behavior specific to alcohol intake, 2) assess if these temporary effects are comparable to those observed in cerebellar patients, 3) evaluate whether the controlled intake of alcohol in healthy subjects represents a valid disease-model for cerebellar degeneration. As suggested in literature, we modeled the nonlinear behavior of eye-drift velocity [65], [207] by tangent function [50]. Such a model is particularly advantageous as it allows to summarize gaze-holding behavior using a two-parameters function, facilitating the quantitative comparison of different datasets (e.g. pre- vs. post-alcohol as well as previously recorded cerebellar patients [53]).

We also investigated asymmetries in gaze-holding control between temporal and nasal eccentricities. While asymmetries in saccadic system [208], [209] and vestibulo-ocular reflex [210] are well known, similar differences in gaze-holding were only hypothesized [64], [67]. We speculate that alcohol, enhancing the eye-drift, may unveil such asymmetries.

3.2. Materials and methods

3.2.1. Subjects

The statistical distribution of the eye-drift velocity in the 20 healthy subjects (6 females, 41 ± 11 years old, mean ± 1 standard deviation [SD]) described by [50], [53], suggested that data from at least 14 subjects are needed to reveal a significant increase of 1°/s in the centripetal drift velocity at extreme gaze, having a power (probability of rejecting the null hypothesis when the alternative hypothesis is true) of 0.80.

Consequently, we recruited two independent groups of fifteen healthy subjects to assess the effect of two different alcohol concentrations: 0.06% (5 females, 31.36 ± 7.3 years, mean age ± 1 SD) and 0.10% (6 females, 28.40 ± 7.7).

The subjects were informed about the nature of the experiment and the whole experimental procedures were fully explained. Every participant signed a written informed consent.

In both groups, none of the participants had a history of neurological disorders including dizziness/vertigo or gait imbalance or took any drugs that may affect gaze-holding. Subjects with myopia were requested to wear contact lenses during the experiment. One subject from 0.06% group was excluded due to an incomplete dataset, as recordings after alcohol intake had to be cancelled because of nausea and vomiting.

3.2.2. Experimental settings

During the entire experiment, each subject was seated upright on a turntable mounted on three servo-controlled motor-driven axes (Acutronic, Jona, Switzerland). In order to stabilize the subject's head and limit head movements, individually molded thermoplastic masks (Sinmed BV, The Netherlands) were used. Safety belts were applied to minimize trunk-movement related artifacts.

The visual stimulus was generated using a remotely controlled LED, attached to a hemispherical full-field screen at 1.5 m distance. The LED was mounted at eye level straight-ahead. The screen was connected to a platform that could be rotated along an earth-vertical axis (position resolution=0.01°).

Horizontal eye movements were recorded using a head-mounted video-oculography (VOG) device (Eyeseecam, Munich, Germany), a video system using two infrared cameras mounted on swimming-like goggles. The position of both eyes were sampled at 220Hz, with a spatial resolution of 0.01° root mean square [211], [212].

A calibration procedure was performed at the beginning of the experiment requiring the subject to look at a sequence of fixation points (21 points forming a grid of gaze angles from -25° to $+25^\circ$ with 10° steps along the horizontal axis, and from -10° to $+10^\circ$ with 10° steps along the vertical axis) projected on the hemispherical screen using a laser galvanometer. The relationship between the output values of the VOG system and eye angular positions on the hemispherical screen was obtained by fitting a second-order polynomial function [50].

3.2.3. Experimental procedure

Every subject underwent two identical sessions: before alcohol intake (baseline recording) and 30 minutes after the ingestion of the amount of

alcohol (in grams) estimated to reach a blood alcohol content (BAC) of 0.06 and 0.1%. The grams of alcohol were calculated on a subject-by-subject basis using the Widmark formula [213] (parameters required: subject's height, weight, gender). The estimated quantity was converted in ml of Red wine 13% alc. vol., for the 0.06% group, while in ml of Vodka 37.5% alc. vol. for the 0.10% group.

The achieved BAC was then estimated from the BrAC (Breath Alcohol content) using a breath alcohol tester (Dräger Alcotest[®] 6510, Lübeck, Germany), with conventional single breath technique to avoid any bias related to different breathing techniques [214]. To confirm that BAC values remained stable during the whole experiment, the BrAC was measured immediately before and after each block of our experiment (i.e., approximately every 10 minutes).

The baseline recording allows discounting any confounding factor known to affect GEN and its prevalence (e.g. lack of sleep, fatigue)[68]–[71]. As each experimental session lasted around one hour and the two sessions were separated by a maximum of one hour the risk that tiredness may change significantly during the test (i.e., before and after alcohol intake) was small.

The paradigm was identical to the one previously described and validated for studying gaze-holding in healthy subjects [50] and patients with cerebellar neurodegeneration [53], respectively. It can be summarized as follows: in a completely dark environment, the subject was asked to fixate a briefly flashing red LED (50ms every 2s) moving at 0.5°/s in the range of horizontal gaze eccentricity from 40° right to 40° left, without moving the head. Both eyes were concurrently recorded, but one eye was covered with an optic filter, allowing eye tracking but preventing vision. This approach was chosen to avoid possible double vision due to GEN.

This paradigm was recorded twice, with the LED initially moving either leftward or rightward (the direction of the first movement was randomized across subjects). During each trial the flashing LED reached an eccentricity of 40° towards the side of the viewing eye and of 20° towards that of the covered eye since the target was usually not visible for larger gaze angles on the side of the covered eye due to both the occlusion from the VOG goggles structure and the subjects' nose. The entire process was repeated changing the covered eye (the order of the covered eye was randomized across subjects).

3.2.4. Data-preprocessing

Eye movement data were analyzed using interactive functions written in MATLAB (MatLab 8.2; The MathWorks, Inc., Natick, MA, USA). Instantaneous eye velocity was obtained computing the derivative of horizontal eye movements.

Only the slow phases of the eye movements were considered when analyzing the eye-drift velocity at different gaze eccentricities, removing

the fast phases (saccades) and eye-blink related artifacts using an automatic custom velocity-based algorithm. Specifically, the algorithm identifies all data points that exceed by a given threshold the median velocity calculated over a time window moving in steps of one third of its width. Consequently, the data points that exceeded the threshold at least two times were considered part of a saccade. The beginning and the end of each saccade were identified by searching for the closer reversals of the eye velocity. Eventually, all data points belonging to saccades were removed. For our analysis the saccade-detection threshold was set to $10^\circ/\text{s}$ and the width of the window was 0.5 seconds.

Missing data (e.g. due to brief interruption of pupil tracking by the VOG software) were not interpolated. Data were down-sampled from 220Hz to 100Hz. No other data preprocessing was done.

3.2.5. Data grouping

We developed three different approaches, which we applied to both concentration (0.06% and 0.1% group), to analyze the eye-velocity data, each time addressing a different question for which a specific procedure for pooling the data was required.

First, we evaluated the alcohol effect on the overall ability to hold gaze on a target. For each subject we pooled the data from both eyes recorded during all trials (trials differ by the starting direction of the target displacement and by the covered eye, see experimental procedure in Section 3.2.3 above for details). To adopt a gaze-based reference system, we took the positions of the eyes when looking at the target straight ahead as zero position and, accordingly, we defined the gaze eccentricity as the angular position of the LED with respect to zero (gaze angles to the subject's right were defined as positive). We estimated the velocity bias when looking straight ahead, by computing the median of instantaneous eye-drift velocities recorded within the range of $\pm 2.5^\circ$ of gaze eccentricity and subtracted it from all data points. This allowed comparing the dependency of eye-drift from gaze eccentricity independently from minor discrepancies of the straight-ahead position across trials and subjects. This analysis compared two conditions: before and after the intake of alcohol (named BA and AA, respectively). This procedure was performed both for 0.06% and 0.10% groups.

Our second analysis considered the behavior of both eyes separately to test for possible disconjugate effects of alcohol. The procedure was identical to the one described above to pool the data, with the exception that the data acquired from each eye were kept separate, building up two subgroups (named LE, for left eye and RE for right eye, respectively) for both conditions studied (i.e., BA and AA).

The third analysis aimed at evaluating asymmetries in gaze-holding mechanisms assessing the differences between eye-drift after fixation in

temporal and nasal hemifields. Such analysis required an additional step to separate the data from the two eyes with respect to the eye null position.

Specifically, while in [64] gaze-holding asymmetries were observed defining an “abducting and adducting eye” using the direction of the previous saccade, we describe our results in terms of the position of the eyes in the orbit, hence considering either the eye in the temporal hemifield or the eye in the nasal hemifield as TH and NH, respectively (Figure 3.1).

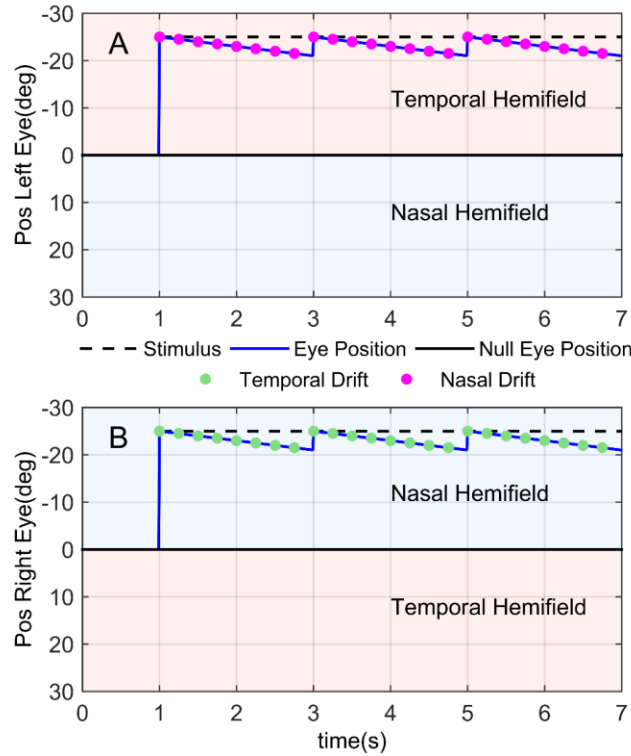


Figure 3.1: Definition of temporal and nasal hemifield for each eye.

Each blue line represents synthetic data of end point nystagmus seen in left eye (A) and right (B) eye maintaining gaze at 25° (dashed black line). Light red and light blue areas represent respectively gaze angles in temporal and nasal hemifield, divided by the null position of eye (solid black line). Due to conjugate eye movements, the magenta data points of left eye temporal-nasal drift was used to build the temporal hemifield PV-plot, while for nasal hemifield the green data points of right eye naso-temporal drift are used.

Therefore, the TH data was obtained pooling data from all fixation points, irrespective of right or left eye, in the temporal hemifield. TH data then comprise gaze angles lesser than eye null position for LE and greater for RE, and therefore producing eye-drift in temporal-nasal direction (TN). Similarly, the NH data was obtained pooling all fixation points in the nasal hemifield, i.e. gaze angles greater than eye null position for LE and lesser for RE, causing eye-drift in naso-temporal direction (NT).

To align left and right eye data for the second analysis and to distinguish temporal and nasal gaze angles in the third analysis, we used the null position of each eye (i.e., the gaze angle showing no drift) as “switch point”. However, we observed that the zero position defined by the target straight ahead as described above, was often not appropriate to describe the actual null of either eye. In darkness each eye drifts toward a resting point corresponding to a subject-specific resting vergence [215]–[217]. Such vergence may not correspond to the one required to look at the target used in this experiment, leading to disconjugate drifts when looking straight ahead. We therefore estimated null position $Null^{eye}$ on the raw data of each single eye, fitting the instantaneous velocity of each eye, V^{eye} with the following linear function of eye eccentricity E^{eye} in range from -15° to 15° (position-velocity linear relationship for small gaze angles [50]):

$$V^{eye} = m^{eye} E^{eye} + q^{eye} \quad \text{with } m^{eye} < 0 \quad (3.1)$$

The null position $Null^{eye}$ was computed as the value of E^{eye} with velocity $V^{eye}=0$, i.e. $Null^{eye} = q^{eye}/m^{eye}$. Fit coefficients, q^{eye} and m^{eye} , were estimated using quantile regression [218]. The $Null^{eye}$ was considered unreliable when the slope m^{eye} was close to zero (threshold: $m^{eye} > 0.002s^{-1}$) and $Null^{eye}$ value was outside the range $-10^\circ < Null^{eye} \vee Null^{eye} > 10^\circ$. In such cases $Null^{eye}$ was set to zero, for both eyes.

Once $Null^{eye}$ was estimated, its value was used to align data points of the two eyes according to their actual null position (i.e., resting point vergence). Such correction allows us to compare left versus right eye and to distinguish nasal gaze angles from temporal ones, avoiding to align incorrectly data points from each eye in PV-plot (discussed in the “Differential analysis for temporal and nasal hemifields” subsection) and to overestimate the slope of PV relationship in temporal hemifield data erroneously using data points from nasal hemifield.

Eventually, the last two procedures, i.e. single eye and direction analysis, were performed for 0.06% group only.

3.2.6. Data analysis

Our data analysis is similar to that described in [50], [53] to study gaze-holding mechanism in healthy subjects and patients with cerebellar disorders. The analysis is based on a position-velocity plot representation (PV-plot, i.e. a plot of the eye-drift velocity as a function of gaze eccentricity), commonly adopted to analyze the VPNI time constant by means of a linear fit modeling, but introduces some important differences [50].

To draw the PV-plot, we sorted the eye-drift velocity of every subject in ascending order of gaze eccentricity. Sorted data were assigned into 17 non-overlapping, 5° wide bins, covering the whole range of gaze angles

tested ($\pm 40^\circ$). For each bin the median values of position and velocity were calculated, reducing data noise caused by outliers.

The three different procedures described in the “data grouping” (see Section 3.2.5) were separately applied to the data acquired in 0.06% groups, for both conditions tested BA and AA. This generated several subsets of data to be compared within the three analyses (as defined in the “data grouping” subsection):

1. Overall gaze BA vs. AA,
2. Left eye BA vs. right eye BA, left eye AA vs. right eye AA, left eye BA vs. AA, right eye BA vs. AA,
3. Temporal hemifield BA vs. nasal hemifield BA, temporal hemifield AA vs. nasal hemifield AA, temporal hemifield BA vs. AA and nasal hemifield BA vs. AA.

For data acquired in 0.10% group, instead, the overall gaze stability was tested before and after alcohol intake, using only the first procedure (see Section 3.2.5).

In all subsets of data formed using either for 0.06% or 0.10% group, each comparison was carried out in two steps: a “direct comparison” of data and a model-based analysis. Consequently, for sake of simplicity, in the following subsection BA and AA indicates the before and after conditions both for 0.06% and 0.10% groups, as the data analysis was identical for both groups.

3.2.6.1. Direct comparison

In the “direct comparison”, for each subject i , we computed the median ratio (r^i) of the median velocities of corresponding bins. This was repeated for each pair of subsets compared, which were in turn named S1 and S2. Formally the computation is expressed by:

$$r^i = \text{median} \left(\frac{V_1^{i,S1}}{V_1^{i,S2}}, \dots, \frac{V_j^{i,S1}}{V_j^{i,S2}}, \dots, \frac{V_{n_{bins}}^{i,S1}}{V_{n_{bins}}^{i,S2}} \right) \quad (3.2)$$

with $i = 1, \dots, n_{subjs}$

where, regarding the i -th subject, $V_j^{i,S1}$ represents the median velocity of the j -th bin in the S1 subset, while $V_j^{i,S2}$ represents the median velocity of the same bin in the S2 subset.

The distribution of median ratios across subjects was tested using the Wilcoxon signed-rank test to verify whether the compared subsets (S1, S2) were statistically different.

3.2.6.2. Model-based approach

In addition to the “direct comparison”, we performed a further analysis using a model-based approach comparing each pair of subsets. As suggested in early studies [65], [207] and recently confirmed [50], we assumed a nonlinear relationship between eye position and drift velocity, conversely to the common assumption of linear growth between drift velocity and gaze eccentricity that does not allow to appreciate the differences observed across a sample of patients with cerebellar diseases [53]. Specifically, in each analyzed subset, for the i -th subject, the instantaneous drift velocity, (V^i) was independently fitted, using the following function of gaze eccentricity (E^i):

$$V^i = \frac{k_2^i}{k_1^i} \tan(k_1^i \cdot E^i) \quad \text{with } i = 1, \dots, n_{\text{subjs}} \quad (3.3)$$

The mathematical model in Eq.(3.3), is a modified version of the ones presented in [50] and [53]. It consists of a tangent function where independent changes of the two parameters k_1 and k_2 lead to changes of two distinct features describing the behavior of the drift velocity V as a function of the gaze angle E . Specifically, the “shaping coefficient” k_1 , modifies the shape of tangent function to capture rapid deterioration of gaze-holding performance beyond a certain eccentricity of gaze, i.e., how marked the nonlinear behavior is; the “scaling coefficient” k_2 instead scales the whole function independently from the gaze angle, keeping the tangent shape unchanged (see Figure 3.2 for a detailed description).

Moreover, compared to the previous versions of the tangent function presented in [50], [53], the modelling in Eq.(3.3) reduces the number of estimated parameters from three to two as we now remove the offset velocity directly on raw data instead of using a third coefficient k_3 . This simplification, although mainly methodological, allowed focusing on the two relevant parameters.

The ratios (r_{k_1}, r_{k_2}) of each fit coefficient in two paired subsets (S1, S2) were then computed for every subject as follows:

$$r_{k_1}^i = k_1^{i,S1} / k_1^{i,S2} \quad \text{and} \quad r_{k_2}^i = k_2^{i,S1} / k_2^{i,S2} \quad \text{with } i = 1, \dots, n_{\text{subjs}} \quad (3.4)$$

The statistical distributions of ratios (r_{k_1}, r_{k_2}) across our subjects were tested by means of a Wilcoxon signed-rank test, and were compared to a population with median equal to one.

3.2.1. Gaze-holding dataset comparison

To verify that our two dataset of 15 subjects (before alcohol intake for both 0.06% and 0.1% groups) were comparable to previously reported gaze-dependent eye-drift, we compared them with a gaze-holding dataset of

20 healthy human subjects described in [50]. For each subject, we independently fitted the median velocity computed over gaze eccentricity bins using Eq. (3.3), pooling all data from left and right eye within each subject, and compared the resulting parameters.

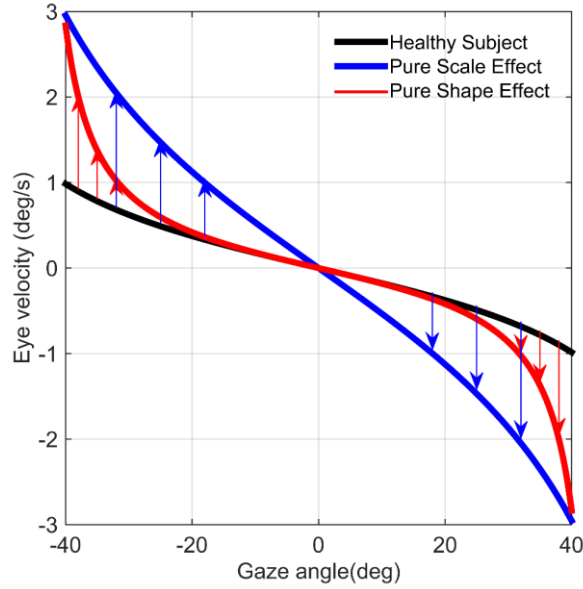


Figure 3.2: Changes in PV-plot by tuning the shaping k_1 and scaling k_2 parameters of the tangent model. Healthy subjects usually show a slightly nonlinear position-velocity relationship (black line). Our 2-parameter tangent model allows to model changes in the PV relationship of VPNI. Specifically, increase of the k_2 scaling factor reflects an increase of eye drift velocity for all gaze angles, called “pure scaling” behavior (blue line). Changes in the value shaping factor k_1 , instead, models a pure shape-changing behavior of eye drift (red line). In such condition, eye drift velocity values remain within normal range up to approximately 20-25° of gaze eccentricity and only for more extreme gaze angles, a significant increase in eye drift velocity can be observed. When both parameters are modified, PV-plot shows patterns between pure shape-changing and pure scaling (adapted from [53]).

3.2.2. Statistical analysis

Median and MAD (median absolute deviation) were used as statistical descriptors of the data, as weakly affected by outliers [219].

For all paired comparisons, we performed a Kolmogorov-Smirnov test. Since our data were non-normally distributed, a bilateral Wilcoxon signed rank test was then used after testing the symmetry of the data by means of the Wilcoxon test for symmetry. In the same way, we tested the difference of two independent samples using the Wilcoxon rank sum test.

For multiple comparisons, a Bonferroni correction was used to ensure a conservative measure of significance. We considered a p -value < 0.05 (after the correction in multiple comparisons) as statistically significant.

Least square regression and quantile regression [218] were used as methods for data fitting, respectively, when normality of the data were confirmed or not.

To measure the strength of the relationship between the tangent coefficients, since linearity of analyzed variables was not confirmed, the Kendall's Tau, a non-parametric correlation index, was used.

3.3. Results

3.3.1. Gaze-holding baseline comparisons

The first two rows of Table 3-1 show the distribution of tangent coefficients estimated using the 0.06% dataset and the gaze-holding dataset described in [50].

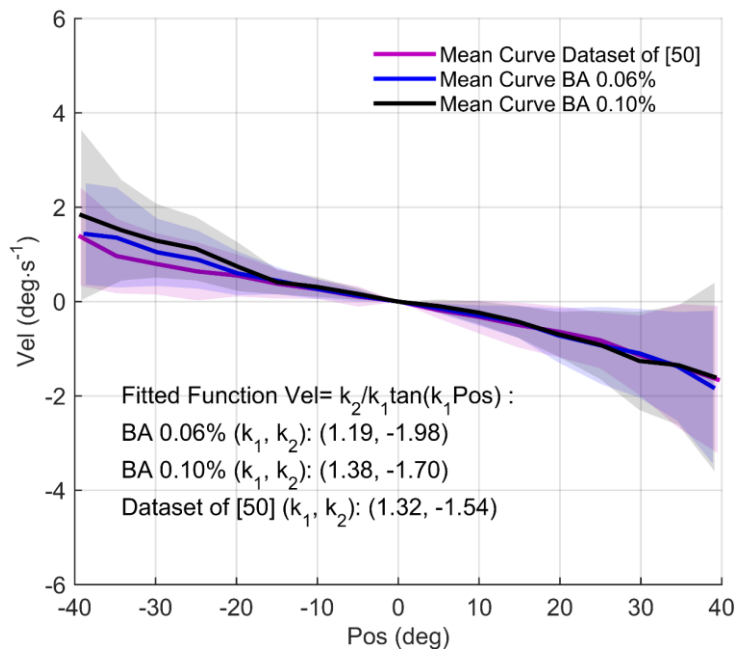


Figure 3.3: PV plot of three different datasets of healthy subjects. Each line represents the mean drift velocity of all subjects, while the shaded area represents the mean \pm sd. Positive angles correspond to right gaze eccentricities as seen by the subject. Data recorded on our two groups of subjects before alcohol intake (blue and black solid line, respective 0.06% and 0.10%) are almost indistinguishable from the dataset of 20 healthy subjects described in [50] (purple solid line), confirming that our dataset includes subjects with physiological gaze dependent eye-drift. The plotted curves were also fitted with the tangent function (the estimated parameters are reported in the figure). Both the shaping (k_1) and scaling (k_2) parameters are comparable in the two datasets.

Despite small differences, neither the shaping coefficient k_1 nor the scaling coefficient k_2 showed any statistical difference with respect to the values of healthy subjects in [50] (Wilcoxon rank sum test: $p=0.79$ and $p=0.24$, respectively).

A similar result was achieved using BA condition of 0.10% group, as shown in Table 3-2. Specifically, both coefficients, k_1 and k_2 , were not statistically different to the reference values estimated on dataset described in [50] (Wilcoxon rank sum test: $p=0.82$ and $p=0.56$, respectively).

The absence of relevant differences emerges also from Figure 3.3, where the averages of individual medians of velocity bins are shown for the BA conditions of our two groups, i.e. 0.06% and 0.10%, and the datasets described in [50].

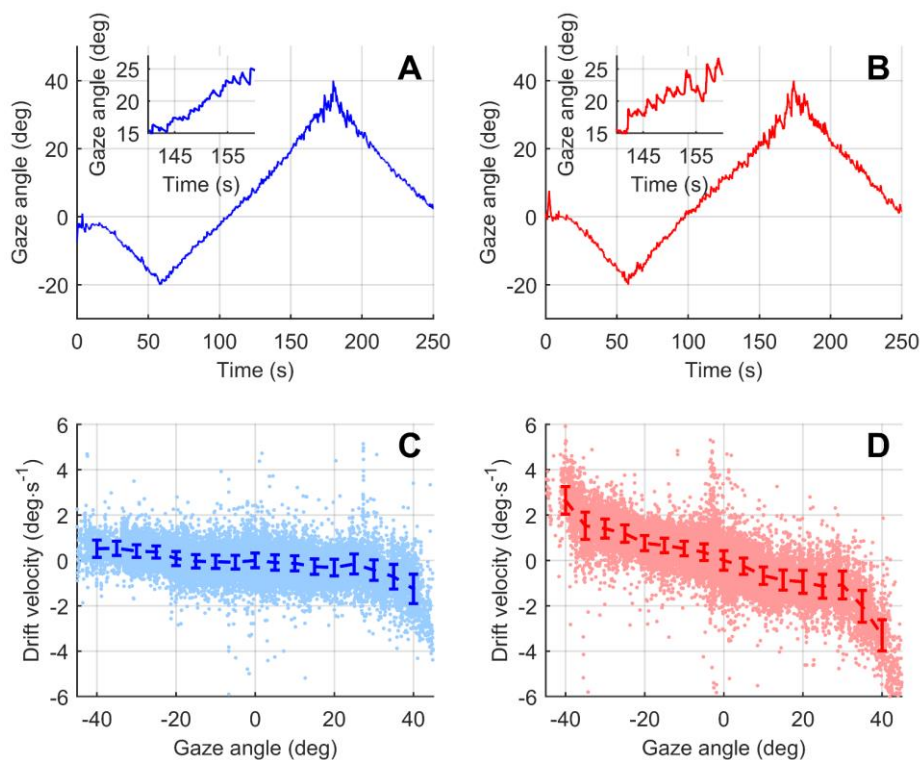


Figure 3.4: Horizontal eye position recorded in a single trial from a typical subject before (A, C) and after alcohol consumption (B, D). Positive angles correspond to right gaze eccentricities as seen by the subject. In (A, B) right eye position is plotted as a function of time. Insets: Centrifugal nystagmus is already present at the same gaze eccentricity, but slow phase velocity of nystagmus is strongly increased by alcohol consumption. In (C, D) horizontal eye-drift velocity is plotted against gaze position. Data points: Instantaneous velocities of slow phases, saccades were removed during preprocessing of data. Blue and red bars: median ± 1 MAD of instantaneous eye-drift velocity. Alcohol intake causes greater gaze instability. Such an effect is visible as a homogenous increase of eye-drift for all gaze angles (D) compared to the baseline condition (C).

3.3.1. BAC 0.06%: Alcohol effects on gaze-holding

At baseline, BAC was zero in all subjects. The median level of BAC across our subjects 30min after alcohol intake was in accordance with Widmark's formula prediction [213]($0.58 \pm 0.06\%$ BAC; 31 ± 4 min). This value remained quite stable during the whole recording period (sample distribution of median of BAC for each subject, $0.61 \pm 0.02\%$ BAC; sample distribution of BAC variability, i.e. MAD, for each subject: $0.03 \pm 0.02\%$ BAC).

A comparison of eye movements recorded in the BA and AA conditions is shown in Figure 3.4A, B for a typical subject. Alcohol consumption reduced the gaze angle where nystagmus becomes clearly recognizable. This is due to a higher eye-drift velocity at the same gaze eccentricity, as illustrated on the PV-plots (Figure 3.4C, D).

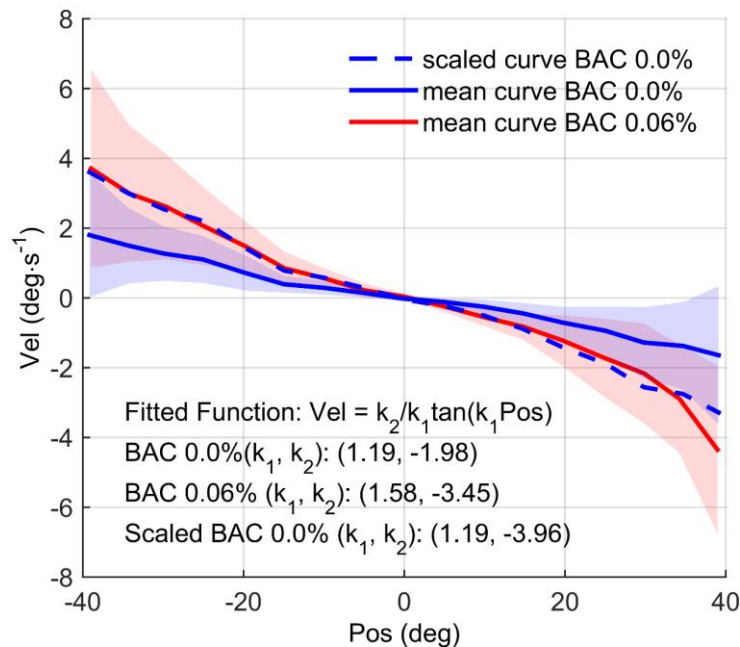


Figure 3.5: Effect of 0.06% BAC on eye-drift velocity (Vel) as a function of eye gaze angle (Pos). Each line represents the mean drift velocity of all subjects in the different conditions, while the shaded area represents the mean ± 1 standard deviation. The blue dashed line is a scaled version of the data recorded before alcohol intake (blue solid line), perfectly overlapping with the data recorded after alcohol intake (red solid line), confirming the pure scaling effect of 0.06% BAC. Such an effect is further confirmed by the scaling parameter of the tangent model (k_2), which was estimated on the plotted curves (the estimated parameters are reported in the figure).

This pattern was confirmed in the whole 0.06% group by computing the median ratio of the AA versus the BA condition for every subject (see “Direct comparison” in the Section 3.2.6.1, and Eq.(3.2)). The Wilcoxon

test for paired data revealed that the median of medians ratios distribution (2.21 ± 0.55) was significantly higher than one (highly significant; $p=0.002$), confirming that a BAC of 0.06% affects gaze-holding by increasing centripetal eye-drift velocity more than two-folds.

Fitting the tangent function in Eq.(3.3) independently for each subject and computing the ratios of estimated coefficients (Eq.(3.4)) allowed investigating the mechanisms behind these increases in drift velocity. No statistical difference was found for the shaping coefficient k_1 (median ratio= 1.09 ± 0.38 , $p=0.22$, Wilcoxon signed-rank test for paired data). On the other hand, the ratio of the scaling coefficient k_2 (1.96 ± 0.82) was statistically different from one ($p=0.001$), suggesting that changes in drift velocity induced by alcohol were due to a proportional increase of drift velocity at all studied gaze angles.

The pure scaling effect induced by alcohol is clearly visible in Figure 3.5, which compares the mean of individual velocity curves before and after alcohol consumption, pooling all subjects. The shape of the curve from the AA condition (red curve) looks indeed almost unchanged when compared to the BA condition, showing a steady increase of eye-drift velocity as a function of gaze eccentricity. A simple algebraic multiplication of the point-by-point velocity from the BA curve (solid blue curve) by a scaling factor of two (dashed blue curve) reproduces the experimental data and thus indicates that a BAC of 0.06% induces no change in the shape of the PV relationship of gaze-evoked eye-drift (red curve).

3.3.2. BAC 0.06%: Differential analysis two eyes

Comparing drift velocities from both eyes, an eye-specific offset in the resting (or null) position was observed in some subjects. Such offset biased the pairing of gaze eccentricity of the two eyes when comparing drift velocities. According to our criterion for a reliable estimate of the null point (for a detailed description of criteria to estimate the null see Data Grouping in Section 3.2.5), we estimated the null position $Null^{eye}$ for each eye. A reliable estimate was possible for 8 of the 14 subjects in 0.06% group from the BA condition (Offset RE: $-4.68 \pm 2.28^\circ$; Offset LE: $4.69 \pm 2.28^\circ$) and for 11 out of 14 subjects from the AA condition (Offset RE: $-4.00 \pm 1.90^\circ$; Offset LE: $5.91 \pm 2.34^\circ$), respectively (see Eq.(3.1)). In order to allow an unbiased comparison of the drift velocity between the two eyes, the reliably estimated offsets were removed. No correction was performed for the remaining subjects (see Section 3.2.5). The results of the bias removal are shown in Figure 3.6B, D for a typical subject. Specifically, the figure demonstrates how the data points from LE and RE (in BA and AA conditions, respectively Figure 3.6B, D) showed a better overlap after bias subtraction than in the original PV-plot (Figure 3.6A, C).

After offset correction, the distributions of median ratios (see Eq.(3.2)) of LE and RE were not statistically different from 1 in any condition (BA:

0.97 ± 0.19 , $p=0.65$; AA: 0.99 ± 0.09 , $p=0.82$; Wilcoxon signed-rank test). This implies that the VPNI acts identically for both eyes with respect to their specific null position, and that this symmetry is not affected by the consumption of alcohol (with 0.06% of BAC).

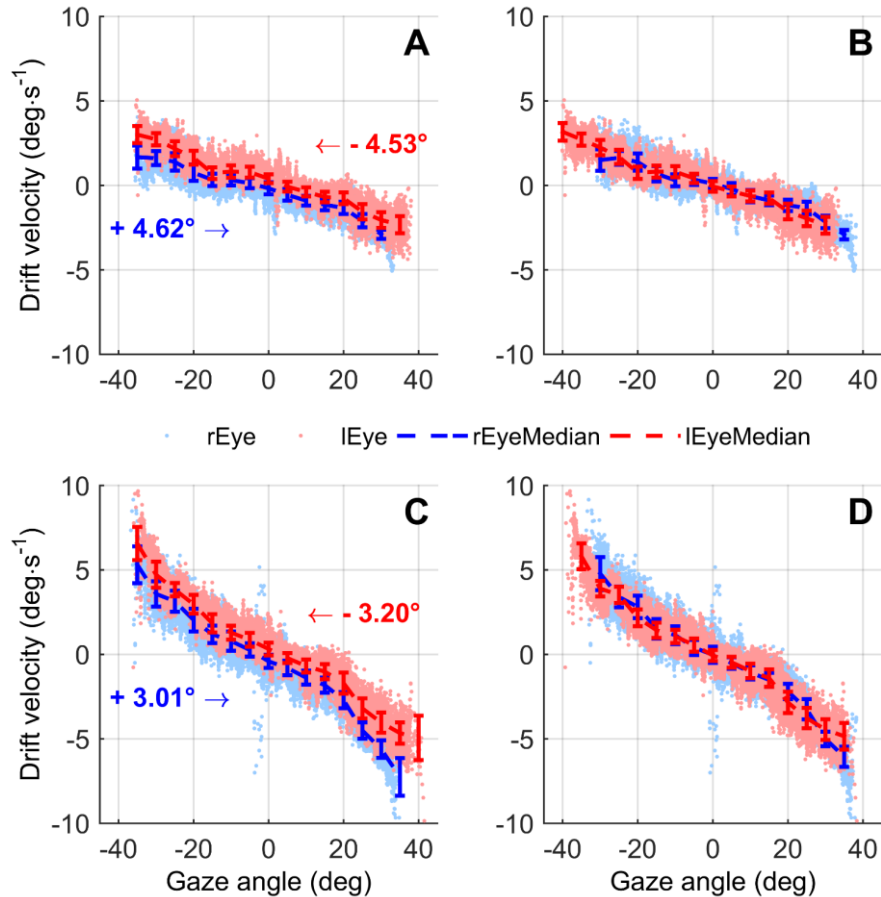


Figure 3.6: PV-plots of a typical subject with data points of the two eyes aligned (B, D) or not (A, C) according to their actual null position. Data from both eyes (blue and red, respectively, for right and left eye) are plotted separately for before (A, B) and after (C, D) alcohol intake (0.06% BAC) conditions. Dots: instantaneous velocities of slow phases, saccades were removed during data preprocessing. Solid bars: median ± 1 MAD of instantaneous drift velocity. In panels (A) and (C), independently of alcohol consumption, an eye-specific offset can be easily observed as the data points for each eye are not overlapping. Such an offset was estimated by means of Eq. (3.1) and used to shift data as shown by color-coded arrows in panels (A) and (C). Only when the eyes are correctly aligned (B, D), their PV-plots can be compared.

The results were further confirmed by comparing the estimated tangent coefficients (Eq. (3.4)) in each data subset (see Table 3-1). The median of k_1 ratios between RE and LE (BA: 1.01 ± 0.34 , $p=0.54$; AA: 1.01 ± 0.18 , $p=0.94$) and that of k_2 ratios (BA: 0.96 ± 0.29 , $p=0.83$; AA: 1.03 ± 0.07 ,

$p=0.21$) were indeed not different from 1 both before and after alcohol consumption.

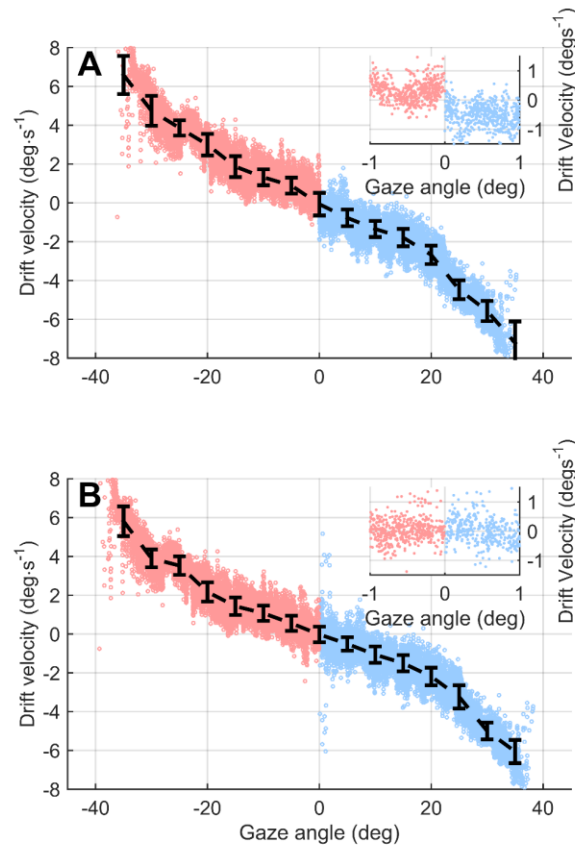


Figure 3.7: Gaze angle drift velocity relationship in the temporal hemifield (TH) estimated on data shown in Figure 3.6C, D, respectively, with (A) and without (B) eye specific positional offset. Red and Blue Dots: instantaneous velocities of slow phases, respectively, from the left and the right eye of Figure 3.6. Black solid bars: median ± 1 MAD of instantaneous drift velocity. In both panels (A) and (B), TH data points were obtained pooling the left and right eye, considering gaze eccentricities being lesser and greater than the null position (i.e., zero of PV-plot), respectively. Using data shown in Figure 3.6C, a discontinuity is visible between data points from the left (red dots) and right eye (blue dots) in the inset of panel (A). Such ambiguity is due to an incorrect alignment of the eyes in Figure 3.6C. Conversely panel (B), using data from correctly aligned eyes (Figure 3.6D), does not show any discontinuity between the data from the left and right eye (inset of panel (B)).

With respect to the effects of BAC 0.06%, our analysis revealed that the same homogeneous scaling effect of eye-drift velocity found for the pooled data (shown in Figure 3.5) was observed for each single eye individually. Specifically, the direct comparison of the AA and BA conditions (computing the distribution of median ratios according to Eq. (3.2)), revealed significant differences in the data of both eyes (RE: 2.08 ± 0.42 ,

$p=0.002$; LE: 1.69 ± 0.30 , $p=0.005$). Similar to the pooled analysis, no significant difference in the shaping coefficient k_1 was found for RE or LE alone (medians of ratio between AA and BA conditions were 1.03 ± 0.44 , $p=0.41$, and 1.07 ± 0.14 , $p=0.31$, respectively for RE and LE), while ratios of k_2 estimated in AA to k_2 estimated in BA condition were statistically higher than one for both eyes (RE: 2.20 ± 1.06 , $p=0.04$; LE: 1.95 ± 0.57 , $p=0.007$).

3.3.3. BAC 0.06%: Differential analysis for temporal and nasal hemifield

By comparing gaze angles in temporal and nasal hemifields considering separately the data acquired in the two tested conditions in group 0.06%, we observed that the different ocular dynamics of the ocular plant shown in saccades data did not affect gaze-holding features. In the BA condition no significant difference was found between NH and TH ($p=0.064$) neither using Eq.(3.2) to compare medians within each bin (where $S1$ and $S2$ represent NH BA and TH BA, respectively, and their median of distribution of medians ratios was 0.68 ± 0.23) nor comparing the tangent coefficients estimated from NH BA and TH BA.

No differences were indeed found either in the shaping coefficient k_1 or the scaling coefficient k_2 , since both median ratios were not statistically different from one ($k_1^{NH_BA}/k_1^{TH_BA}$: 0.99 ± 0.08 , $p=0.52$; $k_2^{NH_BA}/k_2^{TH_BA}$: 0.61 ± 0.35 ; $p=0.084$).

Similarly, in the AA condition a direct comparison of NH and TH did not reveal significant differences (median ratio distribution: 1.0 ± 0.44 , $p=0.52$). The ratios of tangent coefficients k_1 and k_2 in both directions were not different from 1 ($k_1^{NH_AA}/k_1^{TH_AA}$: 0.96 ± 0.43 , $p=0.79$; $k_2^{NH_AA}/k_2^{TH_AA}$: 0.94 ± 0.38 ; $p=0.68$), as shown in Table 3-1.

In line with the results obtained with the other grouping strategies, the analysis of the effects of alcohol consumption, through direct comparison of data pooled by drift direction showed a statistically significant difference between BA and AA conditions (medians of ratio between AA and BA conditions for TH: 1.68 ± 0.42 , $p=0.01$; and NH: 2.76 ± 1.23 , $p=0.004$). The comparison of the parameters of the fitted function (Eq.(3.4)) revealed that the change in the gaze-holding behavior was due to a pure scaling of eye velocity as the Wilcoxon signed-rank test showed that only the median ratio of k_2 , either for TH ($k_1^{TH_AA}/k_1^{TH_BA}$: 1.04 ± 0.19 , $p=0.30$; $k_2^{TH_AA}/k_2^{TH_BA}$: 1.58 ± 0.31 , $p=0.027$) and NH ($k_1^{NH_AA}/k_1^{NH_BA}$: 0.99 ± 0.17 , $p=0.97$; $k_2^{NH_AA}/k_2^{NH_BA}$: 2.46 ± 2.20 , $p=0.019$) was significantly different from one.

3.3.4. BAC 0.10%: Overall effect of acute intoxication on gaze-holding

To further investigate the overall effect of alcohol on gaze-holding, we assessed the effect of acute intoxication, generalizing the results of 0.06% group. Thus, we collected data from a second group of subjects (named 0.10% in the following) before and after alcohol ingestion to reach 0.10% BAC.

At baseline, BAC was zero in all subjects. Similar to 0.06% group, the quantity of alcohol grams was estimated according to Widmark's formula prediction [213]. Despite that, the BAC across subjects after 30min was not homogeneous, obtaining in median a lower BAC than the estimated one ($0.85 \pm 0.12\%$ BAC; 32 ± 3 min). However, such level remained quite stable during the whole recording period (sample distribution of median of BAC for each subject, $0.80 \pm 0.10\%$ BAC; sample distribution of BAC variability, i.e. MAD, for each subject: $0.03 \pm 0.02\%$ BAC).

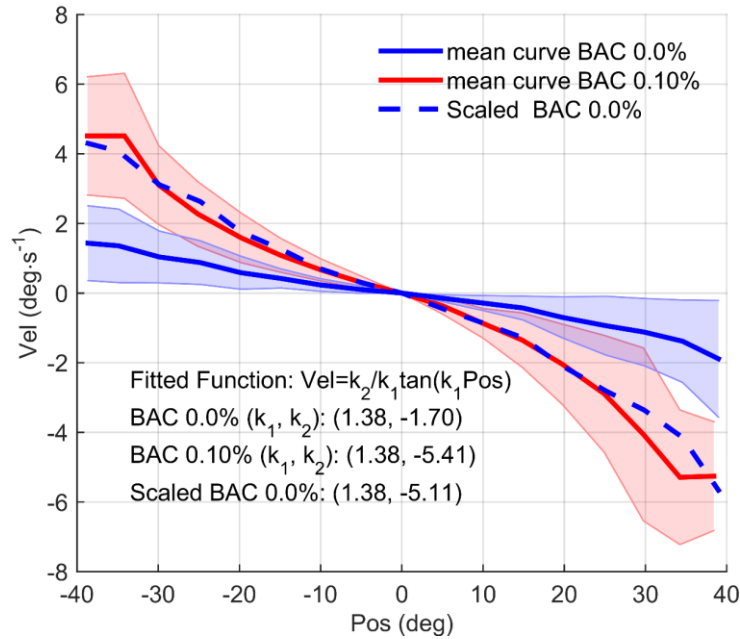


Figure 3.8: Change in position-velocity relationship induced by acute alcohol intoxication of 0.10% BAC. Each line represents the mean drift velocity of all subjects in the different conditions, while the shaded area represents the mean ± 1 standard deviation. The blue dashed line is a scaled version of the data recorded before alcohol intake (blue solid line), overlapping with the data recorded after alcohol intake (red solid line), confirming the pure scaling effect of 0.10% BAC. Such an effect is further confirmed by the scaling parameter k_2 of the tangent model, which was estimated on the plotted curves (the estimated parameters are reported in the figure). Acute alcohol intoxication, instead, seems not affect the non-linearity of PV relationship, as confirmed by the shaping parameter k_1 .

The direct comparison of before and after alcohol conditions in 0.10% group (see Section 3.2.6.1 and Eq.(3.2)) revealed a significant increase in eye drift velocity compared to our data with lower BAC (0.06% group, see Section 3.3.1). Specifically, the ratio of the median ratios distribution (2.40 ± 0.60) was significantly higher than two (Wilcoxon signed rank test, $p=0.01$), suggesting an alcohol effect on gaze-holding mechanism that increases centripetal eye-drift velocity more than two-folds.

The overall alcohol effect is also showed in Figure 3.8 comparing in 0.10% group the mean of PV curves BA and AA intake (data of all subjects are pooled). The increase of drift velocity seems to be homogenous for all gaze angles, while the shape of PV relationship seems unaffected even by a greater BAC. The scaled version of the BA curve, computed multiplying the median baseline PV curve (solid blue curve) by a scaling factor of three, confirmed such hypothesis matching the AA curve (red line).

Despite all these findings suggest direct relationship between the BAC increase and increase of drift velocity (2 and 3 time respectively for 0.06% and 0.10% groups), the model-based approached (see Section 3.2.6.2) unveiled a more complex effect of alcohol in 0.10% group.

Comparing the AA to BA conditions, a clear alcohol-induced effects is visible in both shaping (k_2) and scaling (k_1) distributions (Table 3-2).

The statistical comparison of coefficient ratios confirmed such evidence. Specifically, the Wilcoxon signed-rank test confirmed that the ratio of scaling factor k_2 (2.91 ± 0.79) was statistically different from one ($p=0.0001$), suggesting a proportional increase of drift velocity for all gaze angles, according to previous result achieved through the direct comparison.

On the other hand, even the paired comparison of the shaping coefficient (k_1 ; ratio distribution: 1.20 ± 0.23) revealed a slight but significant change in shape of PV-relationship (Wilcoxon signed-rank test, $H_0: k_1^{AA}/k_1^{BA}=1$; $p=0.01$), conversely to the data shown in Figure 3.8.

3.3.5. BAC 0.10%: Pure scaling vs Shaping and scaling effect

As mentioned in the previous section, statistical comparisons of model parameters suggested that acute alcohol intoxication induced both a scaling and shaping effects on the PV relationship.

Conversely, the preliminarily analysis on “average subject” (Figure 3.8) shows unvaried shaping factors between the BA and AA mean PV curves.

These contrasting findings are due to nonhomogeneous effect of acute alcohol intoxication, suggesting that changes in the shape PV relationship may happen in only few subjects and may be “hidden” in the “average subject”, i.e. the mean curve.

Consequently, the 0.10% dataset was split in two subgroups, respectively: the pure scaling (PS) and the scaling and shaping (SS) group. Each subject was individually assigned to one group, according to a visual

comparison of its PV plot before and after alcohol intake. Accordingly, 8 out of 15 subjects were assigned to the pure scaling subgroup, while 7 out of 15 to the scaling and shaping one.

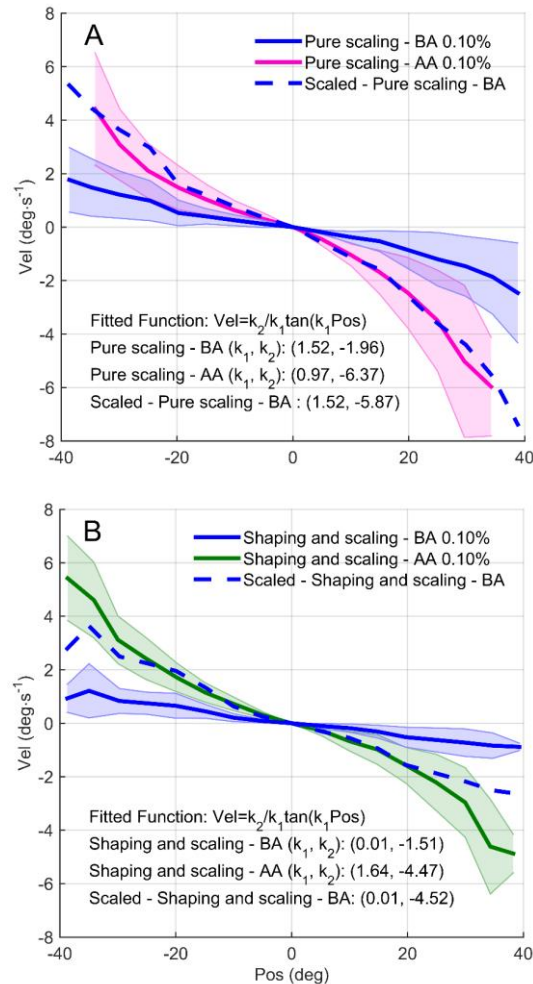


Figure 3.9: Different alcohol-induced effects on PV-plot in two subgroups of subjects from the 0.10% dataset. Each line represents the mean drift velocity of all subjects in the different conditions, while the shaded area represents the mean ± 1 standard deviation. A. In pure shaping subgroup, acute alcohol intoxication induces a homogeneous increase of drift velocity (red curve) respect to its baseline (solid blue curve). A simple algebraic multiplication of the mean recorded before alcohol intake by a factor of 3 (dashed blue curve) correctly models the pure scaling effect of alcohol. B. A differ alcohol-induced effect is shown in the shaping and scaling subgroup. Specifically, the mean curve after alcohol consumption (green curve) shows an increase of drift velocity for all gaze angles and an alteration in nonlinear PV relationship compared to its baseline condition (solid blue curve). Therefore, the scaled version of the data recorded before alcohol intake (blue dashed line) does not match the AA condition, suggesting both scaling and shaping effect. Both effects are further confirmed by the k_1 and k_2 parameters of the tangent model, which was estimated on the plotted curves (the estimated parameters are reported in each panel).

Each subgroup was thus individually tested to verify the subject-dependent effect of acute alcohol intoxication.

The direct comparison in both PS and SS subgroups confirmed our results found in 0.10% dataset analysis. Specifically, the Wilcoxon test for paired samples revealed that the median of ratio distributions between AA and BA was significantly higher than one for both PS (2.49 ± 0.79 ; $p=0.0078$) and SS (2.35 ± 0.58 ; $p=0.01$) datasets. Moreover, the median amount of drift velocity was also comparable between the two subgroups, as the unpaired comparison of their ratio distribution was not statistically significant (Wilcoxon rank sum test, $p=0.95$).

Different results were obtained comparing the two parameters of the tangent model (Eq.(3.1)). As reported in Table 3-2, the distribution of scaling factor k_2 is comparable between the PS and SS groups for both AA and BA conditions, while the distribution of scaling factor k_1 is clearly different between PS and SS subgroups.

Such observations were confirmed by statistical comparison of the AA-BA ratios of the estimated coefficients (Eq.(3.2)). Specifically, Wilcoxon signed-rank test showed that the ratio of the scaling factor (k_2) was statistically different from one for both PS (3.15 ± 1.10 ; $p=0.008$) and SS (2.91 ± 0.65 ; $p=0.02$) subgroup. On the other hand, Wilcoxon rank sum of PS and SS k_2 ratio did not reveal any statistical difference ($p=0.77$) suggesting that alcohol induces a comparable increase (“scaling”) of drift velocity in both subgroups (Table 3-2).

The comparisons of k_1 ratios, instead, revealed a different result in PS and SS subgroups. In PS group the ratio of the shaping coefficient k_1 (1.04 ± 0.07) was not statistically different from one (Wilcoxon signed-rank test, $p=0.001$), suggesting only a steady effect of alcohol on drift velocity independent of gaze angle. Conversely, the shape of PV function in SS subgroup was affected by alcohol, as confirmed by Wilcoxon signed-rank ($H_0: k_1^{AA_SS}/k_1^{BA_SS}=1$; $p=0.02$).

Moreover, the unpaired comparison of k_1 ratio between PS and SS groups confirmed a difference between the datasets (Wilcoxon rank sum test, $p=0.0003$).

Both PS and SS effects induced by alcohol are also clearly visible in Figure 3.9, comparing the mean of individual velocity curves before and after alcohol consumption in both subgroups. Specifically, in SP subgroup (Figure 3.9A), the scaled version of the mean curve before alcohol intake (dashed blue line) well approximates the mean AA curve (magenta curve), while in SS (Figure 3.9B), the algebraic multiplication of BA curve cannot model the shape-change of mean AA curve (green curve).

It is worth noting that the shaping effect induced by acute alcohol intoxication in SS group is likely due to a lower k_1 value (see data distributions in Table 3-2 and Figure 3.10) in the baseline condition (i.e. more linear PV-behavior). The Wilcoxon rank sum test between the two subgroups baseline (i.e. PS-BA versus SS-BA) confirmed such observation, as the median value of k_1 in SS-BA condition was statistically lower than k_1 in SP-BA (Wilcoxon rank sum: $p=0.03$). Conversely, after alcohol

consumption, median value of k_1 was not statistically different between the two subgroups (PS-AA versus SS-AA; $p=0.99$).

Regarding alcohol-induced scaling effect, the k_2 median value was not statistically different between PS and SS, either for BA ($p=0.95$) or AA ($p=0.61$) conditions.

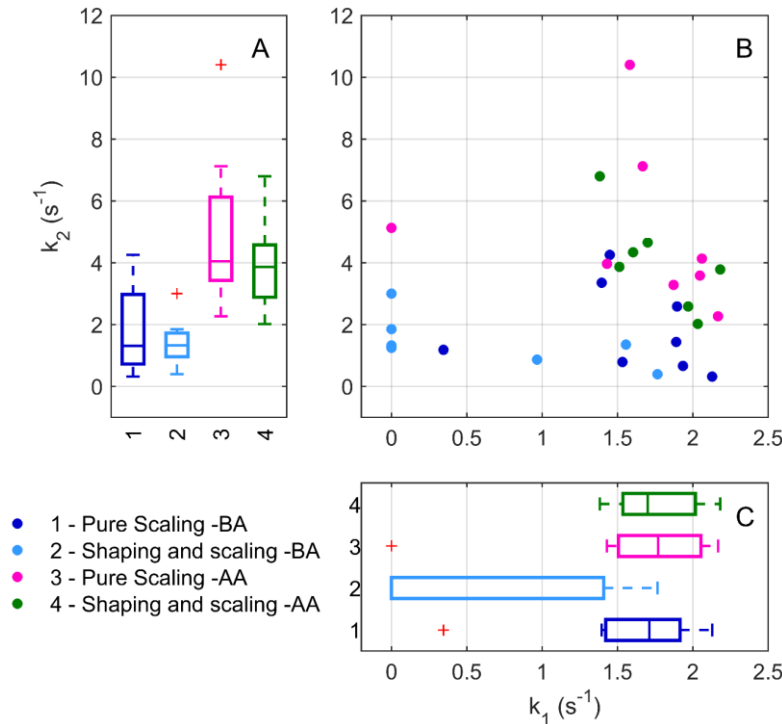


Figure 3.10: Shaping (k_1) and scaling (k_2) factor distribution before and after alcohol consumption in 0.1% subgroups. Boxplot: Central mark indicates the data median, while bottom and top edges of the box indicate the 25th and 75th percentiles, respectively. The alcohol-induced gaze instability is clearly visible in the increase of the scaling factor k_2 in both subgroups after alcohol intake (magenta and green boxes, panel A) compared to their baseline conditions (dark and light blue respectively for pure scaling and shaping and scaling subgroup). In pure scaling subgroup, no changes in nonlinear PV relationship are induced by acute alcohol intoxication as confirmed by comparing the shaping k_1 factor distributions BA and AA conditions (in panel C respectively, dark blue and magenta boxes). Conversely, an increase in nonlinearity is observed in the shaping and scaling subgroup. AA consumption, indeed, the median value of k_1 (green box) is clearly greater than the one in baseline (light blue box). However, such increase is not in absolute terms as the k_1 factor distributions of both subgroups are comparable AA intake (magenta and green boxes, panel C). The overall alcohol effect is visible in panel B, plotting k_1 vs k_2 . Independently of baseline conditions (dark and light blue points), after acute alcohol intake almost all subjects are identified by a $k_1 > 1.4$ and $k_2 > 2$, suggesting a “rule” for classifying intoxicated subjects.

3.3.6. Evaluation of model parameters

The correlation analysis between the coefficients k_1 and k_2 in Eq.(3.3) confirmed that the tangent model allows distinguishing two patterns of gaze-holding behaviors. Independently of the condition and group (0.06 and 0.10%) being analyzed, k_1 and k_2 did not show a significant correlation (BA: $\tau < |0.30|$, $p > 0.05$; AA: $\tau < |0.30|$, $p > 0.05$; using Kendall nonparametric correlation coefficient τ), proving that Eq.(3.3) provides two uncorrelated features to summarize gaze-holding behavior.

Table 3-1: Data distributions in 0.06% group

Pooled data	Shaping coef. k_1 (s^{-1})	Scaling coef. k_2 (s^{-1})
	med \pm MAD	med \pm MAD
Both eye healthy subjects in [50]	1.39 \pm 0.49	1.48 \pm 0.89
Both eyes BA	1.28 \pm 0.55	1.85 \pm 0.83
Both eyes AA	1.66 \pm 0.13	2.98 \pm 1.27
Left eye BA	1.51 \pm 0.21	1.37 \pm 0.97
Right eye BA	1.27 \pm 0.72	1.69 \pm 0.87
Left eye AA	1.42 \pm 0.30	2.77 \pm 0.95
Right eye AA	1.61 \pm 0.47	2.97 \pm 1.24
Nasal eye BA	1.52 \pm 0.44	1.00 \pm 0.74
Temporal eye BA	1.33 \pm 0.39	2.19 \pm 0.63
Nasal eye AA	1.51 \pm 0.72	3.56 \pm 2.06
Temporal eye AA	1.54 \pm 0.19	3.21 \pm 1.35

Table 3-2: Data distributions in 0.10% group

Pooled data	Shaping coef. k_1 (s^{-1})	Scaling coef. k_2 (s^{-1})
	med \pm MAD	med \pm MAD
Healthy subjects in [50]	1.39 \pm 0.49	1.48 \pm 0.89
BA 0.10%	1.45 \pm 0.48	1.32 \pm 0.54
AA 0.10%	1.70 \pm 0.27	3.96 \pm 0.70
Pure scaling - BA	1.71 \pm 0.24	1.32 \pm 0.82
Pure scaling - AA	1.77 \pm 0.28	4.05 \pm 0.92
Shaping and scaling - BA	0.01 \pm 0.70	1.33 \pm 0.46
Shaping and scaling - AA	1.70 \pm 0.27	3.86 \pm 0.79

3.4. Discussion: Alcohol-induced GEN a model of cerebellar GEN

Chronic alcohol consumption causes progressive changes in cerebellar morphology and functionality [147], [206]. Thus, alcoholics can manifest symptoms similar to those typical of patients with hereditary cerebellar disease. Impaired gaze stability, an ocular-motor sign shared by various cerebellar diseases, is encountered also during acute alcohol intoxication, as a consequence of the loss of efficiency of the VPNI due to transient cerebellar impairment.

Using the methodology validated in [50], [53], we quantified the changes in the gaze-holding behavior induced by alcohol. By measuring eye-drift velocity as a continuous function over $\pm 40^\circ$ of gaze eccentricity and fitting a 2-parameters tangent function to the data, we showed a consistent effect of 0.06% BAC in all subjects. The effect was similar at all gaze eccentricities, causing a two-fold increase of the centripetal eye-drift velocity. Similar but increased effect was also shown after acute alcohol intoxication ($>0.08\%$ BAC), causing a three-fold increase of drift-velocity.

Our finding in 0.06% group was confirmed using three different approaches. First, the distribution of median ratios obtained as the ratio of each subject's raw data recorded after alcohol (AA) to that before alcohol (BA) (i.e. without model assumptions) showed a gaze-independent increase of median drift velocity by a factor close to two (2.21 ± 0.55). Second, using the tangent function, we demonstrated that alcohol has a pure scaling effect on eye-drift velocity, since only the scaling coefficient k_2 was significantly increased after alcohol intake. As the ratio of k_2 in AA to BA conditions (1.96 ± 0.82) is also close to two, we conclude that the observed medians' increase could be explained by the scaling factor. Third, the velocity curve "average subject BA" multiplied by a factor of two almost perfectly overlaps with the curve "average subject AA" (Figure 3.5).

Analogous approaches were used for 0.10% group. Specifically, in all subjects, the overall effect of acute alcohol intoxication (BAC $>0.08\%$) was a three-fold increase of drift velocity, as confirmed by the scaled version of "average subject BA" curve (multiplied by a factor of 3) which almost perfectly overlaps the curve of the "average subject AA" (Figure 3.8). Such effect was further confirmed in the ratio of k_2 in AA to BA conditions (2.91 ± 0.79) which is close to three.

Thus, our results in both groups suggest that the alcohol-induced scaling effect is related to BAC, and the increase of drift velocity with respect to BA condition is consistent between subjects. Moreover, scaling effect seems to be "additive" irrespective of the subject's gaze stability in baseline, and it is preserved both in subjects with stable and with leakier VPNI (such as the subjects from the two subgroups in 0.10%).

However, in 0.10% group, a second alcohol-induced effect was not observed in all subjects, identifying two subgroups of subjects. Specifically, 7 out of 15 subjects showed an alcohol-induced alteration of

nonlinear PV relationship in addition to the scaling effect. The other eight subjects instead, just showed a homogenous increase of drift velocity (as in 0.06% group).

The unpaired comparison on model coefficients revealed that such discrepancy between the 0.10% subgroups was mainly due to dissimilar baseline conditions (Figure 3.10). The alcohol-induced shaping effect, in fact, was visible only in subjects characterized by almost linear PV-relationship BA (i.e. more stable VPNI for more eccentric gaze angles), as shown by the k_l distribution (Table 3-2).

Such finding suggests that that alcohol-induced shaping effect is “limited”, and cannot be “accumulated” worsening the nonlinearity of VPNI, which may be already present for the intrinsic VPNI weak performance in more eccentric gaze angles or may be induced by other factors (such as sleepiness or fatigue).

Non-pathological GEN at gaze angles smaller than expected for EPN was previously reported in healthy subjects after alcohol consumption [69], [70], [181], [183]. Previous studies focused on the nystagmic response only considering that the observation of nystagmus is used to assess gaze-holding deficits in patients and to assess the “driving while intoxicated” condition through visual inspection [71], [183], [185], [220], [221]. Yet, the results of these studies are inconsistent and prevented so far the forming of a shared consensus on the use of GEN to assess alcohol intoxication. The core of this dispute [68], [184] lies in the consistency of the alcohol-induced GEN between individuals and on the discriminability of such an effect from normal variations due to other factors.

To our knowledge, the experiment presented in this study is the first to assess the effect of alcohol on the amount of gaze-dependent eye-drift, i.e. the deficit causing nystagmus, and therefore to directly investigate the mechanism of alcohol-induced gaze instability. Due to this approach our results shed new light on the contrasting findings reported in the literature. First, we determined that the effect of alcohol on gaze-holding is consistent across subjects. Second, we evidenced that the eye-drift velocity after alcohol intake depends strictly on the one before alcohol consumption.

The distinction between these two statements is important when evaluating the relationship between GEN and BAC. In our experiments, the impact of alcohol intake was extrapolated from intra-individual comparisons of gaze-holding performance immediately before and shortly after drinking. Despite the eye-drift velocity BA varied considerably among subjects [70], [71], leading to variable drift velocities AA, a BAC of 0.06% always caused BA velocity to roughly double, and such effect is emphasized by $BAC > 0.08\%$, (three-fold increase). Therefore, our results suggest that, even if alcohol effect is consistently increasing eye-drift velocity, the manifestation of nystagmus, which is governed by drift velocity but is also influenced by other factors, will be highly unpredictable due to the large variability of BA drift velocities between subjects.

Hence, our results cast a doubt on the reliability of using GEN for discerning the driving while intoxicated condition, as subjects with the

same amount of BAC may or may not present with GEN as a function of their different BA eye-drift behavior.

As a final remark, it is worth noting that while the drift amount may be used as a valuable criterion to identify acute alcohol intoxicated subjects only ($>0.08\%$), in subjects with lower BAC (as 0.06% , close to legal alcohol limit for driving) the specificity of such criterion (i.e. healthy people who are correctly identified as alcohol intoxicated) may be insufficient.

The findings presented in this study also allow a better understanding of the mechanism linking cerebellar impairment and gaze-holding deficits. In patients with cerebellar disease [53], the tangent function model [50] evidenced three distinct subgroups of patients, namely: a “pure scaling” subgroup, showing a consistent increase of eye-drift velocity with respect to normal values at all gaze angles; a “shape-change” subgroup, with abnormal drift velocity only for large gaze angles, and a subgroup showing a mixture of the two behaviors. Although the authors observed that patients with symptom-onset at a later stage in life presented a “pure scaling” behavior, the heterogeneity of patients populations in [53], prevented linking gaze-holding behaviors and medical findings.

Our experiments evidence that 0.06% and higher BAC cause a “pure scaling” effect. We hypothesize that such a gaze-independent - i.e. global - decrease in gaze-holding abilities reflects diffuse cerebellar loss of function. This decrease, although of lesser magnitude, resembles the change observed in the pure scaling patient subgroup, reinforcing the hypothesis [53] that such patients may suffer from more diffuse cerebellar loss-of-function as compared to patients with a shape-changing pattern.

Such similarity suggests that a controlled amount of alcohol intake provides a promising human model to study the effect of global cerebellar hypofunction to better understand the patho-mechanisms of progressive cerebellar degeneration. As the healthy cerebellum prolongs the VPNI time constant, alcohol intake may reduce this time constant and, consequently, lead to an increase of eye-drift velocity for all gaze angles, i.e. to a “pure scaling effect” due to global reduction of cerebellar control.

Regarding the mechanism inducing such an effect, different explanations are possible. First, it can be linked to the inhibitory effect of alcohol on the cerebellum, reducing cerebellar blood flow [222] or to diffuse alteration of Purkinje cell function [150], [151], [156], [223]. Second, the cerebellar cortex is one of the most sensitive brain regions to alcohol [148], and alcohol consumption seems to alter the firing pattern of cycling and spontaneous activity of Purkinje cells, introducing irregularities in their discharge [150]–[154]. As the firing activity of Purkinje cells encodes specific physiological functions [224], alcohol consumption may alter cerebellar functions affecting motor coordination, equilibrium [154], [156] and gaze-holding mechanisms.

Eventually, in contrast to previous reports [64], [67], the analyses performed separating data from both eyes and hemifields in 0.06% group, showed no differences. The PV-plots of LE and RE, however, did not

completely overlap when plotted separately (Figure 3.6A, C). We believe that such difference represents an artifact induced by the physiological drift of the eyes toward the resting point of vergence. In absence of an adequate visual stimulus (in most gaze-holding studies the target flashes), indeed, the eyes drift towards their resting point, defined not only by vertical and horizontal position, but also by vergence.

As on average the fixation point of vergence at rest lies at about 1m distance [215], [216], although widely variable among subjects, and such distance frequently differs from the one between the target and the subject (e.g. 1.5m in our setup), the eyes frequently perform vergence movements induced by tonic vergence [216], [217].

In the PV-plot this causes eye-specific, positional offsets between the eye null and the null position in the target frame of reference (i.e. the resting point of vergence and our PV-plot zero, respectively). Such eye-specific offsets result in a discrepancy between the null positions of the two eyes matching the one observed in our data shown on the PV-plot (Figure 3.7). These differences need to be taken into account to distinguish gaze angles in temporal from nasal hemifields, as the null position of the eye needs to be extrapolated from the data. Using the fixation straight ahead as null point to separate eye movement directions, may have led to the previously observed asymmetries [64], [67]. We avoided this confounder by shifting PV-curves of each eye on the basis of the null position separately estimated for each eye.

Noteworthy, the comparison of the parameters of the tangent function describing gaze-holding between TH and NH showed no significant differences between directions both in BA and AA (BAC 0.06%) condition. This consistency is important, since the high variability in the values of k_2 coefficient of TH and NH BA might have hidden an actual difference between directions. Alcohol intake, causing a scaling effect on both gaze angles in nasal and temporal hemifields would, however, amplify such difference, making it visible AA in 0.06% dataset. The absence of any significant difference for k_2 in the AA condition (Table 3-1), therefore supports the conclusion that such differences are absent also in the BA condition.

Chapter 4

How can Zebrafish contribute to the understanding of ocular motor disorders?

4.1. Background

Throughout the last decade Zebrafish has been widely used as a model organism in several fields of scientific research from genetics to developmental biology passing through neurophysiology [100]. More recently, Zebrafish has been used as a powerful tool in neuroscience, allowing to study human-like behaviors such as sleep, fear, anxiety, social behavior, learning and neurological conditions such as alcoholism, drug addiction and ocular motor abnormalities [31], [112], [113], [225], [226].

The “versatility” of this bony fish is due to several analogies with other complex vertebrates, making it one of the favorite non-mammal model organisms for analyzing the neural basis of behavior. Moreover, since its CNS presents several neural structures which are physio-anatomically and functionally comparable to human ones, such organism has been used as a model for investigations of the human brain, improving our understanding of complex neural mechanisms [117], [118].

Thus, exploiting the analogies between human and zebrafish CNS together with the advantages of using eye movements in the field of neuroscience (see Section 1.1), zebrafish research has led to new findings on the architecture of neural networks in the brain and has been extensively used as a novel tool for modeling neurological and neuropsychiatric disorders.

Specifically, as mentioned in Section 1.5.2, functional similarity in zebrafish and human brainstem has shed light on the neural implementation of VPNI [75]. Understand such mechanism does not only provide increased knowledge about the ocular motor system and its abnormalities, but even

new insights on temporal integration, which is fundamental to arrange motor, memory and decision-making tasks [76].

The success of zebrafish in eye movements research is also due to two fundamental features of such fish: the analogies between the human visual cortex and the optic tectum (i.e. a primitive visual cortex) in the fish and those between the two visual systems, despite some notable structural differences (e.g. lateral eyes and lack of fovea) [113], [120]. As a consequence, zebrafish has been used as a model to study the cellular and molecular mechanism of pathogenesis of several human eye diseases [112]. At the same time, the benefits related to zebrafish high fertility allow to perform high-throughput screening test for potential drugs used for treating human eye diseases (e.g. gentamicin and paromycin) [227].

Besides the brainstem and visual cortex, the cerebellum also plays a pivotal role in ocular motor control in humans. Such neural structure is preserved in mammals (such as cats and monkeys), which are usually used as the most common model organisms to investigate cerebellar function. Even zebrafish present a cerebellum, as the other vertebrates do, therefore we wondered whether it could be used to pursue the same research goals.

In fact, little is known about the role of zebrafish cerebellum in eye movements control, although it shares functional and anatomical analogies with the cerebellum of human beings [122], [228], [229]. Specifically, a detailed and comprehensive anatomical description of CNS in zebrafish revealed that its cerebellum is composed of three lobes (i.e. valvula cerebelli, corpus cerebelli, and vestibulolateral lobe) like the human one, and presents human-like circuits formed by granule cells parallel fibers and Purkinje cells [121]. Regarding cerebellar functionality instead, optogenetic recording of selected Purkinje cell regions during zebrafish behavior suggests potential analogies in teleost and mammal cerebellum [122]. Such findings confirmed that zebrafish presents a functional regionalization of Purkinje cell efferents revealing their contribution to behavior control as well as their function in controlling lateralized behavioral output.

However, although recent findings suggest that the caudal part of the cerebellar Purkinje cell layer is involved in the control of saccadic eye movements, the lack of deep cerebellar nuclei suggests that cerebellar ocular motor control in zebrafish may be partially different from the human one [229].

Zebrafish may be a perfect model for ocular motor research but only a better understanding of the role of the cerebellum in controlling the eye movements of the fish would allow to rightfully consider it as a model for cerebellar diseases.

Thus, in our research we attempt to shed light on cerebellar functions in the zebrafish exploiting the well-known relationship between cerebellar deficits and ocular motor abnormalities (see Section 2.1). Specifically, we propose here to investigate whether our findings about alcohol-induced effect on the human cerebellum may be generalized to the zebrafish one.

The alcohol-induced gaze instability in humans is indeed provoked by cerebellar impairment, which causes a deficient neural integration. Although another cerebellar mechanism (VSM) has been observed in OKR experiments [230], cerebellar action on VPNI time constant has never been verified in zebrafish.

We thus tried to verify the hypothetical involvement of the cerebellum in the gaze-holding system of the fish by altering its function with alcohol and studying potential ocular motor abnormalities.

To evaluate the effect of alcohol on gaze-holding, we recorded spontaneous zebrafish eye movements for estimating the VPNI time constant, while a main sequence was computed using gaze redirecting fast phases to assess any effects on the saccadic system.

Moreover, since our analysis is the first attempt to measure a possible alcohol impairment of the zebrafish ocular motor system, we analyzed eye movements of both larvae and young adult zebrafish individuals hoping to overcome the possible limitations related to an only partial development of the gaze-holding structures in the larvae [230]. We first performed a preliminary analysis using small sample of larvae to detect a macroscopic ethanol effect, exposing larvae to five different concentrations, which are typically used in toxicological studies. Afterwards, we focused more specifically on ocular motor effects of ethanol, by exposing juvenile zebrafish to typical concentrations used for behavior studies.

4.2. Materials and methods

4.2.1. Maintenance and breeding of Zebrafish

AB wild-type zebrafish strain were bred and maintained as previously described in [231]. Briefly, embryos were raised under a 14-hour light, 10-hour dark cycle in 28°C E3 Medium (in mM: 5 NaCl, 0.17 KCl, 0.33 CaCl₂, and 0.33 MgSO₄) and staged according to development in days post-fertilization (dpf) [232].

Zebrafish specimens were collected for our experiments from two different developmental stages: larval stage at 5 to 6 dpf, and juvenile stage at 38 to 44 dpf. For each experimental condition (see Section 4.2.3) 8 larvae or 14 young adult individuals were tested.

4.2.2. Experimental setup

In order to suppress whole-body motion, two different procedures were used to constrain zebrafish, respectively for larva or juvenile zebrafish.

Single larva was embedded dorsal side up in a transparent 21mm diameter plastic dish filled with 3.5% methylcellulose. Methylcellulose

allows us to embed the larvae without impairing skin respiration through gas diffusion [100].

For juvenile zebrafish, instead, gas exchange happens in gills, which are fully developed. Thus, since gills movements must not be impaired and water must pass through, young adult zebrafish were embedded dorsal side up in the center of a 21mm transparent plastic dish using a 1.8-2% agarose gel (Sigma Type VII-A). Specifically, low gelling temperature agarose was used allowing to handle agarose in the range of fish-life compatible temperatures (i.e. a temperature slightly greater than agarose gelling point 26 ± 2 °C). Once the agarose had set, the gel was covered with E3 Medium water and an ophthalmic scalpel was used to dissect sections away so as to permit free movements of the eyes and gills allowing the fish to breath. During the whole process (less than 1 min), zebrafish were previously anesthetized by using 4% tricaine solution (procedure as in [233]). After the embedding, fish recovery was done using E3 medium water, waiting 20 minutes before starting the experiment. Moreover, to check whether the fish fully recovered from anesthesia or some damages occurred during the embedding process, a brief OKR test was executed.

Once embedding procedure was concluded, the larvae or juvenile zebrafish were placed inside the cylinder at a distance of the fish's eye to the screen of approximately 6.8 cm, and the tube was illuminated from below with infrared (IR)-emitting diodes ($\lambda_{\text{peak}}=875\pm 15$ nm, OIS-150 880, OSA Opto Light GmbH, Germany). IR light allowed us to perform recordings in total darkness without any visual stimuli, as zebrafish eye receptor are not sensitive to light with wavelengths greater than 564 nm [112].

During the whole experiment, movements of both eyes and body were recorded by an IR-sensitive charge-couple device (CCD) camera with a sample rate of 40 frames per seconds.

4.2.3. Experimental procedure

To evaluate the effect of alcohol on the gaze-holding and saccadic systems, spontaneous eye movements in the dark were recorded for 10 min. As alcohol-induced ocular motor abnormalities have never been studied in fish, no previous data about appropriate ethanol concentrations are available. However, since several studies about acute alcohol intoxication were performed on zebrafish, we started off by adapting the most commonly used ethanol concentrations [226], [234]–[238]. Eventually, we followed two different experimental procedures for testing the larvae and young adults.

Procedure for larvae: Following the data on ethanol toxicity available in the literature, we considered ethanol concentrations between 1% and 10%, which are commonly used in toxicological studies on larvae [235], [238]. Four independent groups were formed, randomly selecting larvae from a single clutch. In each group, larvae were individually tested and exposed

for 20 min to 0, 1.25, 2.5, 5 or 10% ethanol solution (ethanol and E3 Medium water). After the ethanol exposure, larvae were immediately embedded (as shown in Section 4.2.2) and the eye movements were recorded for 10 minutes in total darkness. Following the experiment, larvae were euthanized using non-dilute tricaine solution.

Procedure for young adult zebrafish: Three different concentrations (0.2, 0.5 and 0.8%) were used, within the range considered for behavioral assays during acute intoxication [226], [237].

Each group was formed by randomly selecting zebrafish from a different clutch. To limit any potential difference due to possibly altered developmental process, ethanol effects were evaluated comparing zebrafish before and after ethanol exposure (BE and AE, respectively).

Specifically, after embedding (see Section 4.2.2), spontaneous eye movements of single specimen were recorded for 10 minutes in total darkness obtaining the baseline condition (BE). Subsequently, the specimen was exposed to ethanol solution for 20 minutes and recorded for 10 minutes (AE). Lastly, zebrafish were euthanized using non-dilute tricaine solution.

4.2.4. Eye movements extraction

Due to the different stages of the developmental process, larvae and adult zebrafish have different morphological features, which encouraged us to use two different algorithms for the extraction of eye movements from the recorded videos.

Eye movements extraction algorithm for larvae: Larval eye positions were measured and recorded using a real-time video system that was already validated in [30], [230]. Each frame is processed by custom-developed software (LabVIEW 10.0; National Instruments, USA). Exploiting the high transparency of larvae, a simple threshold method allows to identify the opaque eyes in real-time. Therefore, before the recording begins, the user has to manually select three regions of interest (ROI) around each eye and the body, the threshold level and parameters of morphological operators (i.e. number of iterations) allowing accurate image segmentation.

The software extracts the ellipse-like shape of the eye from the ROI by using the user-selected parameters and computes the angular eye position by means of the center of mass and the axis with the lowest momentum of inertia for each eye. A similar process was used to extract body angles.

Video recording and analysis of eye and body positions are achieved in real-time and are displayed on the software user-interface during the experiment. For the subsequent off-line analysis of the eye movement, a vector containing a time stamp, the eye and body position computed on each frame were saved in a text file.

Eye movements extraction algorithm for juvenile and adult zebrafish: Eye movement extraction for juvenile and adult zebrafish was implemented through a second custom-developed algorithm, as their body is also

partially or completely opaque to IR light and therefore the eye cannot be directly identified based on a simple threshold.

Our novel algorithm was fully developed in MATLAB. Specifically, each recording is first acquired and stored through Labview custom-developed software and subsequently analyzed off-line by our algorithm.

Briefly, our algorithm is designed based on two processing steps: segmentation and features extraction. The first step concerns eye recognition using the “Hough Transform” which identifies circle-like shapes and their center of rotation. The second step instead computes the angular positions of the eyes using an “Image registration Method” which estimates the parameters of the affine transformation that minimizes the difference between two subsequent frame. Body angles on each frame, instead, were computed based on the same algorithm described for larvae.

After processing the video frames, in order to standardize the outputs of both algorithms for simplifying further analyses, the time stamp, the eye and body position computed on each frame were saved in a text file.

4.2.5. Data post-processing

Both post-processing and data analysis were implemented in off-line codes written in MATLAB.

Data were imported from our standardized text files, and eye and body angles were resampled at 40 Hz, avoiding erroneous changes in frame rate due to delays in the acquisition process.

Absolute eye position was computed using the body angle, subtracting the temporal median value of the body position signal from eye movements traces. Moreover, we considered positive the clockwise angles and negative the counter-clockwise. Missing data (e.g. due to fish movement) were not interpolated.

Our custom-developed velocity-based algorithm used for analyzing human data, responsible for identifying slow-phases and saccades (see Section 3.2.4 in Material and Methods) was adapted for zebrafish eye movement data by introducing only a few changes. Specifically, two parameters were added for the post-processing of identified saccades: we imposed a maximum duration and a minimum amplitude of saccades, i.e. only saccades shorter than 1 second and with an amplitude greater than 1° were evaluated. One additional parameter was introduced for the post-processing of slow-phases: minimum duration of 1 s, in order to grant enough data points for performing an exponential fit.

The chosen post-processing parameters were not too strict so that only obviously erroneous slow-phases and saccades were removed, without altering the overall analysis.

An additional post-processing step was performed for slow-phases of juvenile zebrafish, as gill breathing superimposed a sinusoidal noise, i.e. the breathing cycle, on eye movements traces. A 4th order Butterworth stopband filter was implemented to individually filter each slow-phase. The

stopband corner frequencies were estimated on the whole signal as the most powerful components of the power spectrum in order to filter the breathing cycle of the fish.

4.2.6. Data analysis

Ethanol-induced effects on cerebellum were evaluated analyzing performances of the saccadic and gaze-holding systems.

4.2.6.1. Data analysis: Saccades

Saccades performance was assessed through main sequence analysis by plotting saccade amplitude (A_S) against peak velocity (V_S^{Peak}). Based on previous studies in goldfish [239] we used a straight line to fit the peak velocity-amplitude relationship instead of the nonlinear relationship typical of human saccades, where large saccades show a soft saturation of peak [240]. Specifically, for each specimen, we summarized the main sequence by computing the slope of best fitting line straight line, m_S :

$$V_S^{Peak} = m_S A_S \quad (4.1)$$

The slope parameter m_S was then used for evaluating ethanol-induced abnormality in neurophysiological control of saccades.

The spontaneous saccade frequency f_S , i.e. the average number of saccades per time unit, was also estimated for each specimen to investigate possible ethanol-induced sedative effect.

4.2.6.2. Data analysis: Slow phases

To assess the function of the gaze-holding system we analyzed the VPNI time constant (see Section 1.3.2) and adopted the most common approaches for both humans and goldfish [50], [84], [124], [239]: direct estimation of the VPNI time constant and PV-plot representation. It is worth noting that both methods assume that all eye positions share a common null point, albeit experimental observations show multiple null points in goldfish [123]. Despite such assumption, both methods were used for ease of interpretation and of comparison of our results with those in the literature.

Direct estimation of VPNI time constant: under the assumption of linear VPNI, the eye drift velocity caused by leaky neural integration is well approximated by a first-order differential equation (see Eq.(1.7)). We thus used the following differential equation to describe the temporal slow phase decay $E(t)$ in zebrafish:

$$E(t) = A e^{-\frac{t}{\tau_c}} \quad (4.2)$$

Each specimen's VPNI the time constant (τ_c) was estimated on all pooled slow-phases using a logarithmic transformation of Eq.(4.2), which allowed to fit a linear function to each slow-phase, as follows:

$$\ln(E(t)) = \ln\left(Ae^{-\frac{t}{\tau_c}}\right) = \ln(A) - \frac{t}{\tau_c} \quad (4.3)$$

Consequently, the VPNI τ_c was estimates as the inverse of the straight line slope, while the intercept ($\ln(A)$) was optimized only to improve the estimate and was not used for the following comparisons.

PV-plot analysis: VPNI performance was evaluated by means of position-velocity plot representation, similarly to gaze-holding analysis in humans (see Chapter 3). The PV-plot representation, instead, allowed us to appreciate potential alcohol-induced changes in the nonlinear relationship between eye position and drift velocity (as with cerebellar deficit in [53]). Such analysis was carried out as detailed in section 3.2.6 (Data Analysis), except for a few adjustments performed to take into account the specific features of zebrafish eye movements.

The main change concerns the estimation of the null eye position. In fact, the absence of a fovea in zebrafish' eyes does not allow us to correctly identify the zero position and thereby align the signals as we did with human data. To remove such offset we estimated the zero position of each eye as the median value of its temporal trace, i.e. the median value of the whole angular trace over the 10 minutes of recordings. Thus, for each eye the PV-plot was centered in zero by subtracting the estimated zero position from all slow phases' data points.

The PV-plot construction, instead, remains basically unchanged. Briefly, for each specimen we considered all data points corresponding to slow phases, sorted them in ascending order of gaze eccentricity and assigned them into non-overlapping, on degree-wide bins. For each bin, the median drift velocity was considered for subsequent analysis, reducing data noise caused by outliers and obtaining a median velocity-position curve.

Afterward, the curves were individually fitted using the mathematical model in Eq.(4.4) and summarizing the PV-relationship with two coefficients, respectively the "shaping" k_1 and "scaling" k_2 coefficients.

$$V = -k_2/k_1 \sinh(k_1 E) \quad (4.4)$$

Note that with respect to the human model in Eq.(3.3), the tangent function was replaced with hyperbolic sine. Although analytically similar, the hyperbolic sine better describes the nonlinear relationship between the instantaneous drift velocity V and gaze eccentricity E in zebrafish.

4.2.7. Statistical analysis

Median and MAD (Median Absolute Deviation) were used as statistical descriptors of the data, while the normality of data distributions was tested through Kolmogorov-Smirnov test for all groups.

Least square regression and quantile regression [218] were used as data fitting methods when normality of the data was confirmed or not, respectively.

Due to the different designs of the experiments involving larvae and juvenile zebrafish, we performed two different statistical procedures.

Analysis of larvae: Multiple comparisons for independent groups were performed to compare the three groups of larvae, i.e. the 0.0, 1.25, 2.50% groups. Since data were non-normally distributed, a non-parametric one-way analysis of variance (Kruskal-Wallis test) was used. For post-hoc test, a Bonferroni correction was used to ensure a conservative measure of significance.

Analysis of juvenile zebrafish: Paired comparisons were performed for juvenile zebrafish, as each fish was tested twice (BE and AE). To remove the dependency between samples, we tested the ratio of each feature following a procedure identical to the one used for GEN analysis in humans (see Section 3.2.6, Eq.(3.4) for further details).

Since data were non-normally distributed, a bilateral Wilcoxon signed rank test was then used after testing for the symmetry of the data by means of the Wilcoxon test for symmetry.

Intergroup comparisons were performed using the Kruskal-Wallis test and comparing the ratio distributions (AE/BE) of the three independent groups, i.e. three concentrations. Bonferroni correction was used for multiple comparisons and post-hoc tests.

In both analyses, we considered a p-value lower than 0.05 (after the correction for multiple comparisons) as statistically significant.

4.3. Results

4.3.1. Ethanol effect on larvae

Ethanol dose-response relationship was evaluated by testing five different concentrations, 0, 1.25, 2.5, 5 and 10% in independent groups of eight specimens.

Ethanol-induced macroscopic effect was first assessed during the data acquisition process, excluding larvae without spontaneous eye movements from subsequent data analysis (to avoid biasing statistics such as saccades frequency).

The highest concentration (10%) was lethal for all larvae, which died after 10 min of exposure. The 5% ethanol solution was also highly toxic, as 3 out of 8 larvae died, while the others did not show any eye movements.

Lower ethanol concentrations (i.e. 2.5 and 1.25%) were not lethal for any zebrafish larvae. However, two larvae were excluded from 2.5% group, while in control (0%) and 1.25% no specimens were excluded.

For the sake of simplicity, in the following paragraphs and figures, each group is named only using the percentage of ethanol concentration.

4.3.1.1. Ethanol effect on the saccadic system

Potential ethanol effect on the larvae's saccadic system was assessed by means of main sequence analysis, evaluating alcohol influence on saccades amplitude-velocity relationship.

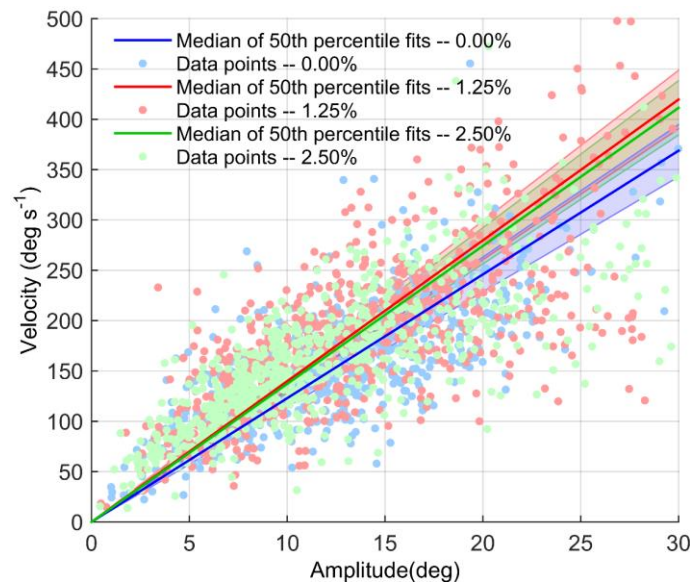


Figure 4.1: Main sequences for 0.0, 1.25 and 2.50% groups. Data points: Saccade amplitude versus peak velocity for all tested larvae within 0.0, 1.25 and 2.50% groups (light blue, red and green dots, respectively). Straight lines and shaded areas: medians of fitted straight lines \pm MAD within each group. Despite the large within-group variability of data points, amplitude-velocity relationship may be unaffected by ethanol in larvae. Indeed, comparison of main sequence slopes (i.e. slope of solid lines) did not reveal any difference, although the control group (blue line) has slightly lower slope ($p=0.22$).

As shown in Figure 4.1, when pooling all saccades within individual groups, we found that the main sequences were almost identical for 0.0, 1.25 and 2.50% groups, as their data points almost overlapped. Consequently, despite large within-group variability, ethanol does not seem to alter the amplitude-velocity relationship of saccades.

Such observation was confirmed comparing the medians of the slopes of the straight-lines (see Paragraph 4.2.6.1) fitted to each individual, within each group (i.e. $m_{S-0.0\%}$ vs $m_{S-1.25\%}$ vs $m_{S-2.50\%}$, solid blue, red and green line in Figure 4.1, respectively). The Kruskal-Wallis test indeed did not reveal any statistically significant difference between such groups ($p=0.22$), as shown by the data distributions of main sequence slopes (in Table 4-1).

Ethanol-induced changes in the saccadic system were further investigated comparing the data distributions of peak velocity and amplitude (Figure 4.2A, B). We tested the medians of both peak velocity and amplitude data distributions (see Table 4-1), and non-parametric ANOVA did not allow us to reject the null hypothesis that all samples are drawn from the same population (Amplitude: $p=0.12$; Peak Velocity $p=0.07$).

Frequency of spontaneous saccades was evaluated to assess the ethanol-induced sedative effect, which has previously been found affecting the motor behavior of adult fish [235]. However, as evident visible in Figure 4.2C, data distributions were not statistically different (Kruskal-Wallis test, $p=0.91$).

It is worth noting that the available video acquisition system, with a sample rate of only 40 Hz may be inadequate to accurately measure saccadic parameters such as peak eye velocity or duration, which likely explains the high variability shown in Figure 4.1.

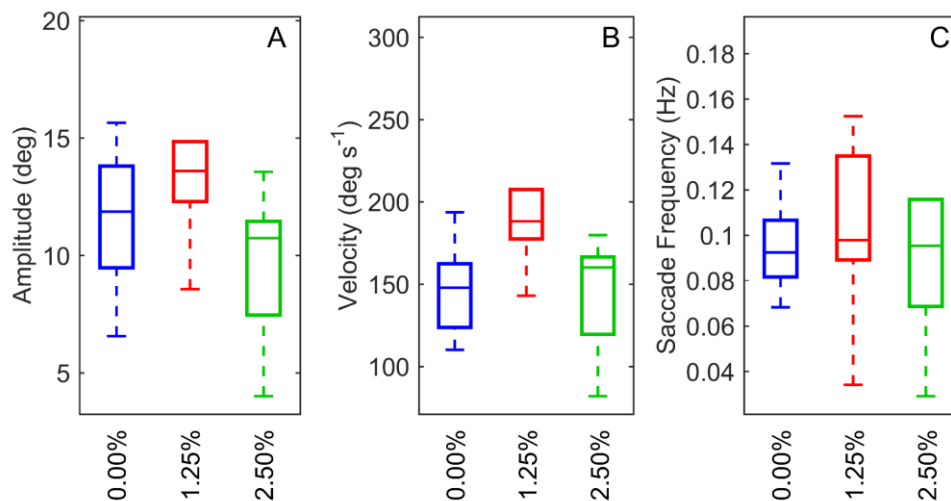


Figure 4.2: Saccade amplitude, peak velocity and frequency data distributions. Boxplot: Central mark indicates the median, while bottom and top edges of the box indicate the 25th and 75th percentiles, respectively. In each subpanel the blue, red and green colors identify 0.0, 1.25 and 2.50% groups. Multiple comparison of saccade features did not reveal an effect of ethanol on amplitude (A), peak velocity (B) or frequency (C) ($p=0.12$, 0.07 and 0.91 , respectively), confirming our finding based on main sequence analysis.

4.3.1.1. Ethanol effect on Gaze stability

Direct estimate of VPNI time constant. To assess gaze stability, we estimated the VPNI time constant τ_c , of each larva group using Eq.(4.2). Data distributions of τ_c in Table 4-1 revealed that larvae VPNI is already leaky in control group ($\approx 8\text{sec}$). Similarly, 1.25 and 2.50% groups showed a shorter but comparable τ_c , in spite of ethanol intoxication. Kruskal-Wallis test, in fact, did not confirm an ethanol-induced effect, resulting in non-statistically significant differences with controls ($p=0.84$).

The absence of relevant differences in slow-phases estimated considering the median τ_c found in 0.0, 1.25 and 2.50% groups also emerges in Figure 4.3, suggesting that a clear ethanol cause-effect on τ_c cannot be identified.

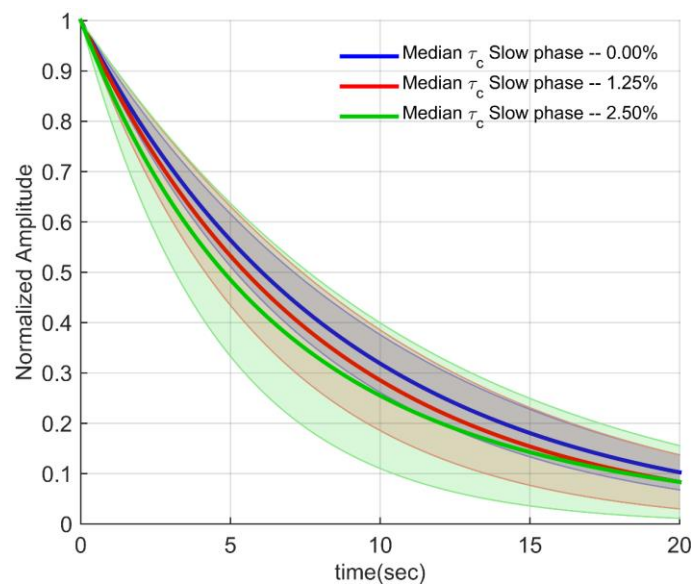


Figure 4.3: VPNI time constant (τ_c) of 0.0, 1.25 and 2.50% groups. Each line represents the estimated exponential decay using median τ_c for the group, while the shaded areas represent the decay with median $\tau_c \pm \text{MAD}$. Despite slightly longer τ_c , the estimated slow-phase of control group is comparable to 1.25 and 2.50% ones (red and green lines, respectively). However, although the leakiness of VPNI seems not to be affected by ethanol intoxication, the higher within-group variability found in 1.25 and 2.50% groups may be due to ethanol-induced effect.

PV-plot analysis. Direct estimate of τ_c may not allow to identify potential ethanol-induced effect on relationship between drift velocity and position of slow phases, since VPNI performance is summarized by one parameter only (i.e. the time constant). As in the previous Chapter, PV-plot analysis was performed individually on each specimen (see Paragraphs 3.2.6.2 and 4.2.6.2 for further details) estimating k_1 and k_2 (shaping and scaling parameters).

The larvae PV-plot (Figure 4.4) differs from the human one (see Figure 3.5) as the range of eye movements is restricted to $\pm 25^\circ$, since large eccentric angles are rare in afoveate organisms [239] and our data considered only spontaneous eye movements. Consequently, while the scaling factor k_2 was properly estimated as it is mainly related to small eye deviations, the shaping factor k_1 was less reliable and almost negligible (≈ 0 , see Table 4-1).

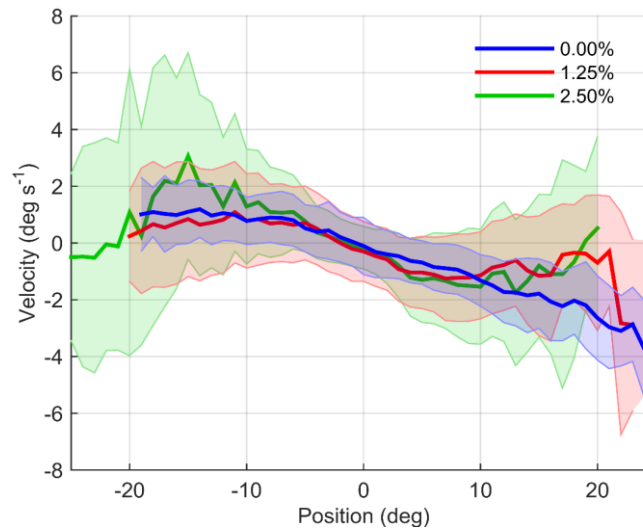


Figure 4.4: Position-Velocity (PV) plot for larvae spontaneous slow phases in all tested conditions. Each line represents the median drift velocity for all larvae in 0.0, 1.25 and 2.50% groups (blue, red and green, respectively), while the shaded area represents the median \pm MAD. Irrespective of concentration, the PV relationship is partially preserved after ethanol exposure. Specifically, no scaling effects are induced by ethanol, conversely to alcohol intoxication in human. However, the huge variability of data in eccentric angles ($>15^\circ$) may hide any potential ethanol effects. The shaping factor, in fact, does not reliably summarize the increased asymmetry in PV-plots (red and green curves), which could be related to ethanol exposure.

Overall PV-plots are shown in Figure 4.4, where medians of velocity curves are computed for 0.0, 1.25 and 2.50% groups (blue, red and green, respectively). As evident, the slope of median curve is almost indiscernible between groups (neglecting some asymmetries). The finding of no statistical difference was also confirmed by multiple comparison of the median k_2 values of each group (Kruskal-Wallis test, $p=0.56$).

Even the k_1 factors were proven to be non-statistically significant (Kruskal-Wallis test, $p=0.16$). However, the meaning of such finding is limited since the k_1 values cannot appropriately summarize both the great variability found in our PV-plot data and its shape in groups such as in 2.50% (green curve and the shading in Figure 4.4). Overall these results suggest that an effect of ethanol affecting the VPNI in the tested larvae is questionable.

4.3.2. Ethanol effect on juvenile zebrafish

Preliminary data in larval zebrafish did not show any significant ethanol-induced effect on the ocular motor system, yet such result left us with one main open question: is there any relationship between the increased within-group variability and ethanol concentration?

To answer this question, we performed a second experiment limiting some of the possible sources of variability, doubling the sample size and performing paired comparisons. Moreover, to avoid uncertainty related to the neural development of VPNI and other neural structures at the larval stage, we considered juvenile zebrafish for further experiments.

Juvenile zebrafish were tested both before and after ethanol exposure (BE and AE). Three concentrations, 0.2, 0.5, 0.8% were used, according to the state of art of behavioral studies on fish.

With an approach similar to the one adopted for experiments on larvae, the fish without spontaneous eye movements were excluded from subsequent data analysis. Specifically, 4 out of 14 fish did not show any eye movements after exposure to the highest concentration (0.8%), while only one fish was excluded from the 0.5% group. All 14 fish exposed to 0.2% concentrations showed eye movements.

4.3.2.1. Ethanol effect on the saccadic system

The saccade amplitude-peak velocity relationship after ethanol (AE) exposure is shown in Figure 4.5. Similar to larvae's main sequences (Figure 4.1), we found that within-groups pooled data were overlapping in all AE conditions, although the slope of the best fitting straight line to the medians for 0.2% was lower than the 1.25% and 2.50% (panel D). Such conflicting result was clarified by comparing the main sequence for BE and AE (Figure 4.5 A-C). The 0.2% group in AE condition (blue line in Figure 4.5B), indeed, showed a lower of slope of the median straight line but comparable to that in BE (black line in Figure 4.5B). Similar findings are also shown in other two AE-BE comparisons (Figure 4.5C, D), suggesting that ethanol may not affect the amplitude-velocity relationship of saccades. Data distribution shown in Table 4-2 and paired comparisons (ratio of AE to BE) confirmed such observations. Specifically, the Wilcoxon signed rank test applied to each group did not reveal any statistical significance of ethanol exposure (testing the null hypothesis H_0 that the slopes before and after exposure are not different, $H_0: m_S^{AE}/m_S^{BE}=1$; 0.2% group: $p=0.08$, 0.5% group: $p=0.38$; 0.8% group: $p=0.93$). No statistical difference was also confirmed by means of Kruskal-Wallis test, performing inter-group comparisons of the ratio of main sequence slopes ($p=0.21$).

Despite the main sequence relationship may not be altered, the distributions of velocities and amplitudes in Figure 4.5A-C show a potential change. Further analyses on the saccadic system were thus

performed individually comparing data distributions of saccade peak velocities and amplitudes (Figure 4.6A, B).

Paired comparison of saccade amplitudes revealed a decrease in 0.5 and 0.8% group AE (Figure 4.6A and Table 4-2), as the median of AE to BE ratios were statistically different from 1 (0.5% group: $p=0.0002$; 0.8% group: $p=0.03$). The lowest concentration, instead, did not elicit any effect (Wilcoxon signed rank test: $p=0.45$).

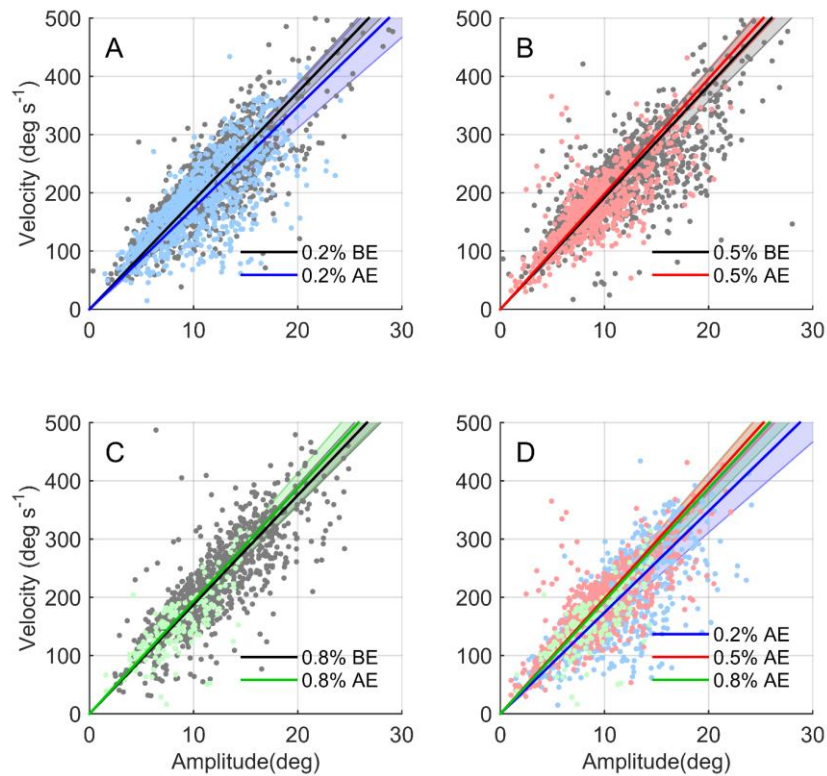


Figure 4.5: Main sequences of juvenile zebrafish. Data points: Saccade amplitude versus peak velocity pooled within groups. Straight lines: Median of straight lines individually estimated on specimen's main sequences. Shaded areas: Median of fitted straight lines \pm MAD. Blue, red and green colors represent the 0.2, 0.5 and 0.8% groups, respectively, after ethanol exposure (AE), while black dots and lines represent the data for the same group in the baseline condition (i.e. before ethanol, BE). **A-C.** Main sequence comparison between AE (colored) and BE (black) conditions for 0.2 (**A**), 0.5 (**B**) and 0.8% (**C**) groups. Irrespectively of ethanol concentration, the saccade amplitude-peak velocity relationship seems to be preserved after ethanol exposure. On the other hand, an absolute reduction in the number of saccades, amplitude and peak velocity is apparent after the exposure to high concentrations, such as for 0.8%. **D.** Comparison of 0.2, 0.5 and 0.8% groups AE. The distributions do not show an evident alteration of the main sequence due to ethanol exposure.

A clear reduction in peak velocity AE is visible in Figure 4.6B. Wilcoxon signed rank test revealed that AE-BE ratio was statistically

different from 1, irrespectively of ethanol concentration ($H_0: A^{AE}/A^{BE}=1$; 0.2% group: $p=0.01$, 0.5% group: $p=0.0002$; 0.8% group: $p=0.04$). Moreover, inter-group comparisons revealed that the highest ethanol concentration (0.08%) induced a greater decrease in velocities compared to 0.02% group (Kruskal-Wallis test: $p=0.04$; post-hoc comparison $H_0 A^{AE-0.2\%}/A^{BE-0.2\%} = A^{AE-0.8\%}/A^{BE-0.8\%}$; $p<0.05$).

Finally, we considered the frequency of spontaneous saccades (Figure 4.6C). A reduction in saccadic frequency was observed for both the highest ethanol concentration groups, suggesting an ethanol-induced sedative effect (Figure 4.6C, red and green boxplots).

Wilcoxon signed rank test confirmed that the ratio of frequencies (AE/BE) was statistically different from 1 in the groups exposed to 0.5% ($p=0.0001$) and 0.8% ethanol solution, while the 0.2% concentration did not cause a significant decrease ($p=0.19$). Furthermore, multiple comparisons unveiled a relationship between ethanol concentration and reduction in spontaneous eye movements, as the 0.8% concentration induced a statistically stronger effect than 0.2 and 0.5% (Kruskal-Wallis test: $p=0.0006$; post-hoc comparisons $p<0.05$).

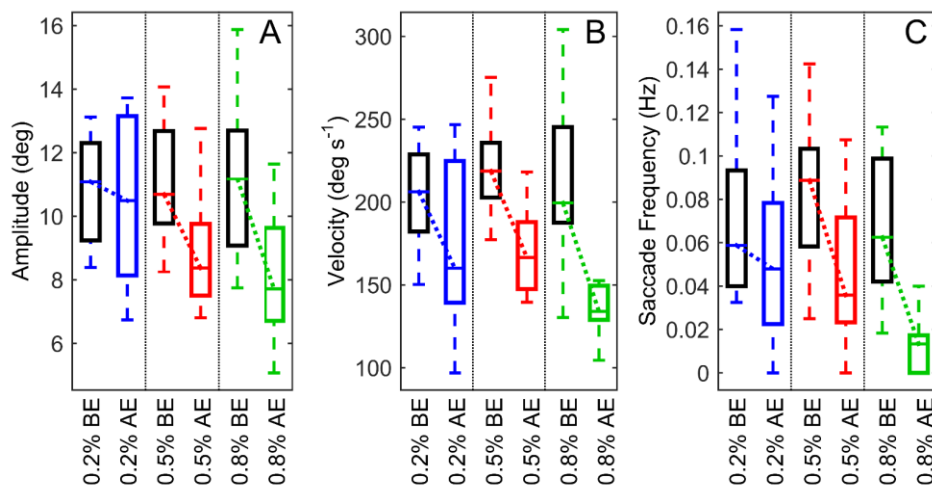


Figure 4.6: Saccade amplitude, peak velocity and frequency data distributions in young adult zebrafish. Boxplot: Central mark indicates the median, bottom and top edges of the box indicate the 25th and 75th percentiles of the data distribution, respectively. In each subpanel the fully colored boxes, i.e. blue, red and green, identify 0.20, 0.50 and 0.80% groups after ethanol exposure (AE), respectively, while the corresponding half black and colored boxes represent the same conditions before ethanol exposure (BE), as indicated by abscissa labels. Paired comparisons of saccade features revealed statistical effects of ethanol on amplitude (A), peak velocity (B) and frequency (C). Moreover, the amount of reduction in all features is clearly related to ethanol concentrations. Specifically, 0.8% exposure induced the strongest reduction in amplitude and velocity, provoking a sedative effect visible in the decrease of spontaneous eye movements, i.e. saccade frequency.

4.3.2.1. Ethanol effect on gaze stability

Direct estimate of VPNI time constant. The estimated VNPI τ_c in young adult zebrafish did not unveil a nearly perfect integrator but a markedly leaky one, as confirmed by data distributions shown in Table 4-2. Consequently, as shown in Figure 4.7, the exponential decays computed using the estimated VPNI τ_c exhibit high drift velocity already in baseline conditions (black curves in A-C panels).

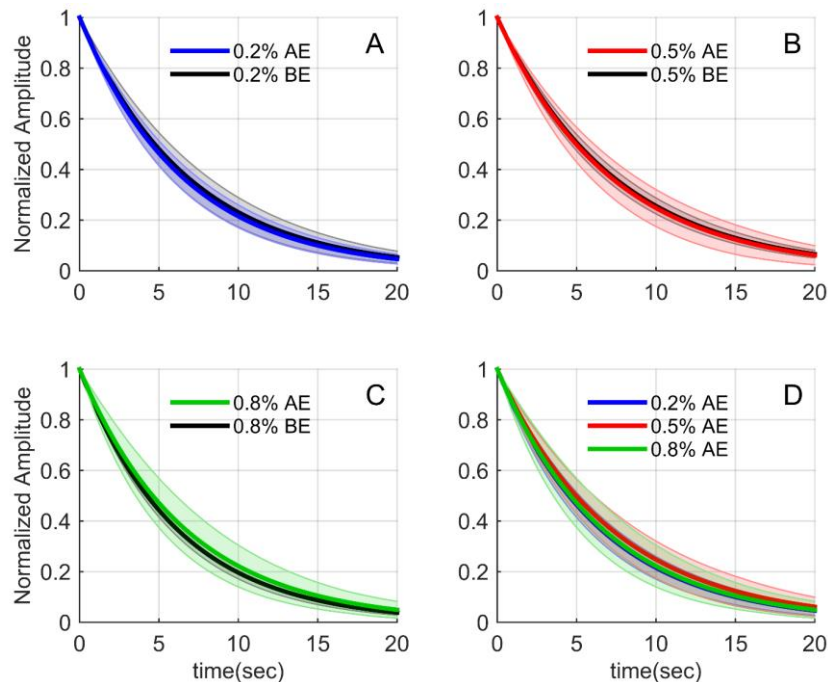


Figure 4.7: Estimated VPNI time constant (τ_c). Each line represents the estimated exponential decay with median τ_c , while the shaded areas represent the decay with median $\tau_c \pm \text{MAD}$. Blue, red and green lines represent the 0.2, 0.5 and 0.8% groups after ethanol exposure (AE), respectively, while black lines identify the same group in baseline condition, i.e. before ethanol (BE). **A-C.** Comparisons between AE (colored) and BE (black) conditions for 0.2 (**A**), 0.5 (**B**) and 0.8% (**C**) groups. Clearly, ethanol exposure does not affect the time constant of VPNI, as the computed decays with median τ_c are almost overlapping in BE and AE. **D.** The comparison of all AE conditions further contradicts the original hypothesis of a relationship between ethanol concentration and VPNI leakiness.

At first visual inspection Figure 4.7A-C suggested that ethanol exposure did not change the VPNI leakiness, although it induced an increase of variability (Table 4-2).

Paired comparison of time constants in AE and BE conditions confirmed, in fact, that no statistical evidence about ethanol-induced effect was inferable, irrespective of the considered concentration (Wilcoxon signed

rank test, $H_0: \tau_c^{AE} / \tau_c^{BE} = 1$; 0.2% group: $p=0.85$, 0.5% group: $p=0.90$; 0.8% group: $p=0.63$). Kruskal-Wallis test also confirmed such result, showing no statistical differences between the ratios of time constants in the three groups ($p=0.83$). No statistical evidence of τ_c changes in every AE condition is evident in Figure 4.7D, where the confidence intervals of median exponential decays are almost overlapping.

PV-plot analysis. The assessment of VPNI performance through direct estimate of its time constant did not reveal any clear ethanol effects. However, our model (see Section 3.2.6.2 for further details about PV-plot) has helped us to interpret the complex effect of ethanol on zebrafish VPNI. PV nonlinear relationship, indeed, appears altered by ethanol, mostly for the more eccentric angles (Figure 4.8A-C), while the PV linear relationship (for small angles approximation Eq.(4.4) $\approx V = k_2 E$) seems to be preserved, in agreement with our findings on VNPI time constants.

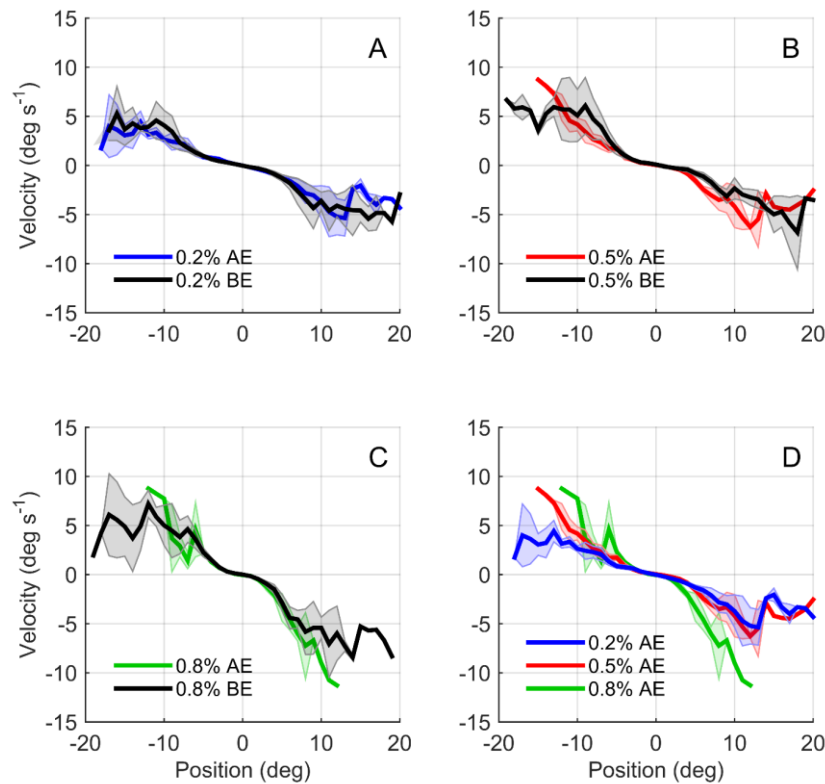


Figure 4.8: Position-Velocity (PV) plots of juvenile Zebrafish. Black and colored solid lines represent the median drift velocity of zebrafish before and after exposure, respectively, to 0.2, 0.5 and 0.8% ethanol solutions (blue, red and green), while the shaded area represents the median \pm MAD. A-C. Irrespective of concentration, the linear PV relationship is partially preserved after ethanol exposure, thus no scaling effect is induced by ethanol. However, an increase of nonlinear behavior in AE eccentric angles ($>|10^\circ$) compared to BE suggested a change in the shaping factor related to ethanol concentration. Such effect is evident comparing all AE conditions (D).

Data distributions (Table 4-2) and statistical comparisons of ratio of both parameters (i.e. k_1^{AE}/k_1^{BE} and k_2^{AE}/k_2^{BE}) confirmed the empirical evidences shown in Figure 4.8.

First, Wilcoxon signed rank test of scaling factors k_2 revealed no statistical difference between BE and AE conditions, for any ethanol concentration (Wilcoxon signed rank test, $H_0: k_2^{AE}/k_2^{BE}=1$; 0.2% group: $p=0.95$, 0.5% group: $p=0.71$; 0.8% group: $p=0.43$).

Second, the limited PV-plot variability (Figure 4.8) allowed us to reliably estimate and compare also shaping factors k_1 , contrary to larvae (Figure 4.4). Specifically, significant differences were shown for higher ethanol concentrations (Wilcoxon signed rank test, $H_0: k_1^{AE}/k_1^{BE}=1$; 0.5% group: $p=0.007$; 0.8% group: $p=0.014$), while the 0.2% groups showed no significant changes ($p=0.32$). However, the positive reinforcement due to alcohol concentration on shaping factor was not confirmed by multiple comparisons (Kruskal-Wallis test, $p=0.15$), suggesting that after the threshold value of 0.5%, the effect of ethanol on the nonlinear PV relationship saturates.

Table 4-1: Data distributions in larvae groups

Feature type		0.00% med \pm MAD	1.25% med \pm MAD	2.50% med \pm MAD
	Main sequence slope (s ⁻¹)	12.30 \pm 0.87	13.78 \pm 0.96	13.71 \pm 0.90
Saccadic System	Amplitude (°)	11.89 \pm 2.16	13.62 \pm 1.28	11.84 \pm 1.77
	Peak velocity (°/s)	147.9 \pm 19.3	188.2 \pm 15.0	160.2 \pm 13.0
	Saccade frequency (mHz)	92.5 \pm 12.5	97.9 \pm 22.9	95.4 \pm 23.6
Gaze-Holding System	Time constant (s)	8.57 \pm 1.34	8.02 \pm 2.12	7.67 \pm 3.16
	Shaping coefficient k_1 (ms ⁻¹)	5.05 \pm 5.00	1.01 \pm 0.50	5.01 \pm 4.99
	Scaling coefficient k_2 (s ⁻¹)	0.11 \pm 0.02	0.08 \pm 0.04	0.10 \pm 0.05

Table 4-2: Data distributions in juvenile zebrafish groups

Feature type		0.20% med \pm MAD	0.50% med \pm MAD	0.80% med \pm MAD	
	Main sequence slope (s ⁻¹)	AE	17.39 \pm 1.83	19.80 \pm 0.81	19.36 \pm 1.32
		BE	18.65 \pm 0.77	19.41 \pm 1.30	18.77 \pm 0.89
Saccadic System	Amplitude (°)	AE	10.49 \pm 2.59	8.37 \pm 1.14	7.72 \pm 1.13
		BE	11.09 \pm 1.35	10.69 \pm 1.04	11.19 \pm 1.55
	Peak velocity (°/s)	AE	160.1 \pm 48.9	166.6 \pm 19.3	133.98 \pm 6.4
		BE	206.2 \pm 23.3	218.7 \pm 16.5	199.5 \pm 36.6

	Saccade frequency (mHz)	AE	47.9 ± 27.9	35.8 ± 13.7	13.3 ± 13.3
		BE	58.8 ± 21.3	88.8 ± 26.3	62.5 ± 25.0
	Time constant (s)	AE	6.51 ± 1.01	6.97 ± 1.68	5.77 ± 1.62
		BE	6.83 ± 1.13	7.34 ± 0.64	6.44 ± 0.48
Gaze-Holding System	Shaping coefficient k_1 (s^{-1})	AE	0.17 ± 0.11	0.31 ± 0.15	0.31 ± 0.39
		BE	0.18 ± 0.13	0.15 ± 0.14	0.13 ± 0.13
	Scaling coefficient k_2 (s^{-1})	AE	0.21 ± 0.06	0.18 ± 0.05	0.14 ± 0.13
		BE	0.20 ± 0.09	0.25 ± 0.11	0.26 ± 0.10

4.4. Discussion: human vs zebrafish, analogies and differences in ethanol intoxication

The majority of the experimental studies establishing the role, location, and mechanisms of VPNI considered mammals as experimental animal model [51], [79], [241], [242]. However, simpler vertebrates such as goldfish and zebrafish have proven to be a better experimental model due to their limited neural complexity. Moreover, as mentioned earlier, the study of VPNI in fish has extensively been used to unravel the mammalian VPNI as the basic hindbrain neural mechanisms, including the vestibular connections, are preserved in vertebrates [243], [244].

The cerebellum is also preserved in zebrafish and goldfish [121], yet its role in VPNI time elongation has not been explicitly tested, and some experimental evidence on goldfish suggests that it may not be involved in prolonging the gaze-holding time constant [245].

Our previous study on ethanol-induced GEN in humans (Chapter 3) suggested that alcohol can be used to alter the cerebellar functionality allowing to better understand its role in eye movements control and to model the common clinical signs of cerebellar patients.

Thus, merging together the unique advantages of using a simpler vertebrate as a model organism and the transient effect and particular affinity of ethanol on the cerebellum, our study aimed at verifying whether ethanol intoxication in the zebrafish was a potential candidate to model cerebellar disease.

To achieve this goal, we tried to answer two main issues: quantifying ethanol effects on the zebrafish ocular motor system, and elucidating the role of the cerebellum on the gaze-holding mechanism in the fish.

Despite several studies investigated alcohol-induced behavioral changes in adult zebrafish [226], [234], [237] or developmental alteration in larvae [235], [236], [246], to our knowledge the present study is the first attempt to quantify alcohol effect on the ocular motor system of the fish. Consequently, we performed our experiments using both larvae and juvenile zebrafish, aiming at taking into account the potential developmental changes in neural structures such as the VPNI.

First, a preliminary study on larvae was performed and, in order to detect a macroscopic effect on their oculomotor system, we tested several alcohol concentrations (range 0.0-10%) adapted from toxicological studies. As explained in the Results section, only three out of the five tested conditions were suitable for eye movement analysis (0.0, 1.25 and 2.50%). However, an effect of ethanol was not statistically proven either for the gaze-holding system or the saccadic mechanism.

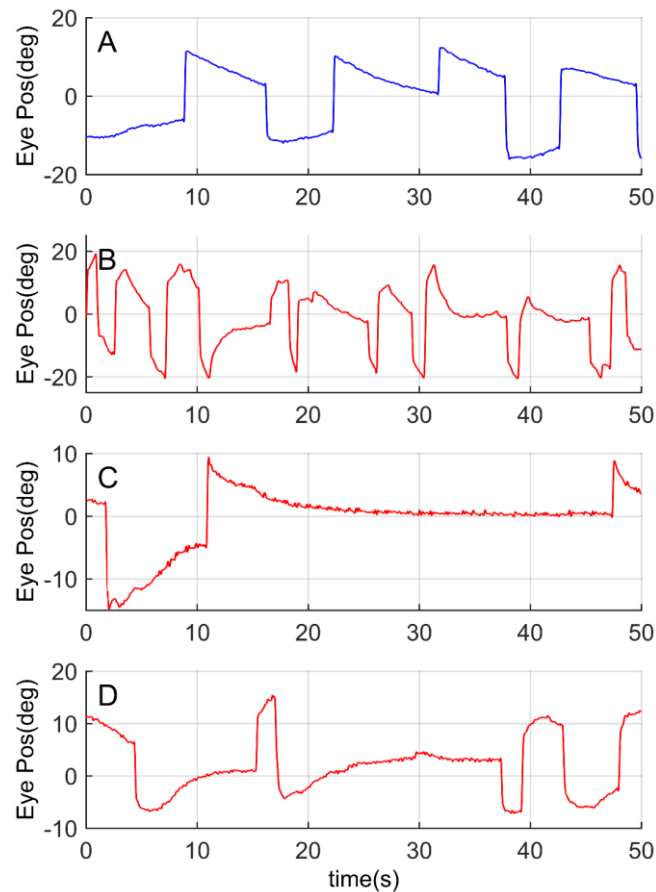


Figure 4.9: Nonhomogeneous effect of ethanol on VPNI. Each line represents the temporal evolution of the right eye position in four larvae. Blue line represents the normal eye movement in darkness in one fish from the 0.0% group (A). Since the VPNI is leaky, the slow phase can be described by a linear or exponential decay. The three red traces (B-D), instead, show a clear but nonhomogeneous ethanol-induced effect in three larvae exposed to 2.50%. Specifically, the larva in (B) shows an increased drift decay, alternating with centrifugal drift towards the temporal side, while in the second specimen (C), ethanol does not seem to affect the leakiness of VPNI. In the last fish (D), after ethanol the entire pattern is altered, with slower and longer slow phases.

Despite such result may be inconsistent with ethanol-induced effect on humans, the reduced number of samples, the normally leaky integrator and

the high variability of larval zebrafish eye movements, may have partially covered a potential effect of alcohol in our data. In particular, the effect of ethanol is nonhomogeneous and varies from fish to fish as shown in Figure 4.9. Strong evidences are shown also in Figure 4.3, where the confidence interval of the exponential decay estimated on the median VPNI time constant increased with the amount of ethanol concentration, suggesting a fish-dependent effect of ethanol.

Also the PV-analysis in larvae did not provide solid results in favor of an effect of ethanol. Using our model, indeed, we took the assumption of single null point according to [123], [239] (where the PV-plot was modeled with a linear function). However, such assumption does not seem adequate to describe the effect of alcohol on larvae. A clear example is shown in the median curve of 2.50% group (Figure 4.4), where the change in PV-plot shape and the instable behavior of the VPNI for eccentric angles, i.e. centrifugal drifts, are not properly model by the shaping factor k_I (see data distributions in Table 4-1).

These findings, together with the mechanism of alcohol absorption (by diffusion through the whole body) and lack of information about the exact internal ethanol concentration in the CNS (usually measured in all tissues), pointed out that the effect of ethanol on the larvae ocular motor system was more complex than expected and hardly extendable to the human one.

As a consequence, our second study was performed on juvenile zebrafish, to characterize its response to ethanol.

At larval stage, in fact, the CNS is still developing, while juvenile zebrafish have an almost fully formed brain [233].

Despite that, it is worth noting that our data suggest that the VPNI may still not be fully developed even in the young adult zebrafish studied here, as the short time constant (≈ 7 sec see Table 4-2) is distinctive of a very leaky integrator. On the other hand, our preliminary data on adults suggest the further increase in time constant in adult fish (>4 months) is only marginal (≈ 9 sec, data not shown). Nonetheless, in this second set of experiments the variability of the data was reduced, and especially so for the study of the VPNI time constant and the PV-plot analysis (Figure 4.7 and Figure 4.8).

Although data showed a similarly leaky integrator in larvae (≈ 7 sec), it must be considered that the different experimental setups make our data not comparable between juvenile and larval zebrafish, as the viscosity of methylcellulose used to embed larvae may have affected eye movements by prolonging VPNI time constant and reducing the slope of the amplitude-peak velocity main sequence (Table 4-1 and Table 4-2).

In spite of these considerations, the study juvenile zebrafish behavior has indeed offered us less variable results than larvae (as shown in data distributions in Table 4-2), thereby allowing a more reliable comparison with humans.

Ethanol concentrations in the range tested here (0.0-1.0%) were previously used in behavioral studies with ethanol diluted in water that demonstrated that the internal ethanol concentrations achieved through these exposures

produced effects on the CNS of adult zebrafish and are within the range of human drinker [226], [237]. Consequently, based on preliminary data in [226], we tested the 0.2, 0.5 and 0.8% ethanol concentrations which induce a BAC in the range of 0.04-0.12%, allowing us to compare them to BAC used in our previous experiment on humans.

Regarding the saccadic system, ethanol does not seem to affect the amplitude-peak velocity relationship as no statistically significant differences were found in the main sequence, similarly to our preliminary data obtained in humans with 0.06% BAC (data not shown). However, the low frame rate of our video acquisition system may have affected our results, increasing data variability and possibly covering more significant findings.

On the other hand, our data showed a significant reduction in saccade peak velocity in intoxicated juvenile zebrafish, which may be in relationship with the common ethanol-induced effect observed in humans [166], [247]–[250]. Despite such promising affinity, other ethanol-induced effects in zebrafish, such as amplitude reduction (Figure 4.6), are not comparable to findings in human, whose saccades were mainly investigated in visually guided experiments, i.e. with subjects performing saccades to visual targets.

Overall both our approaches to study the performance of the gaze-holding mechanism in zebrafish revealed a complex ethanol effect on the neural integrator. Apparently, the direct estimation of its time constant and the PV-plot analysis were contrasting, yet in the following we will argue how both findings describe in fact the same phenomenon.

The VPNI time constant τ_C was estimated using Eq.(4.2), which assumes linear PV relationship for slow phases. Similarly, the scaling factor (k_2) (see Eq.(4.4)) describes the linear portion of the PV plot, i.e. that corresponding to small eccentric angles. Thus, both findings on τ_C and k_2 suggest that ethanol does not seem to affect the VPNI ability to integrate the eye velocity command in the linear range of gaze-holding behavior, i.e. small eccentric angles, which correspond to the preferred eye positions for afoveate animals [239].

Despite that, a specific effect of ethanol on gaze-holding was observed after exposure to the higher concentrations tested here (0.5 and 0.8%). Specifically, both concentrations caused a significant increase of the shaping factor k_I compared the BA condition.

The effect of ethanol, indeed, changed the nonlinear PV relationship, resulting in an increase of drift velocity for more eccentric angles ($>|15^\circ$). Such effect was properly modeled by the shaping factor k_I , which is mainly relevant at more eccentric angles and describes “the overall degree of nonlinearity”, while the estimate of VPNI τ_C was not affected, except for its increased variability.

Our findings on the zebrafish’s gaze-holding system suggested that the effect of alcohol on CNS is different than in the human one. Specifically, the alcohol intake in humans provoked an increase in drift velocity for each

gaze angle (i.e. scaling effect), while ethanol exposure in zebrafish caused a shaping effect only.

As mentioned in the previous chapter, the scaling effect in humans may be due to a diffused action of alcohol on the cerebellum, affecting its role of reinforcing the VPNI neural integration.

The completely different response observed in our zebrafish data (i.e. the shaping effect) suggests that the cerebellum may not be involved in lengthening of VPNI time constant in the fish. The pure shaping effect, in fact, was not induced by alcohol in healthy subjects, but only in cerebellar patients. However, the shape changes observed in zebrafish were hardly comparable with those in cerebellar patients, as cerebellar ataxia induced also saccadic abnormalities.

There are at least two lines of evidence that support our hypothesis that the cerebellum may not be involved in lengthening the VPNI time constant.

First, the cerebellar feedback loop in humans prolonged the short time constant of VPNI from 2 to 20 seconds, approximately, while the zebrafish neural integrator is still extremely leaky ($\tau_C \simeq 7$ seconds), although it succeeds in prolonging the time constant of oculomotor plant (1-2sec measured in goldfish after pharmacological inhibition of hindbrain VPNI [126], [251])

Second, anatomical studies in goldfish showed that the vestibulo-lateral lobe of the cerebellum and hindbrain VPNI have no direct afferent or efferent interconnections [124], [252], and may therefore interact through indirect projections. Furthermore, the anatomy of the goldfish hindbrain circuitry, suggests that all cerebellar-related effects on fixation stability may be mediated through the vestibular nuclei [123].

Consequently, we speculated that the limited ethanol effect on zebrafish eye movements may be induced by its interaction with the hindbrain, occurring only after exposure to higher concentrations (0.5 and 0.8%).

Conclusions

Alcohol intoxicated subjects manifest several deficits of cerebellar functions, e.g. motor impairment, ocular motor abnormality and gait ataxia, comparable to those experienced by patients affected by cerebellar degeneration.

The research presented here is based on the idea that alcohol-induced impairment of cerebellar function may be useful to get new insight about its involvement in motor control. Specifically, my study tried to answer one main question: may the transient alcohol effect on the cerebellum be used as a model of cerebellar diseases?

To answer such question, the research was carried out studying the eye movements, as inherently simpler and more stereotyped than limb or whole body movements, and focusing on one physiological function relying on the cerebellum: the gaze-holding mechanism.

Such mechanism was studied in two species: humans, in order to directly compare the ocular motor deficit caused by alcohol intoxication and cerebellar degeneration; and in zebrafish, one of the most widely used non-mammal model organisms for the surprising similarity of its CNS with the human one.

The results found in humans were promising. Our detailed analysis on the PV-plot, i.e. the relationship between drift velocity and eccentricity of the eye in the orbit, revealed an alcohol-related linear increase of the drift velocity, and, in a subgroup of subjects, a nonlinear alteration of the PV relationship occurring only at higher BAC ($>0.08\%$).

Both pure scaling and scaling and shaping effects, were accurately modeled by a tangent function, revealing the usefulness of our 2-parameter model to assess the gaze-holding performances.

Similar linear and nonlinear transformations were also described in patients affected by cerebellar degenerations, suggesting that alcohol-induced GEN could provide a model of GEN in cerebellar pathology.

On the other hand, alcohol affects homogeneously all neural structures involved in gaze-holding and in general terms the whole cerebellum, suggesting that its application as a model may be limited. A subgroup of cerebellar patients, in fact, demonstrated nonlinear increases of drift velocity in absence of an overall scaling, a condition not reproduced by our results.

Despite alcohol cannot be used to induce localized cerebellar inhibition, the effortless estimation of BAC using a breathalyzer and the rapid transition of ethanol from blood stream to the CNS through the blood-brain barrier are important advantages which allow using alcohol as suitable noninvasive tool for investigating the alteration of cerebellar functions in healthy subjects.

The effects induced by alcohol intoxication in zebrafish, instead, were contrasting with those found in humans, but shed light on the role of the cerebellum in zebrafish' eye movements control.

The first part of our research on larvae did not show any clear alcohol effect on the ocular motor control system. However, some doubts regarding the full development of the CNS in larva motivated us to extend the research to juvenile zebrafish.

The young adult fish, in fact, displayed a range of oculomotor abnormalities related to ethanol concentration. The decrease in saccade peak velocity and amplitude revealed an alcohol-dependent effect on the saccadic system partially comparable to that in humans, although the main sequence relationship was not affected.

Conversely to the results found in humans, only a nonlinear transformation of the PV relationship was found in zebrafish after the exposure to ethanol solution ($>0.5\%$). Such alcohol-induced gaze instability concerned only the more eccentric gaze angles, without affecting the linear range of eye movements, i.e. small angles $<|10^\circ|$, and therefore the leakiness of neural integrator.

Such findings, together with the anatomical evidence shown in goldfish about the lack of a direct connection between the brainstem and the cerebellum, suggest that the cerebellar involvement in the control of eye movements in zebrafish is limited.

Thus, despite the zebrafish may be appropriately considered as a model organism in the field of eye movement research, its use as model for cerebellar-related oculomotor diseases seems to be inadequate.

References

- [1] F. Land and D. Fernald, "The evolution of eyes," *Annu. Rev. Neurosci.*, vol. 15, no. 1990, pp. 1–29, Mar. 1992.
- [2] F. D. Frentiu and A. D. Briscoe, "A butterfly eye's view of birds," *BioEssays*, vol. 30, no. 11–12. Wiley Subscription Services, Inc., A Wiley Company, pp. 1151–1162, Nov-2008.
- [3] D. E. Nilsson, "Eye evolution and its functional basis," *Vis. Neurosci.*, vol. 30, no. 1–2, pp. 5–20, Mar. 2013.
- [4] R. F. Dougherty, V. M. Koch, A. A. Brewer, B. Fischer, J. Modersitzki, and B. A. Wandell, "Visual field representations and locations of visual areas V1/2/3 in human visual cortex.," *J. Vis.*, vol. 3, no. 10, pp. 586–598, Oct. 2003.
- [5] S. Grillner, B. Robertson, and M. Stephenson-Jones, "The evolutionary origin of the vertebrate basal ganglia and its role in action selection," *J Physiol*, vol. 591, no. Pt 22, pp. 5425–5431, Nov. 2013.
- [6] E. R. Kandel, J. H. Schwartz, and T. M. Jessell, *Principles of Neural Science*, vol. 3. 2000.
- [7] R. J. Leigh and D. S. Zee, *The Neurology of Eye Movements*, Fifth Edit. Oxford University Press, 2015.
- [8] B. S. Ballew, "Elsevier's Scopus® Database," *J. Electron. Resour. Med. Libr.*, vol. 6, pp. 245–252, 2009.
- [9] H. Straka and N. Dieringer, "Basic organization principles of the VOR: Lessons from frogs," *Prog. Neurobiol.*, vol. 73, no. 4, pp. 259–309, 2004.
- [10] N. Dieringer, C. Pantle, I. Reichenberger, and H. Straka, "The synaptic organization of the horizontal vestibulo-ocular reflex in the frog.," *Acta Biol. Hung.*, vol. 47, no. 1–4, pp. 61–72, 1996.
- [11] A. Böhmer, V. Henn, and J. ichi Suzuki, "Vestibulo-ocular reflexes after selective plugging of the semicircular canals in the monkey - response plane determinations," *Brain Res.*, vol. 326, no. 2, pp. 291–298, 1985.
- [12] B. Cohen, D. Schiff, and J. Buettner, "Contribution of the nucleus of the optic tract to optokinetic nystagmus and optokinetic afternystagmus in the monkey: clinical implications.," *Res. Publ. Assoc. Res. Nerv. Ment. Dis.*, vol. 67, pp. 233–55, 1990.

References

- [13] K. P. Hoffmann, "Control of the optokinetic reflex by the nucleus of the optic tract in primates.," *Prog. Brain Res.*, vol. 80, pp. 173-182-172, 1989.
- [14] V. Honrubia, W. L. Downey, D. P. Mitchell, and P. H. Ward, "Experimental studies on optokinetic nystagmus. II. Normal humans.," *Acta Otolaryngol.*, vol. 65, no. 5, pp. 441-448, May 1968.
- [15] D. Boghen, B. T. Troost, R. B. Daroff, L. F. Dell'Osso, and J. E. Birkett, "Velocity characteristics of normal human saccades.," *Invest. Ophthalmol.*, vol. 13, no. 8, pp. 619-623, 1974.
- [16] R. J. Krauzlis, "The control of voluntary eye movements: new perspectives.," *Neuroscientist*, vol. 11, no. 2, pp. 124-37, Apr. 2005.
- [17] R. J. Krauzlis, "Recasting the smooth pursuit eye movement system," *J. Neurophysiol.*, vol. 91, no. 2, pp. 591-603, 2004.
- [18] D. A. Robinson, "The mechanics of human smooth pursuit eye movement," *J. Physiol.*, vol. 180, no. 3, pp. 569-591, Oct. 1965.
- [19] D. L. Sparks, "The brainstem control of saccadic eye movements," *Nat. Rev. Neurosci.*, vol. 3, no. 12, pp. 952-964, Dec. 2002.
- [20] S. C. Cannon and D. A. Robinson, "Loss of the neural integrator of the oculomotor system from brain stem lesions in monkey," *J. Neurophysiol.*, vol. 57, no. 5, pp. 1383-1409, May 1987.
- [21] C. Pierrot-Deseilligny, D. Milea, and R. M. Müri, "Eye movement control by the cerebral cortex.," *Curr Opin Neurol*, vol. 17, no. 1, pp. 17-25, 2004.
- [22] D. S. Zee, R. J. Leigh, F. Mathieu-Millaire, J. R. Leigh, and F. Mathieu-Millaire, "Cerebellar Control of Ocular Gaze Stability," *Ann. Neurol.*, vol. 7, no. 1, pp. 37-40, 1980.
- [23] M. B. Bender, "Brain control of conjugate horizontal and vertical eye movements: a survey of the structural and functional correlates.," *Brain*, vol. 103, no. 1, pp. 23-69, Mar. 1980.
- [24] D. A. Robinson and A. F. Fuchs, "Eye movements evoked by stimulation of frontal eye fields.," *J. Neurophysiol.*, vol. 32, no. 5, pp. 637-48, Sep. 1969.
- [25] D. A. Robinson, "Adaptive gain control of vestibuloocular reflex by the cerebellum.," *J. Neurophysiol.*, vol. 39, no. 5, pp. 954-69, Sep. 1976.
- [26] D. A. Robinson, "The effect of cerebellectomy on the cat's vestibulo-ocular integrator," *Brain Res.*, vol. 71, no. 2-3, pp. 195-207, 1974.
- [27] J. O. Schairer and M. V. L. Bennett, "Changes in Gain of the Vestibulo-Ocular Reflex Induced by Sinusoidal Visual-Stimulation in Goldfish," *Brain Res.*, vol. 373, no. 1, pp. 177-181, 1986.
- [28] J. H. J. Allum, W. Graf, J. Dichgans, and C. L. Schmidt, "Visual-vestibular interactions in the vestibular nuclei of the goldfish," *Exp. Brain Res.*, vol. 26, no. 5, pp. 463-485, Dec. 1976.

- [29] J. J. Michnovicz and M. V. L. Bennett, "Effects of rapid cerebellectomy on adaptive gain control of the vestibulo-ocular reflex in alert goldfish," *Exp. Brain Res.*, vol. 66, no. 2, pp. 287–294, Apr. 1987.
- [30] J. C. Beck, E. Gilland, D. W. Tank, and R. Baker, "Quantifying the ontogeny of optokinetic and vestibuloocular behaviors in zebrafish, medaka, and goldfish.," *J. Neurophysiol.*, vol. 92, no. 6, pp. 3546–61, Dec. 2004.
- [31] Y.-Y. Huang, O. Rinner, P. Hedinger, S.-C. Liu, and S. C. F. Neuhaus, "Oculomotor Instabilities in Zebrafish Mutant *belladonna*: A Behavioral Model for Congenital Nystagmus Caused by Axonal Misrouting," *J. Neurosci.*, vol. 26, no. 39, pp. 9873–9880, Sep. 2006.
- [32] Y.-Y. Huang, C. C. Chen, S. P. Huber-Reggi, S. C. F. Neuhaus, and D. Straumann, "Comparison of infantile nystagmus syndrome in achiasmatic zebrafish and humans," *Ann. N. Y. Acad. Sci.*, vol. 1233, no. 1, pp. 285–291, Sep. 2011.
- [33] C. M. Harris and D. M. Wolpert, "Signal-dependent noise determines motor planning.," *Nature*, vol. 394, no. 6695, pp. 780–4, Aug. 1998.
- [34] D. A. Robinson, "Oculomotor unit behavior in the monkey.," *J. Neurophysiol.*, vol. 33, no. 3, pp. 393–403, May 1970.
- [35] A. F. Fuchs and E. S. Luschei, "Firing patterns of abducens neurons of alert monkeys in relationship to horizontal eye movement.," *J. Neurophysiol.*, vol. 33, no. 3, pp. 382–392, May 1970.
- [36] J. M. Miller, "Understanding and misunderstanding extraocular muscle pulleys.," *J. Vis.*, vol. 7, no. 11, p. 10.1-15, Aug. 2007.
- [37] J. M. Miller, "Functional-Anatomy of Normal Human Rectus Muscles," *Vis. Res.*, vol. 29, p. 223-, 1989.
- [38] E. Henneman, G. Somjen, and D. O. Carpenter, "Functional Significance of Cell Size in Spinal Motoneurons.," *J. Neurophysiol.*, vol. 28, no. 3, pp. 560–580, May 1965.
- [39] C. S. Sherrington, "Reciprocal Innervation of Antagonistic Muscles. Fourteenth Note.-On Double Reciprocal Innervation," *Proc. R. Soc. B Biol. Sci.*, vol. 81, no. 548, pp. 249–268, Jul. 1909.
- [40] A. M. F. Wong, J. A. Sharpe, and D. Tweed, "Adaptive Neural Mechanism for Listing's Law Revealed in Patients with Fourth Nerve Palsy," *Invest. Ophthalmol.*, vol. 43, no. 6, pp. 1796–1803, 2002.
- [41] K. Hepp, "Theoretical explanations of Listing's law and their implication for binocular vision," *Vision Res.*, vol. 35, no. 23–24, pp. 3237–3241, 1995.
- [42] A. M. F. Wong, "Listing's law: Clinical significance and implications for neural control," *Survey of Ophthalmology*, vol. 49, no. 6, pp. 563–575, 2004.
- [43] K. Hepp, "On Listing's law," *Commun. Math. Phys.*, vol. 132, no. 1, pp. 285–292, 1990.

References

- [44] D. A. Robinson, "The Mechanics of Human Saccadic Eye Movement.," *J. Physiol.*, vol. 174, no. 2, pp. 245–264, Nov. 1964.
- [45] D. A. Robinson, Z. Kapoula, and H. P. Goldstein, "Holding the Eye Still After a Saccade," in *From Neuron to Action SE - 11*, Berlin, Heidelberg: Springer Berlin Heidelberg, 1990, pp. 89–96.
- [46] M. R. Clark and L. Stark, "Sensitivity of control parameters in a model of saccadic eye tracking and estimation of resultant nervous activity," *Bull. Math. Biol.*, vol. 38, no. 1, pp. 39–57, Jan. 1976.
- [47] E. L. Keller, "Accommodative vergence in the alert monkey. Motor unit analysis," *Vision Res.*, vol. 13, no. 8, pp. 1565–1575, 1973.
- [48] L. M. Optican and F. Miles, "Visually induced adaptive changes in primate saccadic oculomotor control signals.," *J. Neurophysiol.*, vol. 54, no. 4, pp. 940–58, Oct. 1985.
- [49] J. Somers, M. Reschke, A. Feiveson, R. Leigh, S. J. Wood, W. H. Paloski, and L. N. Kornilova, "Studies of the Ability to Hold the Eye in Eccentric Gaze: Measurements in Normal Subjects with the Head Erect," in *Advances in Understanding Mechanisms and Treatment of Infantile Forms of Nystagmus*, Oxford: Oxford University Press, 2008, pp. 129–136.
- [50] G. Bertolini, A. A. Tarnutzer, I. Olasagasti, E. Khojasteh, K. P. Weber, C. J. Bockisch, D. Straumann, and S. Marti, "Gaze Holding in Healthy Subjects," *PLoS One*, vol. 8, no. 4, p. e61389, 2013.
- [51] E. Godaux and G. Cheron, "The hypothesis of the uniqueness of the oculomotor neural integrator: direct experimental evidence in the cat.," *J. Physiol.*, vol. 492, no. Pt 2, pp. 517–527, 1996.
- [52] K. Nakamagoe, Y. Iwamoto, and K. Yoshida, "Evidence for brainstem structures participating in oculomotor integration.," *Science (80-.)*, vol. 288, no. 5467, pp. 857–9, 2000.
- [53] A. A. Tarnutzer, K. P. Weber, B. Schuknecht, D. Straumann, S. Marti, and G. Bertolini, "Gaze holding deficits discriminate early from late onset cerebellar degeneration," *J. Neurol.*, vol. 262, no. May, p. 2015, 2015.
- [54] S. Glasauer, "Cerebellar contribution to saccades and gaze holding: A Modeling Approach," *Ann. N. Y. Acad. Sci.*, vol. 1004, no. 1, pp. 206–219, 2003.
- [55] J. Leech, M. Gresty, K. Hess, and P. Rudge, "Gaze failure, drifting eye movements, and centripetal nystagmus in cerebellar disease.," *Br. J. Ophthalmol.*, vol. 61, no. 12, pp. 774–781, 1977.
- [56] A. Kheradmand and D. S. Zee, "Cerebellum and ocular motor control," *Front. Neurol.*, vol. Sep, p. 53, 2011.
- [57] D. A. Robinson, "Eye movement control in primates," *Science (80-.)*, vol. 165, no. 3847, pp. 1219–1224, Sep. 1968.

-
- [58] D. G. Horner and C. M. Schor, "Chapter 14: Saccade Initiation and Tracking," *Indiana University School of Optometry*, 2004. .
- [59] W. Waespe and V. Henn, "Neuronal activity in the vestibular nuclei of the alert monkey during vestibular and optokinetic stimulation," *Exp. Brain Res.*, vol. 27, no. 5, pp. 523–538, Apr. 1977.
- [60] F. A. Miles and J. H. Fuller, "Visual Tracking and the Primate Flocculus," *Science (80-)*, vol. 189, pp. 1000–1002, 1975.
- [61] R. H. S. Carpenter, "Cerebellectomy and the Transfer Function of the Vestibulo-Ocular Reflex in the Decerebrate Cat," *Proc. R. Soc. London. Ser. B. Biol. Sci.*, vol. 181, no. 1065, pp. 353–374, Jul. 1972.
- [62] D. S. Zee, R. D. Yee, D. G. Cogan, D. A. Robinson, and W. K. Engel, "Ocular motor abnormalities in hereditary cerebellar ataxia," *Brain*, vol. 99, no. 2, pp. 207–234, Jun. 1976.
- [63] G. Westheimer and S. M. Blair, "Functional organization of primate oculomotor system revealed by cerebellectomy," *Exp. Brain Res.*, vol. 21, no. 5, pp. 463–472, Dec. 1974.
- [64] L. A. Abel, L. Parker, R. B. Daroff, and L. F. Dell'Osso, "End-point nystagmus," *Investig. Ophthalmol. Vis. Sci.*, vol. 17, no. 6, pp. 539–544, 1978.
- [65] L. A. Abel, L. F. Dell'osso, and R. B. Daroff, "Analog Model for Gaze-Evoked Nystagmus," *IEEE Trans. Biomed. Eng.*, vol. BME-25, no. 1, pp. 71–75, 1978.
- [66] M. Elzenman, P. Cheng, J. A. Sharpe, and R. C. Frecker, "End-point nystagmus and ocular drift: An experimental and theoretical study," *Vision Res.*, vol. 30, no. 6, pp. 863–877, 1990.
- [67] J. Shallo-Hoffmann, H. Schwarze, H. J. Simonsz, and H. Muhlendyck, "A reexamination of end-point and rebound nystagmus in normals," *Investig. Ophthalmol. Vis. Sci.*, vol. 31, no. 2, pp. 388–392, 1990.
- [68] C. A. Whyte, A. M. Petrock, and M. Rosenberg, "Occurrence of physiologic gaze-evoked nystagmus at small angles of gaze," *Investig. Ophthalmol. Vis. Sci.*, vol. 51, no. 5, pp. 2476–2478, 2010.
- [69] J. L. Booker, "End-position nystagmus as an indicator of ethanol intoxication.," *Sci. justice J. Forensic Sci. Soc. J. Forensic Sci. Soc.*, vol. 41, no. 2, pp. 113–6, 2001.
- [70] J. L. Booker, "The Horizontal Gaze Nystagmus test: fraudulent science in the American courts.," *Sci. justice J. Forensic Sci. Soc.*, vol. 44, no. 3, pp. 133–9, 2004.
- [71] S. J. Rubenzer and S. B. Stevenson, "Horizontal gaze nystagmus: A review of vision science and application issues," *J. Forensic Sci.*, vol. 55, no. 2, pp. 394–409, 2010.
- [72] W. W. P. Chan and H. L. Galiana, "Integrator function in the oculomotor

References

- system is dependent on sensory context.," *J. Neurophysiol.*, vol. 93, no. 6, pp. 3709–17, Jun. 2005.
- [73] D. E. Angelaki, "The oculomotor plant and its role in three-dimensional eye orientation," in *The Oxford Handbook of Eye Movements*, 2012.
- [74] R. A. McCrea, "Neuroanatomy of the oculomotor system. The nucleus prepositus.," *Rev. Oculomot. Res.*, vol. 2, pp. 203–23, 1988.
- [75] E. Aksay, I. Olasagasti, B. D. Mensh, R. Baker, M. S. Goldman, and D. W. Tank, "Functional dissection of circuitry in a neural integrator.," *Nat. Neurosci.*, vol. 10, no. 4, pp. 494–504, 2007.
- [76] A. Miri, K. Daie, A. B. Arrenberg, H. Baier, E. Aksay, and D. W. Tank, "Spatial gradients and multidimensional dynamics in a neural integrator circuit.," *Nat. Neurosci.*, vol. 14, no. 9, pp. 1150–1159, 2011.
- [77] W. Waespe, B. Cohen, and T. Raphan, "Role of the flocculus and paraflocculus in optokinetic nystagmus and visual-vestibular interactions: effects of lesions.," *Exp. brain Res.*, vol. 50, no. 1, pp. 9–33, 1983.
- [78] D. S. Zee, A. Yamazaki, P. H. Butler, and G. Gücer, "Effects of ablation of flocculus and paraflocculus of eye movements in primate.," *J. Neurophysiol.*, vol. 46, no. 4, pp. 878–899, Oct. 1981.
- [79] M. Escudero, G. Cheron, and E. Godaux, "Discharge properties of brain stem neurons projecting to the flocculus in the alert cat. II. Prepositus hypoglossal nucleus.," *J. Neurophysiol.*, vol. 76, no. 3, pp. 1775–1785, Sep. 1996.
- [80] D. G. Cogan, K. Jatho, J. L. Cogan, D.G., and Barrows, M. Victor, and W. F. Bender, M.B., and Gorman, "Down-Beat Nystagmus," *Arch. Ophthalmol.*, vol. 80, no. 6, pp. 757–768, Dec. 1968.
- [81] S. Sharma, P. M. Sumich, I. C. Francis, M. C. Kiernan, and P. J. Spira, "Wernicke's encephalopathy presenting with upbeating nystagmus.," *J. Clin. Neurosci.*, vol. 9, no. 4, pp. 476–8, Jul. 2002.
- [82] B. . Aschoff, C.; Conrad and H. . Kornhurber, "Acquired pendular nystagmus with oscillopsia in multiple sclerosis: a sign of cerebellar nuclei disease," *J. Neurol. Neurosurgery, Psychiatry*, vol. 37, no. 5, pp. 570–577, May 1974.
- [83] G. Major, R. Baker, E. Aksay, B. Mensh, H. S. Seung, and D. W. Tank, "Plasticity and tuning by visual feedback of the stability of a neural integrator.," *Proc. Natl. Acad. Sci. U. S. A.*, vol. 101, no. 20, pp. 7739–44, 2004.
- [84] G. Major, R. Baker, E. Aksay, H. S. Seung, and D. W. Tank, "Plasticity and tuning of the time course of analog persistent firing in a neural integrator.," *Proc. Natl. Acad. Sci. U. S. A.*, vol. 101, no. 20, pp. 7745–50, 2004.
- [85] C. Tiliket, M. Shelhamer, D. Roberts, and D. S. Zee, "Short-term vestibulo-ocular reflex adaptation in humans," *Exp. Brain Res.*, vol. 100, no. 2, pp. 316–327, Aug. 1994.

- [86] D. B. Arnold and D. A. Robinson, "The oculomotor integrator: testing of a neural network model," *Exp. Brain Res.*, vol. 113, no. 1, pp. 57–74, Jan. 1997.
- [87] S. C. Cannon, D. A. Robinson, and S. Shamma, "A proposed neural network for the integrator of the oculomotor system," *Biol. Cybern.*, vol. 49, no. 2, pp. 127–136, Dec. 1983.
- [88] S. C. Cannon and D. A. Robinson, "An improved neural-network model for the neural integrator of the oculomotor system: More realistic neuron behavior," *Biol. Cybern.*, vol. 53, no. 2, pp. 93–108, 1985.
- [89] D. A. Robinson, "Integrating with Neurons," *Annu. Rev. Neurosci.*, vol. 12, no. 1, pp. 33–45, Mar. 1989.
- [90] M. Strupp, K. Hübner, R. Sandmann, A. Zwergal, M. Dieterich, K. Jahn, and T. Brandt, "Central oculomotor disturbances and nystagmus: a window into the brainstem and cerebellum," *Dtsch. Arztebl. Int.*, vol. 108, no. 12, pp. 197–204, Mar. 2011.
- [91] K. Citek, A. D. Elmont, C. L. Jons, C. J. Krezelok, J. D. Neron, T. A. Plummer, and T. Tannenbaum, "Sleep Deprivation Does Not Mimic Alcohol Intoxication on Field Sobriety Testing," *J. Forensic Sci.*, vol. 56, no. 5, pp. 1170–1179, 2011.
- [92] M. Strupp, O. Kremmyda, C. Adamczyk, N. Böttcher, C. Muth, C. W. Yip, and T. Bremova, "Central ocular motor disorders, including gaze palsy and nystagmus," *Journal of Neurology*, vol. 261, no. Suppl. 2. Springer, pp. 542–558, Sep-2014.
- [93] D. S. Zee, D. G. Cogan, D. A. Robinson, and W. K. Engel, "Analysis of eye movements in members of a family with late-onset, dominantly inherited cerebellar ataxia," *Trans. Am. Neurol. Assoc.*, vol. 100, pp. 98–103, 1975.
- [94] U. Büttner and T. Grunzei, "Gaze-evoked nystagmus and smooth pursuit deficits: Their relationship studied in 52 patients," *J. Neurol.*, vol. 242, no. 6, pp. 384–389, 1995.
- [95] C. M. Gomez, R. M. Thompson, J. T. Gammack, S. L. Perlman, W. B. Dobyns, C. L. Truwit, D. S. Zee, H. B. Clark, and J. H. Anderson, "Spinocerebellar ataxia type 6: Gaze-evoked and vertical nystagmus, Purkinje cell degeneration, and variable age of onset," *Ann. Neurol.*, vol. 42, no. 6, pp. 933–950, Dec. 1997.
- [96] T. Hashimoto, O. Sasaki, K. Yoshida, Y. I. Takei, and S. I. Ikeda, "Periodic alternating nystagmus and rebound nystagmus in spinocerebellar ataxia type 6," *Mov. Disord.*, vol. 18, no. 10, pp. 1201–1204, Oct. 2003.
- [97] S. E. Gordon, T. C. Hain, D. S. Zee, and M. Fetter, "Rebound nystagmus in normals subjects," in *ARVO Abstracts. Invest Ophthalmol Visual Sci*, 1986, vol. 27, p. 158.
- [98] R. L. Bondar, J. A. Sharpe, and A. J. Lewis, "Rebound nystagmus in olivocerebellar atrophy: a clinicopathological correlation," *Ann Neurol*, vol. 15, no. 5, pp. 474–477, May 1984.

References

- [99] J. D. Hood, A. Kayan, and J. Leech, “Rebound nystagmus.,” *Brain a J. Neurol.*, vol. 96, no. 3, pp. 507–26, Sep. 1973.
- [100] S. F. (Steve F. Perry, *Zebrafish*. Elsevier/Academic Press, 2010.
- [101] R. A. Kozol, A. J. Abrams, D. M. James, E. Buglo, Q. Yan, and J. E. Dallman, “Function Over Form: Modeling Groups of Inherited Neurological Conditions in Zebrafish,” *Front. Mol. Neurosci.*, vol. 9, p. 55, Jul. 2016.
- [102] K. Howe, M. D. Clark, C. F. Torroja, J. Torrance, C. Berthelot, M. Muffato, J. E. Collins, S. Humphray, K. McLaren, L. Matthews, S. McLaren, I. Sealy, M. Caccamo, C. Churcher, C. Scott, J. C. Barrett, R. Koch, G.-J. Rauch, S. White, W. Chow, B. Kilian, L. T. Quintais, J. A. Guerra-Assunção, Y. Zhou, Y. Gu, J. Yen, J.-H. Vogel, T. Eyre, S. Redmond, R. Banerjee, J. Chi, B. Fu, E. Langley, S. F. Maguire, G. K. Laird, D. Lloyd, E. Kenyon, S. Donaldson, H. Sehra, J. Almeida-King, J. Loveland, S. Trevanion, M. Jones, M. Quail, D. Willey, A. Hunt, J. Burton, S. Sims, K. McLay, B. Plumb, J. Davis, C. Clee, K. Oliver, R. Clark, C. Riddle, D. Elliot, D. Elliott, G. Threadgold, G. Harden, D. Ware, S. Begum, B. Mortimore, B. Mortimer, G. Kerry, P. Heath, B. Phillimore, A. Tracey, N. Corby, M. Dunn, C. Johnson, J. Wood, S. Clark, S. Pelan, G. Griffiths, M. Smith, R. Glithero, P. Howden, N. Barker, C. Lloyd, C. Stevens, J. Harley, K. Holt, G. Panagiotidis, J. Lovell, H. Beasley, C. Henderson, D. Gordon, K. Auger, D. Wright, J. Collins, C. Raisen, L. Dyer, K. Leung, L. Robertson, K. Ambridge, D. Leongamornlert, S. McGuire, R. Gilderthorp, C. Griffiths, D. Manthavadi, S. Nichol, G. Barker, S. Whitehead, M. Kay, J. Brown, C. Murnane, E. Gray, M. Humphries, N. Sycamore, D. Barker, D. Saunders, J. Wallis, A. Babbage, S. Hammond, M. Mashreghi-Mohammadi, L. Barr, S. Martin, P. Wray, A. Ellington, N. Matthews, M. Ellwood, R. Woodmansey, G. Clark, J. D. Cooper, J. Cooper, A. Tromans, D. Grafham, C. Skuce, R. Pandian, R. Andrews, E. Harrison, A. Kimberley, J. Garnett, N. Fosker, R. Hall, P. Garner, D. Kelly, C. Bird, S. Palmer, I. Gehring, A. Berger, C. M. Dooley, Z. Ersan-Ürün, C. Eser, H. Geiger, M. Geisler, L. Karotki, A. Kirn, J. Konantz, M. Konantz, M. Oberländer, S. Rudolph-Geiger, M. Teucke, C. Lanz, G. Raddatz, K. Osoegawa, B. Zhu, A. Rapp, S. Widaa, C. Langford, F. Yang, S. C. Schuster, N. P. Carter, J. Harrow, Z. Ning, J. Herrero, S. M. J. Searle, A. Enright, R. Geisler, R. H. A. Plasterk, C. Lee, M. Westerfield, P. J. de Jong, L. I. Zon, J. H. Postlethwait, C. Nüsslein-Volhard, T. J. P. Hubbard, H. Roest Crollius, J. Rogers, and D. L. Stemple, “The zebrafish reference genome sequence and its relationship to the human genome.,” *Nature*, vol. 496, no. 7446, pp. 498–503, Apr. 2013.
- [103] R. White, K. Rose, and L. Zon, “Zebrafish cancer: the state of the art and the path forward.,” *Nat. Rev. Cancer*, vol. 13, no. 9, pp. 624–36, Aug. 2013.
- [104] J. M. Fadool and J. E. Dowling, “Zebrafish: A model system for the study of eye genetics,” *Prog. Retin. Eye Res.*, vol. 27, no. 1, pp. 89–110, 2008.
- [105] C. B. Kimmel, W. W. Ballard, S. R. Kimmel, B. Ullmann, and T. F. Schilling, “Stages of embryonic development of the zebrafish.,” *Dev. Dyn.*, vol. 203, no. 3, pp. 253–310, Jul. 1995.
- [106] E. Menelaou, E. E. Husbands, R. G. Pollet, C. A. Coutts, D. W. Ali, and K. R. Svoboda, “Embryonic motor activity and implications for regulating motoneuron axonal pathfinding in zebrafish,” *Eur. J. Neurosci.*, vol. 28, no. 6,

- pp. 1080–1096, Sep. 2008.
- [107] B. D. Olson, P. Sgourdou, and G. B. Downes, “Analysis of a zebrafish behavioral mutant reveals a dominant mutation in *atp2a1/SERCA1*,” *Genesis*, vol. 48, no. 6, pp. 354–361, Jun. 2010.
- [108] I. H. Bianco, A. R. Kampff, and F. Engert, “Prey capture behavior evoked by simple visual stimuli in larval zebrafish,” *Front. Syst. Neurosci.*, vol. 5, no. December, p. 101, 2011.
- [109] S. S. Easter and G. N. Nicola, “The development of vision in the zebrafish (*Danio rerio*).,” *Dev. Biol.*, vol. 180, no. 2, pp. 646–63, Dec. 1996.
- [110] S. S. Easter and G. N. Nicola, “The development of eye movements in the zebrafish (*Danio rerio*).,” *Dev. Psychobiol.*, vol. 31, no. 4, pp. 267–276, Dec. 1997.
- [111] S. C. F. Neuhauss, “Behavioral genetic approaches to visual system development and function in zebrafish,” *Journal of Neurobiology*, vol. 54, no. 1, pp. 148–160, Jan-2003.
- [112] J. Chhetri, G. Jacobson, and N. Gueven, “Zebrafish- on the move towards ophthalmological research.,” *Eye (Lond)*, vol. 28, no. 4, pp. 367–80, Apr. 2014.
- [113] G. Gestri, B. A. Link, and S. C. F. Neuhauss, “The visual system of zebrafish and its use to model human ocular Diseases,” *Dev. Neurobiol.*, vol. 72, no. 3, pp. 302–327, Mar. 2012.
- [114] Y.-Y. Huang, M. Tschopp, D. Straumann, and S. C. F. Neuhauss, “Vestibular deficits do not underlie looping behavior in achiasmatic fish.,” *Commun. Integr. Biol.*, vol. 3, no. 4, pp. 379–381, 2010.
- [115] Y.-Y. Huang, C. C. Chen, S. P. Huber-Reggi, S. C. F. Neuhauss, and D. Straumann, “Comparison of infantile nystagmus syndrome in achiasmatic zebrafish and humans,” *Ann. N. Y. Acad. Sci.*, vol. 1233, no. 1, pp. 285–291, Sep. 2011.
- [116] Y.-Y. Huang and S. C. F. Neuhauss, “The optokinetic response in zebrafish and its applications,” *Technology*, vol. 13, no. January 1, pp. 1899–1916, 2008.
- [117] M. Hashimoto and M. Hibi, “Development and evolution of cerebellar neural circuits,” *Dev. Growth Differ.*, vol. 54, no. 3, pp. 373–389, Apr. 2012.
- [118] M. F. Wullimann, T. Mueller, M. Distel, A. Babaryka, B. Grothe, and R. W. Köster, “The long adventurous journey of rhombic lip cells in jawed vertebrates: a comparative developmental analysis.,” *Front. Neuroanat.*, vol. 5, no. April, p. 27, 2011.
- [119] M. Joshua and S. G. Lisberger, “A tale of two species: Neural integration in zebrafish and monkeys,” *Neuroscience*, vol. 296, pp. 80–91, 2014.
- [120] P. Sajovic and C. Levinthal, “Visual cells of zebrafish optic tectum: Mapping

References

- with small spots,” *Neuroscience*, vol. 7, no. 10, pp. 2407–2426, Oct. 1982.
- [121] C. C. Bell, V. Han, and N. B. Sawtell, “Cerebellum-Like Structures and Their Implications for Cerebellar Function,” *Annu. Rev. Neurosci.*, vol. 31, no. 1, pp. 1–24, 2008.
- [122] H. Matsui, K. Namikawa, A. Babaryka, and R. W. Köster, “Functional regionalization of the teleost cerebellum analyzed in vivo.,” *Proc. Natl. Acad. Sci. U. S. A.*, vol. 111, no. 32, pp. 11846–51, Aug. 2014.
- [123] O. Debowy and R. Baker, “Encoding of eye position in the goldfish horizontal oculomotor neural integrator.,” *J. Neurophysiol.*, vol. 105, no. 2, pp. 896–909, Feb. 2011.
- [124] E. Aksay, R. Baker, H. S. Seung, and D. W. Tank, “Anatomy and discharge properties of pre-motor neurons in the goldfish medulla that have eye-position signals during fixations.,” *J. Neurophysiol.*, vol. 84, no. 2, pp. 1035–1049, Aug. 2000.
- [125] M. S. Goldman, A. Compte, and X. J. Wang, “Neural Integrator Models,” in *Encyclopedia of Neuroscience*, 2010, pp. 165–178.
- [126] E. Aksay, G. Gamkrelidze, H. S. Seung, R. Baker, and D. W. Tank, “In vivo intracellular recording and perturbation of persistent activity in a neural integrator.,” *Nat. Neurosci.*, vol. 4, no. 2, pp. 184–193, Feb. 2001.
- [127] E. Aksay, R. Baker, H. S. Seung, and D. W. Tank, “Correlated discharge among cell pairs within the oculomotor horizontal velocity-to-position integrator.,” *J. Neurosci.*, vol. 23, no. 34, pp. 10852–10858, Nov. 2003.
- [128] D. Purves, G. J. Augustine, D. Fitzpatrick, W. C. Hall, A.-S. Lamantia, J. O. Mcnamara, and S. M. Willians, *Neuroscience*, vol. 3. 2004.
- [129] K. Ohtsuka and T. Enoki, “Transcranial magnetic stimulation over the posterior cerebellum during smooth pursuit eye movements in man.,” *Brain*, vol. 121 (Pt 3, pp. 429–435, Mar. 1998.
- [130] M. F. Walker, J. Tian, X. Shan, R. J. Tamargo, H. Ying, and D. S. Zee, “Lesions of the Cerebellar Nodulus and Uvula Impair Downward Pursuit,” *J. Neurophysiol.*, vol. 100, no. 4, pp. 1813–1823, Oct. 2008.
- [131] S. H. Lee, S. H. Park, J. S. Kim, H. J. Kim, F. Yunusov, and D. S. Zee, “Isolated unilateral infarction of the cerebellar tonsil: Ocular motor findings,” *Ann. Neurol.*, vol. 75, no. 3, pp. 429–434, Mar. 2014.
- [132] H. K. Park, J. S. Kim, M. Strupp, and D. S. Zee, “Isolated floccular infarction: Impaired vestibular responses to horizontal head impulse,” *J. Neurol.*, vol. 260, no. 6, pp. 1576–1582, Jun. 2013.
- [133] R. F. M. Bispo, A. J. C. Ramalho, L. C. B. de Gusmão, A. P. de H. Cavalcante, A. C. da Rocha, and C. F. de Sousa-Rodrigues, “Cerebellar Vermis: Topography and Variations,” *Int. J. Morphol.*, vol. 28, no. 2, pp. 439–443, Jun. 2010.

- [134] B. Cohen, P. John, S. B. Yakushin, J. Buettner-Ennever, and T. Raphan, "The nodulus and uvula: Source of cerebellar control of spatial orientation of the angular vestibulo-ocular reflex," in *Annals of the New York Academy of Sciences*, 2002, vol. 978, pp. 28–45.
- [135] W. Waespe, B. Cohen, and T. Raphan, "Dynamic modification of the vestibulo-ocular reflex by the nodulus and uvula.," *Science*, vol. 228, no. 4696, pp. 199–202, Apr. 1985.
- [136] J. Laurens and D. E. Angelaki, "The functional significance of velocity storage and its dependence on gravity.," *Exp. brain Res.*, vol. 210, no. 3–4, pp. 407–22, May 2011.
- [137] A. Radtke, A. M. Bronstein, M. A. Gresty, M. Faldon, W. Taylor, J. M. Stevens, and P. Rudge, "Paroxysmal alternating skew deviation and nystagmus after partial destruction of the uvula.," *J. Neurol. Neurosurg. Psychiatry*, vol. 70, no. 6, pp. 790–3, Jun. 2001.
- [138] Y. Hayakawa, T. Nakajima, M. Takagi, N. Fukuhara, and H. Abe, "Human cerebellar activation in relation to saccadic eye movements: A functional magnetic resonance imaging study," *Ophthalmologica*, vol. 216, no. 6, pp. 399–405, 2002.
- [139] S. Barash, A. Melikyan, A. Sivakov, M. Zhang, M. Glickstein, and P. Thier, "Saccadic dysmetria and adaptation after lesions of the cerebellar cortex.," *J. Neurosci.*, vol. 19, no. 24, pp. 10931–10939, Dec. 1999.
- [140] J. C. Aschoff and B. Cohen, "Changes in saccadic eye movements produced by cerebellar cortical lesions," *Exp. Neurol.*, vol. 32, no. 2, pp. 123–133, Aug. 1971.
- [141] M. Takagi, D. S. Zee, and R. J. Tamargo, "Effects of lesions of the oculomotor cerebellar vermis on eye movements in primate: Smooth pursuit," *J. Neurophysiol.*, vol. 83, no. 4, pp. 2047–2062, 2000.
- [142] M. Takagi, D. S. Zee, and R. J. Tamargo, "Effects of lesions of the oculomotor vermis on eye movements in primate: saccades.," *J. Neurophysiol.*, vol. 80, no. 4, pp. 1911–1931, 1998.
- [143] Y. Kojima, R. Soetedjo, and A. F. Fuchs, "Effect of inactivation and disinhibition of the oculomotor vermis on saccade adaptation," *Brain Res.*, vol. 1401, pp. 30–39, Jul. 2011.
- [144] F. R. Robinson, A. F. Fuchs, and C. T. Noto, "Cerebellar influences on saccade plasticity.," *Ann. N. Y. Acad. Sci.*, vol. 956, pp. 155–63, Apr. 2002.
- [145] W. M. Pardridge, "The blood-brain barrier: bottleneck in brain drug development.," *NeuroRx*, vol. 2, no. 1, pp. 3–14, 2005.
- [146] J. Lathera, R. Keep, L. A. Betz, and G. W. Goldstein, "Blood-Brain Barrier," in *Basic Neurochemistry: Molecular, Cellular and Medical Aspects*, 6th edition, Philadelphia: Lippincott-Raven, 1999.
- [147] F. Fadda and Z. L. Rossetti, "Chronic ethanol consumption: From

References

- neuroadaptation to neurodegeneration,” *Prog. Neurobiol.*, vol. 56, no. 4, pp. 385–431, 1998.
- [148] W. R. Klemm, C. G. Mallari, L. R. Dreyfus, J. C. Fiske, E. Forney, and J. A. Mikeska, “Ethanol-induced regional and dose-response differences in multiple-unit activity in rabbits,” *Psychopharmacology (Berl.)*, vol. 49, no. 3, pp. 235–244, 1976.
- [149] C. F. Valenzuela and K. Jotty, “Mini-review: Effects of ethanol on GABAA receptor-mediated neurotransmission in the cerebellar cortex-recent advances,” *Cerebellum*, vol. 14, no. 4, pp. 438–446, 2015.
- [150] F. George and N.-S. Chu, “Effects of ethanol on Purkinje cells recorded from cerebellar slices,” *Alcohol*, vol. 1, no. 5, pp. 353–358, Sep. 1984.
- [151] J. G. Sinclair and G. F. Lo, “The effects of ethanol on cerebellar purkinje cell discharge pattern and inhibition evoked by local surface stimulation,” *Brain Res.*, vol. 204, no. 2, pp. 465–471, 1981.
- [152] C. L. Franklin and D. L. Gruol, “Acute ethanol alters the firing pattern and glutamate response of cerebellar Purkinje neurons in culture,” *Brain Res.*, vol. 416, no. 2, pp. 205–218, 1987.
- [153] W. S. Seo and C. K. Suh, “Acute effect of ethanol on firing patterns of Purkinje cells in the rat cerebellar slice preparation,” *Yonsei Med. J.*, vol. 42, no. 4, pp. 384–389, 2001.
- [154] L. Servais, B. Bearzatto, V. Delvaux, E. Noël, R. Leach, M. Brasseur, S. N. Schiffmann, and C. Guy, “Effect of chronic ethanol ingestion on Purkinje and Golgi cell firing in vivo and on motor coordination in mice,” *Brain Res.*, vol. 1055, no. 1–2, pp. 171–179, 2005.
- [155] J. Luo, “Effects of ethanol on the cerebellum: Advances and prospects,” *Cerebellum*, vol. 14, no. 4, pp. 383–385, 2015.
- [156] M. Carta, M. Mamei, and C. F. Valenzuela, “Alcohol Potently Modulates Climbing Fiber-->Purkinje Neuron Synapses: Role of Metabotropic Glutamate Receptors,” *J. Neurosci.*, vol. 26, no. 7, pp. 1906–1912, Feb. 2006.
- [157] M. S. Dar, “Ethanol-Induced Cerebellar Ataxia: Cellular and Molecular Mechanisms,” *The Cerebellum*, vol. 14, no. 4, pp. 447–465, 2015.
- [158] R. Barany, “Experimentelle alkoholintoxikation,” *Monatsschr Ohrenheilkd*, vol. 45, pp. 959–962, 1911.
- [159] H. H. Samson and R. A. Harris, “Neurobiology of alcohol abuse,” *Trends Pharmacol Sci*, vol. 13, no. 5, pp. 206–211, 1992.
- [160] H. J. Little, “Mechanisms that may underlie the behavioural effects of ethanol,” *Prog. Neurobiol.*, vol. 36, no. 3, pp. 171–194, 1991.
- [161] M. E. Charness, R. P. Simon, and D. A. Greenberg, “Ethanol and the nervous system,” *N. Engl. J. Med.*, vol. 321, no. 7, pp. 442–454, 1989.

- [162] G. Aschan and M. Bergstedt, "Positional alcoholic nystagmus (PAN) in man following repeated alcohol doses," *Acta Otolaryngol Suppl*, vol. 330, no. S330, pp. 15–29, 1975.
- [163] F. Modig, *Effects of acute alcohol intoxication on human sensory orientation and postural control*. Lund University, 2013.
- [164] R. G. Watten and I. Lie, "Visual functions and acute ingestion of alcohol," *Ophthalmic Physiol. Opt.*, vol. 16, no. 6, pp. 460–466, 1996.
- [165] H. J. Hanchar, P. D. Dodson, R. W. Olsen, T. S. Otis, and M. Wallner, "Alcohol-induced motor impairment caused by increased extrasynaptic GABA(A) receptor activity.," *Nat. Neurosci.*, vol. 8, no. 3, pp. 339–345, Mar. 2005.
- [166] I. M. Wilkinson and R. Kime, "Alcohol and human eye movement.," *Trans. Am. Neurol. Assoc.*, vol. 99, no. 4, pp. 38–41, 1974.
- [167] R. W. Baloh, S. Sharma, H. Moskowitz, and et al., "Effect of alcohol and marijuana on eye movements," *Aviat. Sp. Environ. Med.*, vol. 50, pp. 18–23, 1979.
- [168] W. Collins, D. Schroeder, and R. Hill, "Some effects of alcohol on vestibular responses," *Curr. Stud. Otoneurology*, 1973.
- [169] D. J. Schroeder, "Some effects of alcohol on nystagmus and vertigo during caloric and optokinetic stimulation," *Ann. Otol. Rhinol. Laryngol.*, 1972.
- [170] D. J. Schroeder, "Influence of alcohol on vestibular responses to angular accelerations," *Aerosp Med*, vol. 42, no. 9, pp. 959–970, 1971.
- [171] R. J. Hill, D. J. Schroeder, and W. E. Collins, "Vestibular response to angular accelerations and to Coriolis stimulation following alcohol ingestion," *Aerosp Med*, vol. 43, no. 5, pp. 525–532, 1972.
- [172] C. H. Markham and S. G. Diamond, "The effect of alcohol ingestion on ocular counterrolling.," *J. Vestib. Res.*, vol. 16, no. 4–5, pp. 193–199, 2006.
- [173] T. N. Roth, K. P. Weber, V. G. Wettstein, G. B. Marks, S. M. Rosengren, and S. C. A. Hegemann, "Ethanol consumption impairs vestibulo-ocular reflex function measured by the video head impulse test and dynamic visual acuity," *J. Vestib. Res. Equilib. Orientat.*, vol. 24, no. 4, pp. 289–295, 2014.
- [174] F. Schmääl, O. Thiede, and W. Stoll, "Effect of ethanol on visual-vestibular interactions during vertical linear body acceleration.," *Alcohol. Clin. Exp. Res.*, vol. 27, no. 9, pp. 1520–1526, 2003.
- [175] M. Nawrot, B. Nordenstrom, and A. Olson, "Disruption of eye movements by ethanol intoxication affects perception of depth from motion parallax," *Psychol. Sci.*, vol. 15, no. 12, pp. 858–865, 2004.
- [176] S. M. Rosengren, K. P. Weber, S. C. A. Hegemann, and T. N. Roth, "The effect of alcohol on cervical and ocular vestibular evoked myogenic potentials in healthy volunteers.," *Clin. Neurophysiol.*, vol. 125, no. 8, pp. 1700–1708,

References

- 2013.
- [177] P.-A. Fransson, F. Modig, M. Patel, S. Gomez, and M. Magnusson, "Oculomotor deficits caused by 0.06% and 0.10% blood alcohol concentrations and relationship to subjective perception of drunkenness," *Clin. Neurophysiol.*, vol. 121, no. 12, pp. 2134–2142, 2010.
- [178] G. R. Barnes, "The effects of ethyl alcohol on visual pursuit and suppression of the vestibulo-ocular reflex," *Acta Otolaryngol.*, vol. 98, no. Suppl. 406, pp. 161–166, 1984.
- [179] I. Lehtinen, A. Lang, V. Jäntti, and E. Keskinen, "Acute effects of alcohol on saccadic eye movements," *Psychopharmacology (Berl.)*, vol. 23, no. 1, pp. 17–23, 1979.
- [180] T. Harder and U. Reker, "Influence of low dose alcohol on fixation suppression," *Acta Otolaryngol Suppl*, vol. 520 Pt 1, pp. 33–36, 1995.
- [181] G. S. Goding and R. A. Dobie, "Gaze nystagmus and blood alcohol.," *Laryngoscope*, vol. 96, no. 7, pp. 713–7, 1986.
- [182] H. M. J. Lehti, "The effect of blood alcohol concentration on the onset of gaze nystagmus," *Blutalkohol*, vol. 13, no. 6, pp. 411–414, 1976.
- [183] K. Citek, B. Ball, and D. A. Rutledge, "Nystagmus testing in intoxicated individuals.," *Optometry*, vol. 74, no. 11, pp. 695–710, 2003.
- [184] K. Citek, "Gen is not HGN," *Investig. Ophthalmol. Vis. Sci.*, vol. 51, no. 12, pp. 6900–6901, 2010.
- [185] V. Tharp, M. Burns, H. Moskowitz, and NHTSA, "Development and Field Test of Psychophysical Tests for DWI Arrest," U.S. Department of Transport, National Highway Traffic Safety Administration, Final Report, Publication No. DOT-HS-805-864, 1981.
- [186] D. G. Newman, *Alcohol and Human Performance from an Aviation Perspective : A Review*. Canberra: Australian Transport Safety Bureau, 2004.
- [187] W. N. Mughni and L. E. Ross, "Alcohol and workload as factors affecting the detection of angular acceleration," *Aviat. Sp. Environ. Med.*, vol. 67, no. 12, pp. 1148–1151, 1996.
- [188] L. E. Ross and W. N. Mughni, "Effect of alcohol on the threshold for detecting angular acceleration," *Aviat. Sp. Environ. Med.*, vol. 66, no. 7, pp. 635–640, 1995.
- [189] T. Seno and S. Nakamura, "Alcohol consumption enhances vection," *Perception*, vol. 42, no. 5, pp. 580–582, 2013.
- [190] G. Bertolini, S. Ramat, C. J. Bockisch, S. Marti, D. Straumann, and A. Palla, "Is vestibular self-motion perception controlled by the velocity storage? insights from patients with chronic degeneration of the vestibulo-cerebellum," *PLoS One*, vol. 7, no. 6, 2012.

- [191] S. M. De La Monte and J. J. Kril, "Human alcohol-related neuropathology," *Acta Neuropathologica*, vol. 127, no. 1. pp. 71–90, 2014.
- [192] M. Manto and J. Jacquy, "Alcohol toxicity in the cerebellum: Clinical aspects," in *The Cerebellum and Its Disorders*, M. Manto and M. Pandolfo, Eds. Cambridge: Cambridge University Press, 2002, pp. 336–341.
- [193] E. Sullivan and M. Rosenbloom, "Alcohol and the cerebellum: effects on balance, motor coordination, and cognition," *Alcohol Res.*, 1995.
- [194] N. M. Zahr, A. L. Pitel, S. Chanraud, and E. V. Sullivan, "Contributions of studies on alcohol use disorders to understanding cerebellar function," *Neuropsychol. Rev.*, vol. 20, no. 3, pp. 280–289, 2010.
- [195] E. V Sullivan, "Human brain vulnerability to alcoholism: Evidence from neuroimaging studies," in *Review of NIAAA's Neuroscience and Behavioral Research Portfolio, NIAAA Research Monograph No. 34*, 2000, pp. 473–508.
- [196] K. G. Baker, A. J. Harding, G. M. Halliday, J. J. Kril, and C. G. Harper, "Neuronal loss in functional zones of the cerebellum of chronic alcoholics with and without Wernicke's encephalopathy," *Neuroscience*, vol. 91, no. 2, pp. 429–438, 1999.
- [197] S. Gilman, R. A. Koeppe, K. Adams, D. Johnson-Greene, L. Junck, K. J. Klun, J. Brunberg, S. Martorello, and M. Lohman, "Positron emission tomographic studies of cerebral benzodiazepine-receptor binding in chronic alcoholics.," *Ann. Neurol.*, vol. 40, no. 2, pp. 163–71, Aug. 1996.
- [198] N. M. Zahr, K. L. Kaufman, and C. G. Harper, "Clinical and pathological features of alcohol-related brain damage.," *Nat. Rev. Neurol.*, vol. 7, no. 5, pp. 284–294, 2011.
- [199] P. R. Martin, C. K. Singleton, and S. Hiller-Sturmhöfel, "The role of thiamine deficiency in alcoholic brain disease.," *Alcohol Res. Health*, vol. 27, no. 2, pp. 134–142, 2003.
- [200] E. V Sullivan, A. Deshmukh, J. E. Desmond, K. O. Lim, and A. Pfefferbaum, "Cerebellar volume decline in normal aging, alcoholism, and Korsakoff's syndrome: relation to ataxia.," *Neuropsychology*, vol. 14, no. 3, pp. 341–352, Jul. 2000.
- [201] D. A. Robinson, "Models of the saccadic eye movement control system.," *Kybernetik*, vol. 14, no. 2, pp. 71–83, 1973.
- [202] T. Klockgether, "Chapter 15 - Sporadic adult-onset ataxia of unknown etiology," in *Handbook of Clinical Neurology*, vol. Volume 103, H. S. Sankara and D. Alexandra, Eds. Elsevier, 2012, pp. 253–262.
- [203] G. Aschan and M. Bergstedt, "Positional alcoholic nystagmus (PAN) in man following repeated alcohol doses," *Acta Otolaryngol Suppl*, vol. 330, no. S330, pp. 15–29, 1975.
- [204] K. H. Mauritz, J. Dichgans, and A. Hufschmidt, "Quantitative Analysis of Stance in Late Cortical Cerebellar Atrophy of the Anterior Lobe and Other

References

- Forms of Cerebellar Ataxia,” *Brain*, vol. 102, no. 3, pp. 461–482, 1979.
- [205] F. Setta, J. Jacquy, J. Hildebrand, and M. U. Manto, “Ataxia induced by small amounts of alcohol,” *J. Neurol. Neurosurg. Psychiatry*, vol. 65, no. 3, pp. 370–373, 1998.
- [206] T. Klockgether, “Sporadic ataxia with adult onset: classification and diagnostic criteria,” *Lancet Neurol.*, vol. 9, no. 1, pp. 94–104, 2010.
- [207] L. M. Optican and D. S. Zee, “A hypothetical explanation of congenital nystagmus,” *Biol. Cybern.*, vol. 50, no. 2, pp. 119–134, 1984.
- [208] M. Versino, O. Hurko, and D. S. Zee, “Disorders of binocular control of eye movements in patients with cerebellar dysfunction,” *Brain*, vol. 119, no. 6, pp. 1933–1950, 1996.
- [209] S. Ramat, V. E. Das, J. T. Somers, and R. J. Leigh, “Tests of two hypotheses to account for different-sized saccades during disjunctive gaze shifts,” *Exp. Brain Res.*, vol. 129, no. 4, pp. 500–10, 1999.
- [210] G. Bertolini and S. Ramat, “Velocity storage in the human vertical rotational vestibulo-ocular reflex,” *Exp. Brain Res.*, vol. 209, no. 1, pp. 51–63, Mar. 2011.
- [211] T. Dera, G. Boning, S. Barete, and E. Schneider, “Low-latency video tracking of horizontal, vertical and torsional eye movements as a basis for 3DOF realtime motion control of a head-mounted camera,” *IEEE Int. Conf. Syst. Man Cybern.*, vol. 6, pp. 5191–5196, 2006.
- [212] E. Schneider, K. Bartl, S. Bardins, T. Dera, G. Boening, and T. Brandt, “Eye movement driven head-mounted camera: It looks where the eyes look,” *IEEE Int. Conf. Syst. Man Cybern.*, vol. 3, pp. 2437–2442, 2005.
- [213] E. M. P. Widmark, *Principles and Applications of Medicolegal Alcohol Determination*. Biomedical Publications, 1981.
- [214] A. W. Jones, “How Breathing Technique Can Influence the Results of Breath-Alcohol Analysis,” *Med. Sci. Law*, vol. 22, no. 4, p. 275, 1982.
- [215] W. Jaschinski-Kruza, “Eyestrain in VDU users: viewing distance and the resting position of ocular muscles,” *Hum. Factors*, vol. 33, no. 1, pp. 69–83, Feb. 1991.
- [216] M. Rosenfield, “Tonic vergence and vergence adaptation,” *Optom. Vis. Sci.*, vol. 74, no. 5, pp. 303–328, 1997.
- [217] W. Jaschinski, S. Jainta, J. Hoormann, and N. Walper, “Objective vs subjective measurements of dark vergence,” *Ophthalmic Physiol. Opt.*, vol. 27, no. 1, pp. 85–92, 2007.
- [218] R. W. Koenker and G. Bassett, “Regression Quantiles,” *Econometrica*, vol. 46, no. 1, pp. 33–50, 1978.
- [219] C. Leys, C. Ley, O. Klein, P. Bernard, and L. Licata, “Detecting outliers: Do

- not use standard deviation around the mean, use absolute deviation around the median,” *J. Exp. Soc. Psychol.*, vol. 49, no. 4, pp. 764–766, 2013.
- [220] J. R. Meaney, “Horizontal Gaze Nystagmus: A Closer Look,” *Jurimetrics*, pp. 383–407, 1996.
- [221] A. J. McKnight, E. A. Langston, A. S. McKnight, and J. E. Lange, “Sobriety tests for low blood alcohol concentrations,” *Accid. Anal. Prev.*, vol. 34, no. 3, pp. 305–311, 2002.
- [222] N. D. Volkow, N. Mullani, L. Gould, S. S. Adler, R. W. Guynn, J. E. Overall, and S. Dewey, “Effects of acute alcohol intoxication on cerebral blood flow measured with PET,” *Psychiatry Res.*, vol. 24, no. 2, pp. 201–209, May 1988.
- [223] A. Basile, B. Hoffer, and T. Dunwiddie, “Differential sensitivity of cerebellar purkinje neurons to ethanol in selectivity outbred lines of mice: maintenance in vitro independent of synaptic transmission,” *Brain Res.*, vol. 264, no. 1, pp. 69–78, 1983.
- [224] L. K. Kaczmarek and I. B. Levitan, *Neuromodulation: The Biochemical Control of Neuronal Excitability*. Oxford University Press, 1987.
- [225] A. M. Stewart, O. Braubach, J. Spitsbergen, R. Gerlai, and A. V Kalueff, “Zebrafish models for translational neuroscience research: From tank to bedside,” *Trends Neurosci.*, vol. 37, no. 5, pp. 264–278, May 2014.
- [226] D. J. Echevarria, C. N. Toms, and D. J. Jouandot, “Alcohol-induced behavior change in zebrafish models,” *Rev. Neurosci.*, vol. 22, no. 1, pp. 85–93, 2011.
- [227] C. Santoriello and L. I. Zon, “Hooked! modeling human disease in zebrafish,” *Journal of Clinical Investigation*, vol. 122, no. 7. American Society for Clinical Investigation, pp. 2337–2343, Jul-2012.
- [228] Y. K. Bae, S. Kani, T. Shimizu, K. Tanabe, H. Nojima, Y. Kimura, S. ichi Higashijima, and M. Hibi, “Anatomy of zebrafish cerebellum and screen for mutations affecting its development,” *Dev. Biol.*, vol. 330, no. 2, pp. 406–426, Jun. 2009.
- [229] L. A. Heap, C. C. Goh, K. S. Kassahn, and E. K. Scott, “Cerebellar output in zebrafish: an analysis of spatial patterns and topography in eurydendroid cell projections.,” *Front. Neural Circuits*, vol. 7, no. April, p. 53, 2013.
- [230] C. C. Chen, C. J. Bockisch, G. Bertolini, I. Olasagasti, S. C. F. Neuhaus, K. P. Weber, D. Straumann, and Y.-Y. M. Huang, “Velocity storage mechanism in zebrafish larvae.,” *J. Physiol.*, vol. 592, no. Pt 1, pp. 203–14, Jan. 2014.
- [231] M. C. Mullins, M. Hammerschmidt, P. Haffter, and C. Nusslein-Volhard, “Large-scale mutagenesis in the zebrafish: In search of genes controlling development in a vertebrate,” *Curr. Biol.*, vol. 4, no. 3, pp. 189–202, Mar. 1994.
- [232] P. Haffter, M. Granato, M. Brand, M. C. Mullins, M. Hammerschmidt, D. a Kane, J. Odenthal, F. J. van Eeden, Y. J. Jiang, C. P. Heisenberg, R. N. Kelsh, M. Furutani-Seiki, E. Vogelsang, D. Beuchle, U. Schach, C. Fabian, and C.

References

- Nüsslein-Volhard, “The identification of genes with unique and essential functions in the development of the zebrafish, *Danio rerio*,” *Development*, vol. 123, pp. 1–36, 1996.
- [233] M. Westerfield, *The Zebrafish Book. A Guide for the Laboratory Use of Zebrafish (Danio rerio)*, 5th Editio. 2007.
- [234] C. A. Dlugos and R. A. Rabin, “Ethanol effects on three strains of zebrafish: Model system for genetic investigations,” *Pharmacol. Biochem. Behav.*, vol. 74, no. 2, pp. 471–480, 2003.
- [235] B. Lockwood, S. Bjerke, K. Kobayashi, and S. Guo, “Acute effects of alcohol on larval zebrafish: A genetic system for large-scale screening,” *Pharmacol. Biochem. Behav.*, vol. 77, no. 3, pp. 647–654, 2004.
- [236] R. C. MacPhail, J. Brooks, D. L. Hunter, B. Padnos, T. D. Irons, and S. Padilla, “Locomotion in larval zebrafish: Influence of time of day, lighting and ethanol,” *Neurotoxicology*, vol. 30, no. 1, pp. 52–58, 2009.
- [237] P. Mathur, M. A. Berberoglu, and S. Guo, “Preference for ethanol in zebrafish following a single exposure,” *Behav. Brain Res.*, vol. 217, no. 1, pp. 128–133, 2011.
- [238] S. Ali, D. L. Champagne, A. Alia, and M. K. Richardson, “Large-scale analysis of acute ethanol exposure in zebrafish development: A critical time window and resilience,” *PLoS One*, vol. 6, no. 5, p. e20037, 2011.
- [239] B. D. Mensh, E. Aksay, D. D. Lee, H. S. Seung, and D. W. Tank, “Spontaneous eye movements in goldfish: Oculomotor integrator performance, plasticity, and dependence on visual feedback,” *Vision Res.*, vol. 44, no. 7, pp. 711–726, 2004.
- [240] A. T. Bahill, M. R. Clark, and L. Stark, “The main sequence, a tool for studying human eye movements,” *Math. Biosci.*, vol. 24, pp. 191–204, 1975.
- [241] T. J. Anastasio and D. A. Robinson, “Failure of the oculomotor neural integrator from a discrete midline lesion between the abducens nuclei in the monkey,” *Neurosci. Lett.*, vol. 127, no. 1, pp. 82–86, 1991.
- [242] M. P. Arts, C. I. De Zeeuw, J. Lips, E. Rosbak, J. I. Simpson, C. I. D. E. Zeeuw, J. Lips, E. Rosbak, and J. I. Simpson, “Effects of nucleus prepositus hypoglossi lesions on visual climbing fiber activity in the rabbit flocculus,” *J. Neurophysiol.*, vol. 84, no. 5, pp. 2552–63, 2000.
- [243] W. Graf, R. Spencer, H. Baker, and R. Baker, “Excitatory and inhibitory vestibular pathways to the extraocular motor nuclei in goldfish,” *J. Neurophysiol.*, vol. 77, no. 5, p. 2765–79., 1997.
- [244] E. Gilland and R. Baker, “Evolutionary patterns of cranial nerve efferent nuclei in vertebrates,” *Brain. Behav. Evol.*, vol. 66, no. 4, pp. 234–254, 2005.
- [245] E. Marsh, “Brainstem and cerebellar organization contributing to goldfish visuomotor behaviors,” PhD Thesis. New York: NYU, 1998.

-
- [246] J. I. Matsui, A. L. Egana, T. R. Sponholtz, A. R. Adolph, and J. E. Dowling, "Effects of ethanol on photoreceptors and visual function in developing zebrafish," *Investig. Ophthalmol. Vis. Sci.*, vol. 47, no. 10, pp. 4589–4597, 2006.
- [247] D. Roche and A. King, "Alcohol impairment of saccadic and smooth pursuit eye movements: impact of risk factors for alcohol dependence," *Psychopharmacology (Berl.)*, 2010.
- [248] M. A. H. W, and K. D, "The effect of oral ethanol consumption on eye movements in healthy volunteers.," *J. Neurol.*, vol. 245, no. 8, pp. 542–50, 1998.
- [249] D. W. H. Holdstock L., "Ethanol impairs saccadic and smooth pursuit eye," *Alcohol. Clin. Exp. Res.*, 1999.
- [250] A. Griffiths, R. W. Marshall, and A. Richens, "Saccadic eye movement analysis as a measure of drug effects on human psychomotor performance.," *Br. J. Clin. Pharmacol.*, vol. 18 Suppl 1, p. 73S–82S, 1984.
- [251] A. M. Pastor, R. R. de la Cruz, and R. Baker, "Cerebellar role in adaptation of the goldfish vestibuloocular reflex.," *J. Neurophysiol.*, vol. 72, no. 3, pp. 1383–1394, Sep. 1994.
- [252] H. Straka, J. C. Beck, A. M. Pastor, and R. Baker, "Morphology and physiology of the cerebellar vestibulolateral lobe pathways linked to oculomotor function in the goldfish.," *J. Neurophysiol.*, vol. 96, no. 4, pp. 1963–80, Oct. 2006.